EXTRACTION, ISOLATION AND PHYSICOCHEMICAL STUDIES OF NATURAL PHEOPHYTIN COMPLEXES

0600017910

North-West University
Mafikeng Campus Library

11862492.0

by

EZEKIEL DIXON DIKIO

Submitted in fulfilment of the requirements for the Degree of Doctor of Philosophy in the Department of Chemistry, Faculty of Agriculture, Science and Technology, North-West University, Mafikeng.

SUPERVISOR:

Dr. D. A. ISABIRYE

DATE SUBMITTED:

JUNE 2005

b16902671

LIBRARY
MAFIKENG CAMPUS
Call No.: TH 572.46
2006 -02- 13 DIK
Acc. No.: 0600299
NORTH-WEST UNIVERSITY

DECLARATION

"I hereby declare that this thesis for the degree of Doctor of Philosophy, at the North West University hereby submitted, has not previously been submitted by me for a degree at this or any other university, that it is my own work in design and execution that all material contained herein has been duly acknowledged."



EZEKIEL DIXON DIKIO

CERTIFICATE OF ACCEPTANCE FOR EXAMINATION

This thesis entitled "Extraction, isolation and physicochemical studies of natural pheophytin complexes" written by Ezekiel Dixon Dikio, Student Number 10336168 of the Department of Chemistry in the Faculty of Agriculture, Science and Technology is hereby recommended for acceptance for examination.



Supervisor:	Dr. David A. Isabirye
Department:	Chemistry
Faculty:	Agriculture, Science and Technology
University:	North-West University (Mmabatho)

ACKNOWLEDGEMENT

I gratefully acknowledge the assistance of my supervisor Dr. David Isabirye for his valuable advice, encouragement and discussion throughout the work presented in this thesis.

I am thankful to the all staff members of the Department of Chemistry North-West University for their support and interest in my work.

Thanks to the staff of the Department of Chemistry, University of Botswana and University of Cape Town for mass Spectrometric analysis and elemental microanalysis, respectively.

I am sincerely thankful to Mr. Fanyana Mtunzi and his family for accommodating me and providing an atmosphere conducive to this work.

I thank Prof. Azibakene Ogulu, Department of Physics, University of Durban-Westville and Dr. and Prof. (Mrs.) Aganga at the Botswana College of Agriculture for their encouragement.

I am thankful to the Almighty God for his grace, love, guidance and protection throughout my study.

Last, but not least, I am grateful to my wife and children for encouragement and forbearance throughout this study.

ABSTRACT

A simple, rapid and efficient method for the extraction and purification of chlorophyll-*a* from plant sources has been developed. And with it, a new method for the extraction of chlorophyll in winter, which has been previously problematic, has been developed. The methods are summarized in flow diagrams showing the elimination of carotene and xanthophylls.

The chlorophyll-*a* isolated has been demetallated to obtain pheophytin-*a* that in turn has been complexed with cobalt(II), copper(II), zinc, nickel(II) and chromium(III) ions. The resulting metal pheophytin complexes, chlorophyll-*a* and pheophytin-*a* have been fully characterized by ultraviolet-visible and Fourier transform infrared spectroscopies, electrospray ion mass spectrometry and elemental analysis.

For the first time, the kinetics of the oxidation of cobalt(II) pheophytin-*a* by chromium(III) has been followed spectrophotometrically at temperatures ranging from 313 to 333 K. The reaction has been found to be first order in the concentration of the hexaaquachromium(III) cation. The oxidation-reduction mechanism proposed for the reaction is an outer-sphere electron tunneling mechanism.

The ease of demetallation and complexation of chlorophyll-*a* has highlighted the problem caused by acidity and the presence of these metal ions in soils, on the chlorophyll content of leaves.

ABBREVIATIONS

HPLC	High performance liquid chromatography
RPHPLC	Reversed phase high performance liquid chromatography
Cophe	Cobalt(II) pheophytin-*a* complex
Cuphe	Copper(II) pheophytin-*a* complex
Znphe	Zinc pheophytin-*a* complex
Niphe	Nickel(II) pheophytin-*a* complex
Crphe	Chromium(III) pheophytin-*a* complex
DMF	Dimethylformamide
TMU	Tetramethylurea
NH	Nitrogen-hydrogen
TCNE	Tetracyanoethylene
TTP	Tetrahydroporphyrin
H_2TTP	Demetalled tetrahydroporphyrin
CD	Circular dichroism
Redox	Oxidation-reduction
ESI-MS	Electrospray ion mass spectrometry
EI-MS	Electron impact mass spectrometry
sh	Sharp
m	Medium
w	Weak
vw	Very weak
s	Strong
vs	Very strong
Chla	Chlorophyll-*a*

Chla.chla	Chlorophyll-*a* plus chlorophyll-*a*
Phe-a	Pheophytin-*a*
Chl_2	Chlorophyll dimer
$Chl.H_2O$	Chlorophyll water aggregate
LUMO	Lowest unoccupied molecular orbital
HOMO	Highest occupied molecular orbital

TABLE OF CONTENTS

PAGE

CHAPTER ONE INTRODUCTION.....1

1.1 **Introduction**.....1
1.2 Problem statement 8
1.3 Objectives.....9

CHAPTER TWO LITERATURE REVIEW.....10

2.1 Chlorophyll 10
2.2 Structure.....13
2.3 Extraction 20
2.4 Analysis of chlorophyll 22
2.5 Chlorophyll estimation.....24
2.6 Methods of metal insertion.....26
2.6.1 Acetate method.....26
2.6.2 Dimethylformamide method.....27
2.6.3 Successful metal insertion.....27
2.7 Degradation process & products.....28
2.8 Reactions.....32

2.8.1	Solubility	32
2.8.2	Enolization & Tautomerization	32
2.8.3	Allomerization	34
2.8.4	Photosensitization	35
2.8.5	Photosynthesis	36
2.9	**Spectroscopic studies**	**37**
2.9.1	Infrared spectroscopy	37
2.9.2	Raman spectroscopy	39
2.9.3	Ultraviolet-visible spectroscopy	39
2.9.4	Mass spectrometry	42
2.10	Metal macrocycles	45
2.11	**Kinetic studies**	**46**
2.12	**Mechanisms of inorganic oxidation-reduction reactions**	**47**
2.13	**Inner sphere and outer-sphere mechanism**	**48**
2.13.1	Inner sphere	49
2.13.2	Outer-sphere	50
2.13.3	Frank-Condon restriction	51

CHAPTER THREE EXPERIMENTAL 53

3.1	**Reagents**	**53**
3.2	**Extraction of chlorophyll**	**54**
3.2.1	Alumina column method (method 1)	54
3.2.2	Silica gel method (method 2)	57

3.2.3	Improved silica gel method (method 3)	59
3.2.4	Winter extraction method (method 4)	62
3.3	**Precautions taken during extraction**	**64**
3.4	**Characterization of chlorophyll**	**64**
3.4.1	Ultraviolet-visible absorption spectra	64
3.4.2	Determination of chlorophyll and pheophytin content	65
3.4.3	Infrared spectra	66
3.4.4	Mass spectrometry	66
3.5	**Removal of magnesium**	**66**
3.6	**Insertion of metal ion in pheophytin**	**67**
3.6.1	Cobalt insertion	67
3.6.2	Copper insertion	68
3.6.3	Zinc insertion	69
3.6.4	Nickel insertion	69
3.6.5	Chromium insertion	70
3.7	**Characterization of metal pheophytin complexes**	**71**
3.7.1	Ultraviolet-visible spectroscopy	71
3.7.2	Infrared spectroscopy	71
3.7.3	Mass spectrometry	71
3.7.4	Elemental analyses	72
3.8	**Procedure for kinetic study of reduction reaction**	**72**
3.9	**Computation of rate constants and activation parameters**	**73**

3.10 Computation of the amount of chlorophyll-*a* and pheophytin-*a* 74

CHAPTER FOUR RESULTS.....75

4.1 Extraction of chlorophyll.....75
4.1.1 Alumina column method (method 1).....75
4.1.2 Silica gel column method (method 2).....79
4.1.3 Improved silica gel column method (method 3).....84
4.1.4 Winter extraction method (method 4) 93
4.1.5 Summary of quantities of chlorophyll extracted 103
4.2 Demetallation of chlorophyll-*a*.....104
4.3 Complexation of pheophytin-*a*.....107
4.4 Elemental analysis.....121
4.5 Kinetics of oxidation of cobalt(II) pheophytin-*a* by hexaaquachromium(III) cation.....127
4.5.1 The oxidation of cobalt(II) pheophytin-*a* by hexaaquachromium(III) cation at 313 K.....130
4.5.2 The oxidation of cobalt(II) pheophytin-*a* by hexaaquachromium(III) cation at 323 K.....133
4.5.3 The oxidation of cobalt(II) pheophytin-*a* by hexaaquachromium(III) cation at 333 K.....136
4.5.4 Arrhenius parameters.....139

CHAPTER FIVE DISCUSSION.....142

5.1. Extraction.....142
5.1.1 Alumina column method (method 1).....142
5.1.2 Silica gel column method (method 2).....144
5.1.3 Improved silica gel column method (method 3).....146
5.1.4 Winter extraction method (method 4).....149
5.2 Characterization.....151
5.2.1 Ultraviolet-visible spectroscopy.....151
5.2.2 Infrared spectroscopy.....153
5.2.3 Mass spectrometry.....157
5.3 Metal insertion.....164
5.3.1 Ultraviolet-visible spectra of metallochlorophylls.....164
5.3.2 Infrared spectra of metallochlorophylls.....169
5.3.3 Elemental analyses.....175
5.3.4 Mass spectra of cobalt(II) pheophytin-*a*.....176
5.4 Kinetics of oxidation of cobalt(II) pheophytin-*a*.....178
5.5 Mechanism of oxidation.....180
5.6 Role of magnesium in chlorophyll.....181

CHAPTER SIX CONCLUSION.....184

6.1 Conclusion.....184

REFERENCES.....186

CHAPTER ONE

INTRODUCTION

1.1 INTRODUCTION

Chlorophyll is an important pigment found in the chloroplast of plants.[1,2] It is the green colouring matter of leaves and green stems whose presence is essential for photosynthesis. [3-8] There are several forms of chlorophyll. The major chlorophylls in land plants are designated *a* and *b*, with chlorophyll-*a* several times more abundant than chlorophyll-*b*.[9-18] Chlorophyll-*a* is now known to have the formula $C_{55}H_{72}N_4O_5Mg$ and relative molecular mass (M_r) 893.503. [19,20]

The chemical name for chlorophyll is [3,7,11,15-tetramethyl-2-hexadecenyl-9-ethenyl-14-ethyl-21-(methoxycarbonyl)-4,8,13,18-tetramethyl-20-oxo-3-phorbinepropanoato(2-)-N^{23},N^{24},N^{25},N^{26}] magnesium. The structures of chlorophyll-*a* and chlorophyll-*b* are shown in Figure 1.1 below. [19,21]

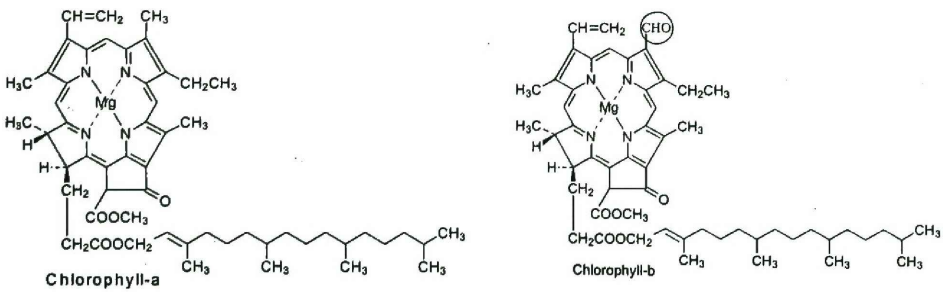


Figure 1.1 Structures of chlorophyll-*a* and chlorophyll-*b*. showing the difference between chlorophyll-*a* and chlorophyll-*b* at position 3 where the CH_3 is replaced by the CHO group.

The biological significance of the chlorophylls stems from their role in photosynthesis. Chlorophyll is capable of channelling the energy of sunlight into chemical energy through the process of photosynthesis.[6] In photosynthesis, the energy absorbed by chlorophyll transforms carbon dioxide and water into carbohydrates and oxygen. Thus chlorophyll is at the centre of the oxidation-reduction reaction between carbon dioxide and water. While it is known that most of the energy fixed in photosynthesis is absorbed originally by the chlorophylls, the exact reactions which they undergo to initiate the process of reduction are not yet understood.[6] The overall process of photosynthesis is shown below Equation [1.1], where carbon dioxide and water combine in the presence of light and chlorophyll to form carbohydrate and oxygen. CH_2O is the empirical formula for carbohydrate. [2]

$$nCO_2 + nH_2O \rightarrow (CH_2O)_n + nO_2 \qquad [1.1]$$

The chlorophylls have been subjected to extensive structural investigations in the 20th century due to their specific chemical properties and their fundamental importance in nature.[22]

The reason why nature selected chlorophyll as the one molecule around which to construct the process of photosynthesis, whereby carbon dioxide, water and sunlight are converted into food and oxygen to breath, has stimulated an immense amount of research and speculation.[14] Much of this effort has taken the form of constructing and studying model systems of chlorophyll, in which some properties

of the physiological system are abstracted from the many others, which make the study of the whole system difficult.[14]

In view of the essential role chlorophylls play as the primary photo-acceptors in plants and bacterial photosynthesis, a great deal of work has focused on their molecular structure, their interactions in solution and their structure-function relationship. [1,10,23]

Studies in the field of artificial photosynthesis require molecular systems, which play the role of chlorophyll. Although chlorophyll contains the magnesium ion at the centre, most studies in artificial photosynthesis have employed zinc, ruthenium and manganese rather than magnesium complexes. [24-26]

Studies on the interactions between two different cyclodextrins and chlorophyll-*a* in the presence of an electrolyte indicate that the presence of both cyclodextrins gives rise to an increase in chlorophyll-*a* solubility. The effect of solvent coordination on the excited states of chlorophyll-*a* and chlorophyll-*b* has been studied. Calculations predict solvent-induced spectroscopic shifts of Q_x and Soret transition, but have the Q_y transition almost unshifted. This is a result of solvent-induced energy-level shifts and charge redistribution on the magnesium atom of chlorophyll in the excited state. [27-29]

The effect of magnesium coordination in chlorophyll has also been the subject of investigation by Boxer, Closs and Katz.[30] The magnesium

produces a redistribution of charge density within the molecule accompanied by a reduction in the energy separations among low-lying $n\pi^*$ states. Besides structural functions, it is conceived that the magnesium atom also plays an important electronic role in the excited state of chlorophyll. The electronic state of the chlorophylls is fundamental for understanding their function in various environments, in solution, in self-assembled aggregates and in photosynthetic complexes. It is not very well understood why the Q_x and Soret bands are much more sensitive to solvent effects than the Q_y band. Very little is also known of the origin of the transition energies of chlorophylls in various environments. [29]

X-ray analyses performed on crystals of ethyl chlorophyllide-*a* dihydrate, ethyl chlorophyllide-*b* dihydrate and other chlorophyll macrocycles have shown the magnesium atom to be coordinated to four pyrrole nitrogens and a water molecule (axial ligand). The magnesium atom in chlorophyll is therefore five-coordinated. [31]

High performance liquid chromatographic separation and isolation of methanolic allomerization products of chlorophyll-*a* have been investigated by Hynninen and co-workers.[32] Reversed-phase HPLC did not result in an acceptable separation of allomerization products in spite of using several different brands of reversed-phase C_{18} columns and mobile phase compositions. [32]

Workers in various scientific disciplines have continued to focus on the chlorophylls.[33-50] In food science, the chlorophylls and their derivatives are of interest as food dyes. They are also used as markers of food processing because of the sensitivity of chlorophylls to light, pH, temperature, oxygen and enzymatic degradation.[51]

In agriculture and industry, the study of colour change from the bright green of chlorophyll to the olive brown of pheophytin during storage and processing is of major interest and importance for technologists and other researchers. This is due to the fact that colour, the major quality attribute of vegetables and fruits, may finally make the consumer decide whether to buy or not.[25]

The tetrapyrroles in chlorophyll are of interest to bioinorganic chemists because of their central importance in metabolism, thus research in this area offers huge opportunity for breaking new grounds. Metal complexes of the tetrapyrroles provide essential cofactors in a large number of protein and enzyme reactions.[38]

Environmental scientists monitor the fate of algae in seawater by studying and measuring chlorophyll degradation products in the seawater.[33,45] In oceanography, the determination of particulate chlorophylls and their degradation products in natural samples is an important measurement to estimate biomass from the sea, lakes, rivers and other sources. It also provides valuable information about the biological activity in different environments. [52]

Medical scientists investigate chlorophyll, porphyrins and their degradation products as potential photosensitizers in photodynamic therapy (PDT) for the treatment of cancer and hyperproliferative diseases, which are also based on photosensitizers in the presence of oxygen and light. The use of metal porphyrins as surrogates for chlorophyll in photosynthetic model systems and molecular photonic devices has also increased. The versatile optical (absorption & emission), redox and photochemical properties of the porphyrins make them ideally suited as components of nanostructures with optical features in the visible or near-infrared spectral regions.[22,27,43,53-55]

Biochemists studying photosynthetic systems of green plants, utilize chlorophyll-*a* and chlorophyll-*b* molecules in light-induced excitation transfer in light-harvesting complexes. In addition, chlorophyll-*a* molecules contribute to charge separation and transfer processes in the photosystems. Their detailed structural features are under investigation because the exceptional efficient energy and electron transfer mechanism of green plants is evidently connected to them.[32]

Studies of various chlorophyll derivatives and porphyrins have been motivated by their importance in the primary photosynthetic events.[9] First, a great number of artificial models for natural photosynthetic processes have been constructed with model tetrapyrroles other than chlorophyll derivatives, poorly mimicking their natural counterparts. Secondly, the use of chlorophyll derivatives as photosensitizers in photodynamic cancer therapy treatment has increased.[53-55]

Much research effort has aimed at preparing artificial systems that can convert solar light into useful chemical energy or give increased understanding of the mechanism of photosynthesis.[22]

In spite of these research endeavours and many more on chlorophyll and its derivatives, the need for research on natural chlorophyll-*a* and its derivatives continues to exist.

Until the mid-1970s, preparative scale isolation and microanalyses of chlorophylls relied mainly on column chromatography and thin layer chromatography (TLC) respectively.[14] In general, these procedures were thought not to be effective in separating the pigments.[14,56]

In recent years, the high performance liquid chromatography (HPLC) technique has been applied to the separation of plant pigments.[32,56] This method did not result in acceptable separation even when different brands of reversed-phase C_{18} columns and mobile phase compositions have been employed, thus necessitating further purification and preparative scale isolation.[24] The separation and isolation of chlorophyll and its derivatives continue to prove difficult in situations where high performance liquid chromatographic technique is lacking. [56]

There have been several attempts to insert metal ions in place of magnesium in the chlorophyll photosynthetic unit. It is reported[56] that, replacing magnesium with copper or zinc results in the formation of

metallochlorophylls with higher stability to photochemical decomposition. These metal ions play a decisive but little understood role in the chlorophyll photosynthetic unit.[56] Chemical examination of chlorophyll derivatives in which the magnesium is replaced by other metal ions (metallochlorophylls) are valuable in that they provide information about the contribution of the metal to the various properties and function of chlorophyll.[57,58]

1.2 PROBLEM STATEMENT

The outline highlights the need for further investigation into chlorophyll and its derivatives. The effect of chemical reagents like acids and metal salts has to be clearly understood in the light of their effect on the chlorophyll content of leaves.

The isolation of some metal pheophytin complexes[9,19] has not been proven by elemental analysis thus casting doubts on the structures and nature of these compounds.

Further, the entire unexplored area of mechanism of electron transfer in these systems warrants clear investigation. This would go a long way towards the understanding of the mechanism of photosynthesis.

In order to achieve all these, a relatively cheap, simple and efficient method of obtaining chlorophyll has to be developed.

1.3 OBJECTIVES

The objectives of this study are therefore:

1.3.1 Extraction of chlorophyll from spinach leaves.

1.3.2 Separation of chlorophyll-*a* by column chromatography.

1.3.3 Demetallation of chlorophyll-*a* to obtain pheophytin-*a*.

1.3.4 Complexation of pheophytin-*a* with various metal ions.

1.3.5 Purification and crystallization of crystals of pheophytin metal complexes.

1.3.6 Characterization of chlorophyll-*a*, pheophytin-*a* and pheophytin metal complexes by Ultraviolet-visible and Fourier transform infrared spectroscopy, elemental analysis and mass spectroscopy.

1.3.7 Investigation of the kinetics and mechanism of the oxidation-reduction reactions of some of the metal-pheophytin complexes.

CHAPTER TWO

LITERATURE REVIEW

2.1 CHLOROPHYLL

Chlorophyll is the most widely distributed natural pigment in nature. Every organism capable of undergoing photosynthesis (including algae and some photosynthetic bacteria) owe their green colour to chlorophyll.[1,4,59] The intense green colour of chlorophyll is due to its strong absorbance in the red and blue regions of the electronic spectrum. [4,60]

The generic name chlorophyll, of these green pigments, was given by Pelletier and Caventou[61a] in 1818. The "chloro" in the name chlorophyll is derived from the Greek word *chloros*, which means yellowish green.[4]

Chlorophyll is the substance at the centre of the photosynthetic oxidation-reduction reaction between carbon dioxide and water that takes place in plants in which carbohydrates and oxygen are produced. It assists in the transfer of electrons from water to carbon dioxide during this process.[2] The chemical structure of chlorophyll-*a* is shown in Figure 2.1.

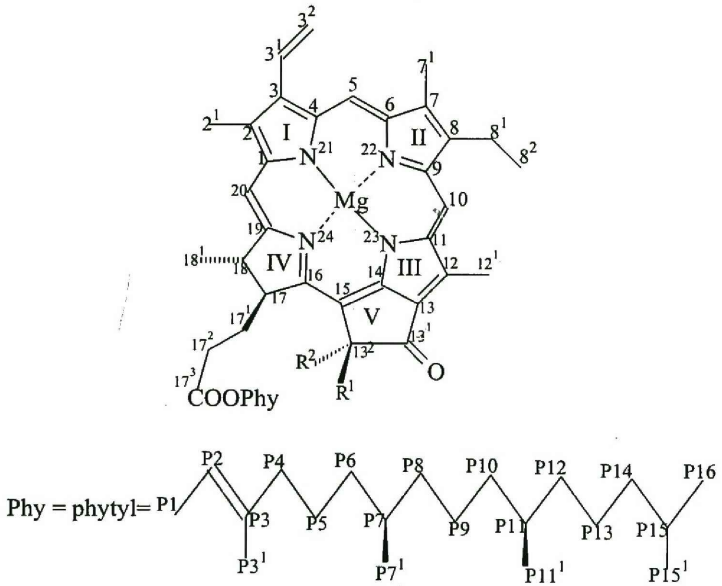


Figure 2.1 Structure of chlorophyll-*a* and the phytyl chain.

The primary process of photosynthesis in plants and algae is a light-induced redox reaction driven by chlorophylls and bacteriochlorophylls.[34] These pigments absorb sunlight in light-harvesting pigment-protein complexes and transfer the energy to reaction centre complexes where chlorophylls and bacteriochlorophylls initiate electron-transfer.[34]

Other molecules with similar structures to that of chlorophyll play important roles in other biochemical electron transfer reactions. Heme[17] for example, consists of a porphyrin ring similar to that in chlorophyll with iron(II) (Fe^{2+}) at the centre of the porphyrin, while

vitamin B_{12} contains cobalt(III) ion (Co^{3+}) in the centre of a corin macrocyclic. [4]

It was assumed initially that chlorophyll was a single compound but in 1864 Stokes[61b] showed by spectroscopy that chlorophyll was a mixture. The chlorophylls are therefore porphyrins in that they are magnesium complexes of compounds derived from porphin and its *di-* and *tetrahydro-* derivatives as shown in Figure 2.2. [9,10,23]

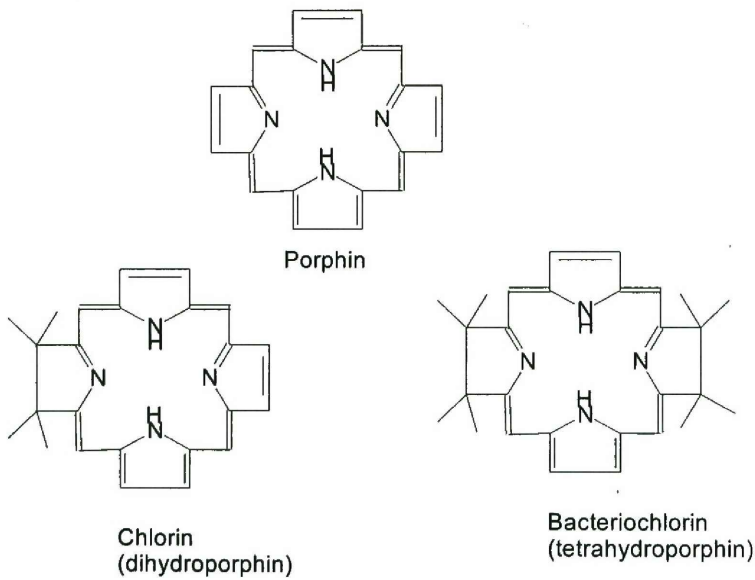


Figure 2.2 Structure of porphin, chlorin and bacteriochlorin

Porphyrins, metalloporphyrins, chlorophylls and metallochlorophylls exhibit many potentially important medicinal and industrial properties. They are being examined as possible blood substitutes and as electrocatalyst for fuel cells and for the electrochemical generation of hydrogen peroxide.[10] The porphyrins are also showing strong potential

in the treatment of a wide range of diseases including cancer using photodynamic therapy.[10]

Metalloporphyrins are being examined as potential catalysts for a variety of processes, including catalytic oxidation.[10] The porphyrins have unique optical properties that make them usable in photovoltaic devices in photocopying, and other optical devices.[6,10]

Phthalocyanine,[62] another cyclic tetrapyrrole has obvious structural similarities with porphyrin and chlorophyll. As with porphyrin and chlorophyll, various metals can be incorporated into the central cavity of phthalocyanine. Like the porphyrins, they are both colourful, stable and used industrially to colour blue-jeans and automobiles.[10,62-65]

An interesting property of the porphyrins is that a small variation in the basic structure of the tetrapyrrole macrocycle leads to a wide diversity of biochemical functions.[10] The main function of porphyrins and porphyrin-like compounds, such as chlorophyll, in nature is to bind metal ions, which act as centres for specific biochemical processes.[6,10]

2.2 STRUCTURE

The earliest systematic investigation of chlorophyll chemistry was carried out by Willstätter and Stoll.[66] The essential structures of chlorophylls-*a* and -*b* as well as bacteriochlorophyll were established by the work of Fischer[67,68] during the 1920s and 1930s.[9] Systematic

evidence for the structure of chlorophyll-*a* was first provided by Fischer[67] in which he also completed the synthesis of some related porphyrins. The absolute configuration of chlorophyll-*a* was first elucidated by a combination of synthetic and spectroscopic methods. Later the three-dimensional (3D) structure was established by the X-ray analysis of chemically modified chlorophyll-*a*. [4,9] Fischer's method was used in the synthesis of methyl pheophobide-*a*.
TheHarvard synthesis of methyl pheophobide-a was done by joining two dipyromethane units.[4,9,10]

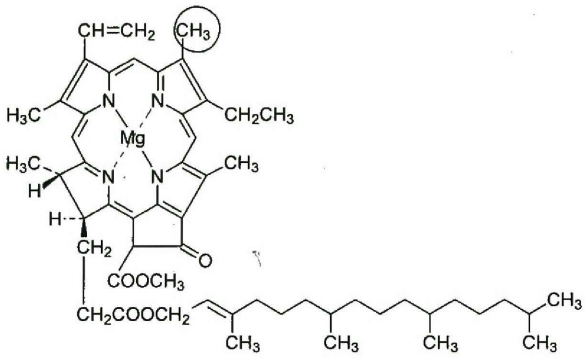
The absolute stereochemistry of chlorophyll-*a* was shown by Fleming[69] by means of a chemical correlation of a degradation product. In their studies of chlorophylls-*a* and -*b*, Strain and Manning[70] chromatographically separated small quantities of two minor green pigments designated chlorophyll-*a'* and *b'*, (chlorophyll-*a'* and chlorophyll-*b'* are derivatives of chlorophyll-*a* and chlorophyll-*b*, respectively) which were almost indistinguishable spectroscopically from the main pigments.[9]

The elucidation of the complete structures of chlorophylls-*a* and -*b* involved many researchers.[9,14] The basic structure of chlorophyll is made up of four pyrrole rings, a tetrapyrrole which is also named porphyrin.[7] The four pyrrole rings are joined together by methine bridges to form the ring structure.[4,14] This structure was put forward by Fischer and Wenderoth (1939).[71] Magnesium is present at the centre of the ring; it is covalently bonded to two nitrogen atoms and

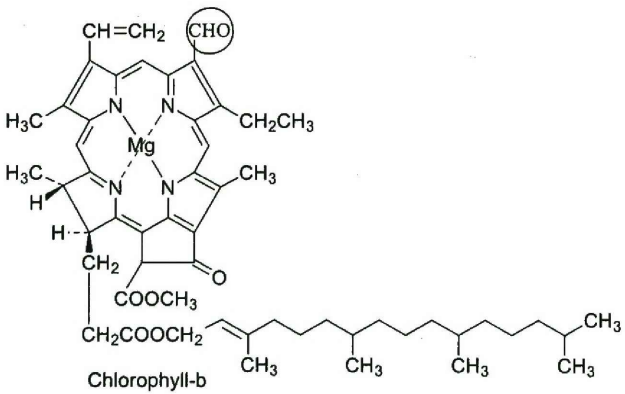
co-ordinately bonded to two other nitrogen atoms of the tetrapyrrole ring.[7,9,10]

There are a number of chlorophylls in plants all with the same basic structure but show basic variations in the nature of substituents on the porphyrin ring. [9,19] Some of the chlorophylls that are recognised presently are chlorophylls *a, b, c, d, e*, protochlorophyll, bacteriochlorophyll and chlorobium chlorophyll as shown in Figure 2.3.[9,12,19] Chlorophyll-*a* differs from chlorophyll-*b* in having a methyl group instead of an aldehyde group in one of the pyrrole rings. [12]

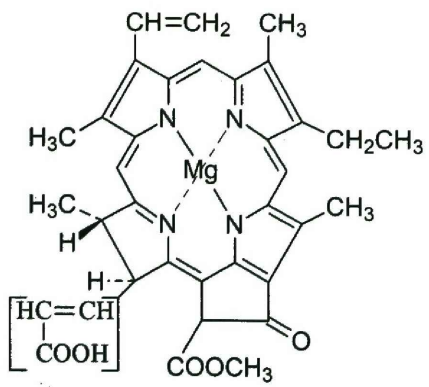
Chlorophyll-*a*, chlorophyll-*b* and chlorophyll-*d* have a long hydrocarbon (phytyl) side chain (Figure 2.3) attached to the porphyrin macrocycle through a carboxylic acid group. This phytyl side chain is not present in chlorophyll-*c*. (Figure 2.3). The structure of chlorophyll-*e* is not yet known. It has only been demonstrated in *Tribonema bombycinum*, a member of the xanthophyceae.[19-21] Protochlorophyll differs from chlorophyll-*a* by loss of two hydrogen atoms from the β-position in ring IV and formation of a double bond.[44] Chlorobium chlorophyll is found in green sulphur bacteria. It does not have a phytyl chain.[19] Bacteriochlorophyll-*a* is found in purple and brown photosynthetic bacteria and in some green sulphur bacteria.[19] It is more reduced than chlorophyll-*a* with two hydrogen atoms at carbons 3 and 4 (which are joined by a single bond) and with $—COCH_3$ attached at carbon 2 instead of $—CH=CH_2$ (Figure 2.3).[3]



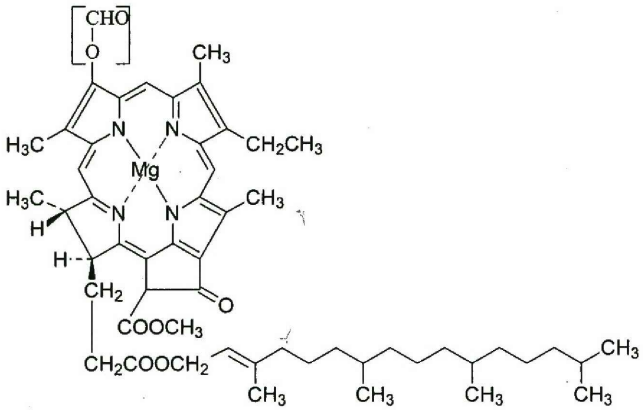
Chlorophyll-a



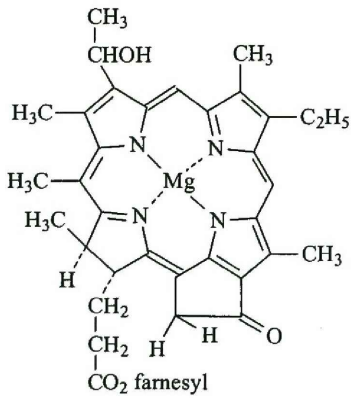
Chlorophyll-b



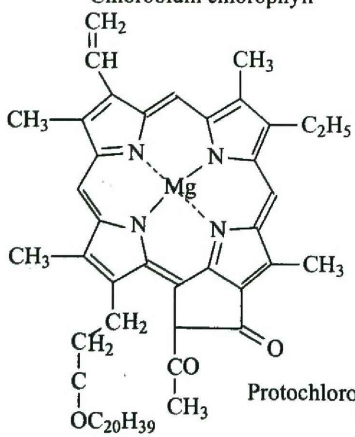
Chlorophyll-c



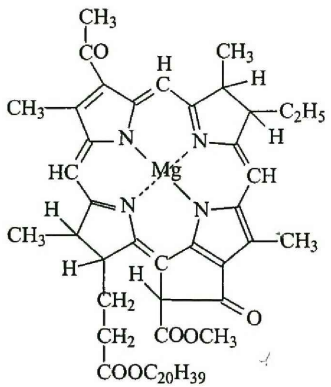
Chlorophyll-d



Chlorobium chlorophyll



Protochlorophyll



Bacteriochlorophyll-a

Figure 2.3 Structures of chlorophylls *a, b, c* and *d* chlorobium chlorophyll and protochlorophyll.

The principal chlorophyll is chlorophyll-*a* (Figure 2.4); it is found in all photosynthetic plants, organisms and photosynthetic bacteria that evolve oxygen.[2] Chlorophyll-*b* is found in virtually all higher plants.[59] Chlorophylls-*a* and *b* are generally found associated with each other in the leaves of green plants. Chlorophyll-*a* is several times more abundant than chlorophyll-*b* with a ratio of about 3 : 1.[9,12,19,72-74] Chlorophyll-*c* is found in diatoms and brown algae while chlorophyll-*d* can be isolated from marine red algae. [19] Chlorophyll-*e* has been isolated from cultures of two algae, *tribonema bombycium* and *vaucheria bamata.*[18,19]

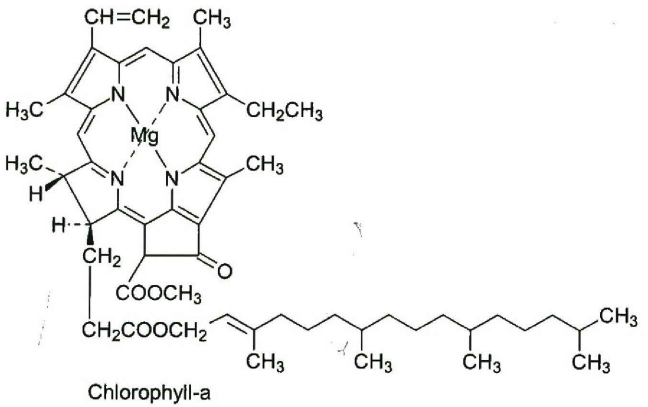


Figure 2.4 Structure of chlorophyll-*a*.

The peripheral carbon atoms in chlorophyll are numbered 1-8 and the methine (or meso) bridge carbon atoms are designated $\alpha,\beta,\gamma,\delta$ in the Fischer system, Figure 2.5.[9] The chlorophylls contain another ring in addition to the four pyrrole rings unlike the haems,[38] the isocyclic ring is labelled E in Fischer's system, Figure 2.5. [9,19,71]

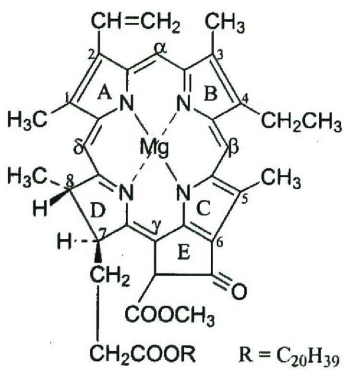


Figure 2.5 Numbering of carbon atoms in the Fischer system.

2.3 EXTRACTION

Extraction of chlorophylls, especially chlorophyll-*a*, has been the subject of many research studies.[19,75-78] A number of methods have been employed in the extraction of chlorophyll pigments from fresh plant material. The method of extraction depends on the type and form of tissue used, the scale of the extraction and the chlorophylls required. [9,10,12,14]

Some workers have immersed the plant material in boiling water to kill it before extracting with an organic solvent. This causes isomerization of chlorophylls -*a* and -*b* with the formation of chlorophylls *a'* and *b'*. The method of Strain[70] causes isomerization of chlorophyll-*a* and chlorophyll-*b* forming chlorophyll-*a'* and chlorophyll-*b'*.[59] Boiling also causes the breakdown of chlorophyll to pheophytin. [9,14,19,59]

Acetone and methanol are the most frequently used solvents in the extraction of chlorophyll.[10,14] Acetone has been preferred by some workers because of the possibility of allomerization in methanol, but as aqueous solvents are almost always used, allomerization is not likely to occur.[59] Hynninen[79] has shown that extracting chlorophyll with methanol causes allomerization of chlorophyll. If samples of young undamaged leaves are soaked in acetone or methanol, the chlorophyll may be completely extracted into the solvent making grinding unnecessary.[10,59]

In this method, leaves placed in boiling water for 2 minutes are washed with cold water, and then transferred separately to methanol (500 ml) plus petroleum ether (125 ml). After a few minutes, the deep green extract is filtered through a pad of cotton wool.[9,10,14] The leaves are extracted twice more with methanol-petroleum ether and the extract (separately) is diluted with saturated brine (1 litre) thereby transferring the pigment to the petroleum ether layer. Separation on a sugar chromatographic column serves to remove the by-products and separate the two major chlorophylls.[14,59,80-85]

Chlorophyll may also be extracted from most green plants by means of 80% aqueous acetone. Chlorophyll and xanthophylls, but not all the carotenes, are extracted by this method.[41,59]

Reversed-phase partition thin layer chromatography appears suitable for analytical purposes, but is unsuitable for preparative isolation since the impregnating triglyceride is eluted from the chromatograms and interferes seriously with subsequent chromatographic analyses.[32,52,86-90] A two-phase isolation method with a precipitation and a separation of the precipitated chlorophylls on a sucrose column has been reported by Hynninen.[32,76-79]

Chlorophyll extraction from spinach by liquid chromatography using zinc phthalocyanine as internal standard was performed by Bohn and Walczyk.[51] This research was conducted because chlorophyll analysis at high precision and accuracy is limited by a lack of suitable

commercially available internal standards. Bohn and Walczyk found zinc phthalocyanine to be sufficiently suitable as an internal standard.[51]

Macías-Sánchez *et al*[81] have reported that the traditional methods for the extraction of chlorophyll and carotenoids from sources such as micro algae frequently require more than one extraction step with organic solvents which are forbidden in processing food additives. They have therefore employed the method of supercritical fluid in the extraction of chlorophyll.[81] Their results indicate that the amount of chlorophyll extracted with supercritical carbon dioxide is always higher than the amount of chlorophyll obtained from methanol extraction. [81]

2.4 ANALYSIS OF CHLOROPHYLL

After pigments have been extracted, chlorophyll can be analysed by various methods based on spectrophotometry and fluorimetry, both with and without further separation of the individual pigments. Extracts should be analysed as soon as possible after being made, otherwise they should be kept in a cold and dark place. [59]

High performance liquid chromatography (HPLC) has been employed in the analysis of the chlorophylls, pheophytins and carotenoids. Angelo Cichelli and Pertesana,[90] used high performance liquid chromatography in the determination of photosynthetic pigments in virgin olive oil. Their analysis showed that the greenish yellow colour

of olive oil is due to various pigments contained in the oil. These natural pigments can also affect the preservation of the products. [90,91]

In order to determine chlorophyll in plant samples, Bohn and Walczyk[51] used HPLC. This technique was applied to chlorophyll analysis of a selection of vegetable foods. Chlorophyll-*a*, -*a'*, -*b*, & *b'* and corresponding pheophytins were separated by HPLC using a C_{18} reverse-phase column and fluorescence detection. [92] The polar nature of the chlorophylls and their oxidation products permit their separation by HPLC. Reversed-phase high performance liquid chromatography (RPHPLC) has been utilized in the study of allomers of chlorophyll-*a*.[93]

High performance liquid chromatography was used in the isolation, analyses and characterisation of mercury(II) pheophytin.[80] Photometric methods have been used in the quantification of the chlorophylls. The method is based on the description of each pigment spectrum by a series of Gaussian peaks.[94]

2.5 ESTIMATION OF CONTENT OF CHLOROPHYLL

The chlorophyll content in a plant extract can be determined easily. Measurement of chlorophyll content can be made by direct determination of the absorbance at different wavelengths using a standard Uv-visible spectrophotometer. The wavelength of maximum absorption varies according to the solvent being used. The chlorophyll

content of a tissue is therefore best determined by measurement in the solvent used for extraction.[3,59,95]

The spectrophotometric determination of chlorophyll is dependent on the Beer-Lambert law; however, various equations have been derived for determining the concentration of total chlorophyll and of chlorophyll-*a* and chlorophyll-*b* in a mixture.[1,3,9,19,59] The absorbance at definite wavelength and thickness of the solution is measured and the specific absorption coefficients of the pure pigment at these wavelengths must be known. [5]

The specific absorption coefficient α is D/dc

Where D is the absorbance

d is the length of light path in cm

c is the concentration of pigment in g/L

In 80% aqueous acetone,[3,10,19,59]

Total chlorophyll (mg/L) = $20.2D_{645} + 8.02D_{663}$

Chlorophyll-*a* (mg/L) = $12.7D_{663} - 2.69D_{645}$

Chlorophyll-*b* (mg/g) = $22.9D_{645} - 4.68D_{663}$

In methanol,[19] total chlorophyll, chlorophyll-*a* and chlorophyll-*b* are calculated as follows:

Total chlorophyll (mg/L) = $25.5D_{650} + 4.0D_{665}$

Chlorophyll-*a* (mg/L) = $16.5D_{665} - 8.3D_{650}$

Chlorophyll-*b* (mg/g) $= 33.8D_{650} - 12.5D_{665}$

In 96% ethanol[59]
Total chlorophyll (mg/L) $= 20.0D_{649} + 6.1D_{665}$
Chlorophyll-*a* (mg/L) $= 13.7D_{665} - 5.7D_{649}$
Chlorophyll-*b* (mg/g) $= 25.8D_{649} - 7.6D_{665}$

In diethyl ether[19,59]
Total chlorophyll (mg/L) $= 7.12D_{660} + 16.8D_{642.5}$
Chlorophyll-*a* (mg/L) $= 9.93D_{660} - 0.78D_{642.5}$
Chlorophyll-*b* (mg/g) $= 17.6D_{642.5} - 2.8D_{660}$
Total pheophytin (mg/L) $= 6.75D_{666} + 26.03D_{655}$
Pheophytin-*a* (mg/L) $= 20.15D_{666} - 5.87D_{655}$

Other equations were given making use of the absorption at 666 nm and 536 nm.[19,59]

$$\text{Chlorophyll-a (mg/g)} = \frac{12.3D_{663} - 0.86D_{645}}{ax100xW} xV$$

where D_{663} and D_{645} are the absorbance at 645 nm and 663 nm.
V is the volume in ml,
a is the length of light path in the cell (1cm),
W is the fresh weight in gram.

2.6 METHODS OF METAL INSERTION[10]

A number of methods used for metal insertion have been reported in the literature. Some of the more frequently used are:

(a) Acetate method

(b) Pyridine method

(c) Acetylacetone method

(d) Phenoxide method

(e) Benzonitrile method

(f) Dimethylformamide method

(g) Metal organyl method

(h) Metal carbonyl method

The methods of metal insertion that will be used in this research work are the acetate and dimethylformamide methods due to their simplicity and ease of isolation of the final product.

2.6.1 THE ACETATE METHOD

The acetate method can be performed very conveniently by extracting gram quantities of chlorophyll from a thimble into the boiling solution of the metal carrier in glacial acetic acid containing sodium acetate. [48] On cooling, the metallochlorophyll or metalloporphyrin frequently crystallises directly from the solution. Thus, it is assured that no crystalline starting material is left when the reaction is complete.

Alternatively, addition of hot water or methanol accomplishes the precipitation. The product may then be purified by chromatography on alumina grade(III) with dichloromethane ($CH_2C\ell_2$), or trichloromethane ($CHC\ell_3$), as eluent.[10]

2.6.2 THE DIMETHYLFORMAMIDE METHOD

More than 68 different metalloporphyrins have been prepared using oxygen donor solvents such as dimethylformamide (DMF), tetramethylurea (TMU) and sulpholane, which are good solvents for the metal carriers and the porphyrins. Best results have been obtained with anhydrous metal chlorides. The high boiling point employed drives off the hydrochloric acid produced during the reaction. Equation [2.2] shows the reaction of a metal chloride with demetallated porphyrin in the presence of oxygen.[10]

$$4MC\ell_2 + 4H_2TPP + O_2 \rightarrow 4M(TPP)C\ell + 2H_2O + 4HC\ell \qquad [2.2]$$

By this method, H_2(TPP) (10 g) are reacted with DMF (1L). The crude product crystallises simply by the addition of water (1L) and cooling. This method may cause surprising results with catalytically active transition metal compounds. [10]

2.6.3 SUCCESSFUL METAL INSERTION

A successful metal insertion can be established by various methods, which allow one either the absence of the chlorophyll adduct or the presence of the metallochlorophyll product.

The methods of visible absorption spectroscopy, observation of fluorescence and infrared spectroscopic analysis, require taking a small sample of the reaction mixture to dryness. For the infrared assay, even the metal carrier should be removed by washing with water. The absence of NH-bands from the infrared spectrum of the reaction mixture then indicates the end of the reaction.

The easiest procedure is to take a small volume from the reaction mixture with a syringe, dilute and measure the electronic absorption spectrum in the visible region. The end of the reaction is indicated by the disappearance of the pheophytin band. [10]

2.7 DEGRADATION PROCESS & PRODUCTS

(a) Colour Change

The loss of chlorophyll is responsible for the symptom of yellowing during senescence. Ethylene has been reported to promote the degradation of chlorophyll during fruit ripening. [11] The mechanism of chlorophyll degradation remains fragmentary. It is generally assumed that chlorophyll is degraded to colourless products thus exposing carotenoids. The initial step in chlorophyll breakdown in plant tissue involves hydrolysis to chlorophyllide and phytol. [11,96]

This hydrolysis is catalyzed by the enzyme chlorophyllase. The degradation of chlorophyll is completed within a relatively short period of time in senescent plant tissue although the intermediates and final products have not been identified *in vivo*.

One of the main reactions in the degradation of chlorophyll is the replacement of the magnesium ion in chlorophyll by hydrogen ions under acidic conditions (Figure 2.6) that results in the formation of pheophytin. The formation of pheophytin is associated with colour change from a bright green to a dull olive green. The rate of

conversion of chlorophyll to pheophytin has been shown to be first order with respect to the acid concentration. [97]

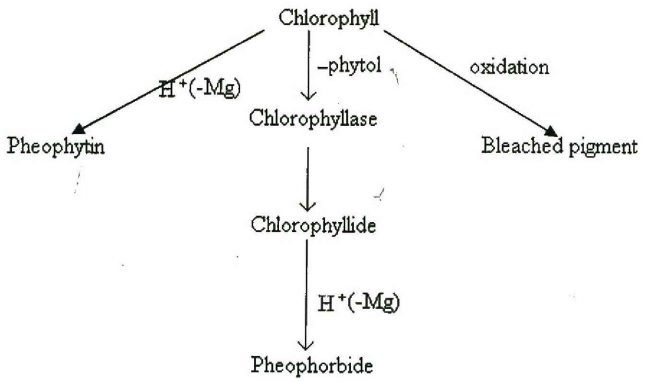


Figure 2.6 Schematic diagram showing chlorophyll degradation products.

(b) Pheophytin

Chlorophylls are relatively unstable molecules in solution and easily convert during handling into derivatives. Both acidic and alkaline solutions affect chlorophyll.[11,97]

Mild acid treatment of chlorophyll produces a derivative of chlorophyll without the magnesium in the centre of the tetrapyrrole ring called pheophytin.[7,12]

Pheophytin are olive green in colour and are more stable.[10,59,97]

Ion exchange column of dowex resins in the H^+ form is able to remove magnesium from chlorophyll and form pheophytin.

Pheophytin-*a*, could be separated from chlorophyll and other derivatives by column chromatography using sugar or silica gel.

When analysed spectroscopically in the Uv-visible region of the spectrum, pheophytin-*a* shows absorptions in the following wavelengths, as reported by Jackson[9] (example 2.1) and Long[19] (example 2.2):

Example 2.1	409 nm, 506 nm, 535 nm, 608 nm, 666 nm
Example 2.2	409 nm, 505 nm, 534 nm, 610 nm, 667 nm

(c) Chlorophyllide

Chlorophyllide is formed from chlorophyll when the enzyme chlorophyllase in aqueous acetone hydrolyses the phytyl ester.

(d) Epichlorophylls

Epichlorophylls (chlorophyll-*a'* and chlorophyll-*b'*) are formed when chlorophyll-*a* and chlorophyll-*b* are warmed or left standing in the presence of trace amounts of a base. These chlorophylls a' and b' can be separated from chlorophyll-*a* and chlorophyll-*b* by chromatography.[14,19]

(e) Pyrochlorophyll

Pyrolysis of chlorophyll at 100°C in pyridine for 24 hrs splits the 10-$COOCH_3$ group forming pyrochlorophyll.

(f) Mesochlorophyll

Mesochlorophyll is produced when chlorophyll is carefully hydrogenated catalytically.

(g) Deuteriochlorophyll

Deuteriochlorophyll is formed when the C10-hydrogen is replaced by water in a base catalysed reaction of chlorophyll. Algae grown in heavy water produces deuterated chlorophyll.[14,19]

(h) Phyllins

These are formed from chlorophyll derivatives containing magnesium by hydrolysis.

(i) Pheophorbides

Pheophorbides are formed when the magnesium is removed and the phytyl ester hydrolysed.

2.8 REACTIONS

2.8.1 SOLUBILITY

Chlorophylls and pheophytins are usually soluble in organic solvents such as ether, acetone, methanol, chloroform and pyridine but relatively insoluble in hydrocarbons when pure. Pheophytins are soluble in warm acetic acid and formic acids.[3,14,19]

2.8.2 ENOLIZATION & TAUTOMERIZATION

The derivatives obtained from chlorophyll are many. The prime derivatives are formed via enolization of the β-ketoester in the isocyclic ring V of chlorophyll. The enolization takes place easily in polar organic solvents such as diethyl ether, tetrahydrofuran, methanol, acetone, pyridine and trimethylamine where the chlorophyll occurs as a solvated monomer. The tautomerization results in an equilibrium mixture containing about 20% of structure 1 and 80% of structure 2, (Figure 2.7) in most polar solvents. [98,99]

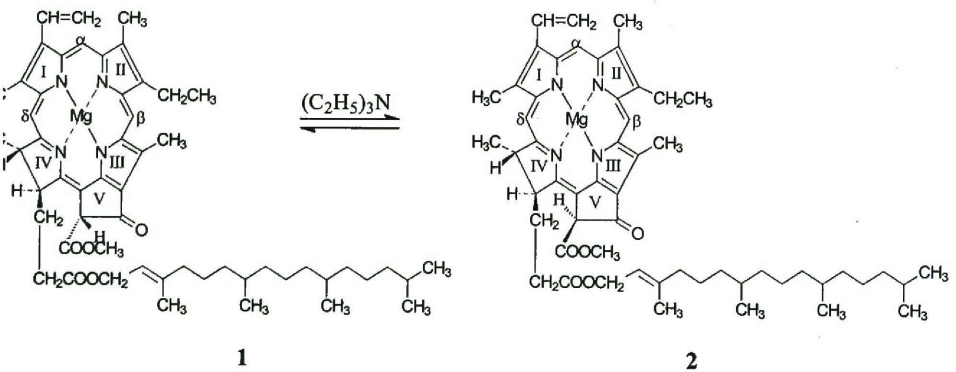


Figure 2.7 Tautomerization of chlorophyll in trimethylamine giving rise to difference in structure in the isocyclic ring V.

The conventional method for the preparation of magnesium free chlorophyll derivatives such as pheophytins and pheophorbides involves treatment of ethereal solution of chlorophyll-*a* or chlorophyll-*b* with aqueous hydrochloric acid.[77,99] This method is not suitable for all purposes because it yields stereochemically impure products. This is due to the configurational instability of C-10 in the substituted phorbins possessing an enolizable β-ketoester structure in their isocyclic ring V. This is because hydrochloric acid catalyses the

enolization in diethyl ether giving a mixture of chlorophyll epimers are obtained. At thermodynamic equilibrium, the mixture consists of about 85% of pheophytin-*a* and 15% of pheophytin-*b*.

Nevertheless, the hydrochloric acid/ether method is quite satisfactory for the preparation of pheophytin-*a* from chlorophyll-*a* provided that dilute hydrochloric acid with a concentration of $\leqq$12.5% is used at a sufficiently low temperature (0°C).[98]

Chlorin e_6 (a derivative of pheophorbide-*a* resulting from the cleavage of the isocyclic ring E) and rhodin g_7 (a derivative of pheophorbide-*b*) as well as their trimethyl esters are important chlorophyll derivatives. These derivatives, which are formed by enolization, have frequently been used in electrochemical, chiroptical and biosynthetic investigations.[19,100]

2.8.3 ALLOMERIZATION

Alcoholic solutions of chlorophyll have been observed to undergo a reaction in which the C-13^2 of chlorophyll is oxidized, a reaction called allomerization. This reaction, which was first observed by Willstäter and Stoll,[66] forms products which are called allomers. These allomers have an oxygen atom instead of a hydrogen atom bonded to carbon at C-13^2, Figure 2.8. The autooxidation of C-13^2 is facilitated by triplet oxygen making it difficult to isolate chlorophyll from natural

sources and in the handling of chlorophyll to yield chlorophyll related chlorin and porphyrin derivates.[66,89,93,101,102]

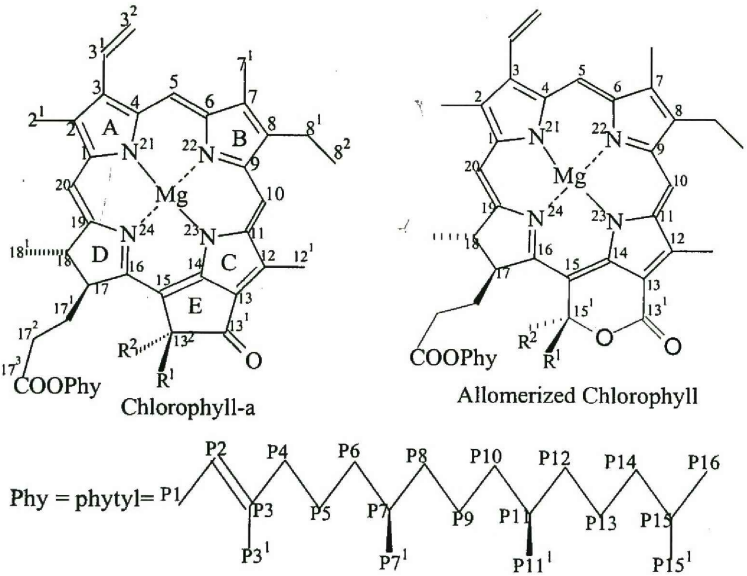


Figure 2.8 Structure of chlorophyll-*a* and allomerized chlorophyll showing allomerization on ring E

2.8.4 PHOTOSENSITIZATION

Chlorophyll-*a* is used in the enzymatic production of hydrogen from oligosaccharide degradation with platinum colloids.[54] The chlorophyll is photosensitized by photoinduction with visible light. Chlorophyll is employed because it acts as a photosensitizer in photosynthesis with absorption maxima around 670 nm. A photosensitizer is an electron donor, electron relay and catalyst. The oxidized photosensitizer is reduced by an electron-donating reagent such as reduced nicotinamide adenine dinucleotide. Hydrogen is produced and this system is usable

as renewable energy source. Photosynthetic pigments have redox characteristics which suggest use of electrochemical methods in their characterization.[54,55]

Electrochemical systems are a common combination of photophysical, photochemical and electrochemical events and electrodes could be directly involved in the exchange of electrons. [55] This reaction involves the interphase of metal electrodes with complex biological systems due to recent improvements in electrochemical devices and biochemical preparation methods together with theoretical models. This has made the electrochemical methods of analysis highly sensitive to redox path of biological systems competitive to supply thermodynamic and kinetic information. Although electrochemical behaviour of chlorophyll-*a* has been studied by cyclic voltammetry in solutions of organic solvents or with water mixtures which show a strong dependence on adsorption potential of the molecule, Cosmas *et al*[55] have shown that chlorophyll-*a* could be used in the electrochemical characterization of proteins. Enzyme electrodes exploiting direct electron transfer between an enzyme and an electrode have also been fabricated for use as biosensors.[27,43,103]

2.8.5 PHOTOSYNTHESIS

Chlorophyll as a pigment is utilized in the photosynthetic conversion of solar light energy into chemical energy in the form of reduced organic compounds such as carbohydrates. It is used in the design of artificial photosynthetic systems for energy conversion. In these

systems, manganese complexes of chlorophyll and tyrosine have been employed as electron carriers covalently linked to a photosensitizer.[91] Inhibition of photosynthetic activity by high irradiation is a known phenomenon.

β-Carotene is a plant pigment that ameliorates photo-inactivation by converting excited energy harmlessly into heat. Cheng-Wei Yang and coworkers[47] have studied the effects of β-carotene feeding on chlorophyll. When chlorophyll is extracted, β-carotene, xanthophylls, zeaxanthin and other plant pigments are also extracted. These pigments are employed to protect the plant by converting excited energy harmlessly into heat thereby preventing the formation of reactive oxygen species.[41,81,94]

The carotenoids interfere most seriously in their contribution to the absorbance of plant extracts near 434 nm where pheophytin-*b* has an absorption peak. To improve analytical methods for chlorophyll estimation in green plants, tetracyanoethylene was used to remove visual carotenoid spectra from solutions of the pigment. The carotenoid reacted completely with the tetracyanoethylene (TCNE)[104] at room temperature with no loss of pheophytin. [4,8,11,49,81,90,104-108]

2.9 SPECTROSCOPIC STUDIES

Stokes[61b] was the first in 1864 to provide a spectrophotometric definition of the photosynthetic pigments that cause light energy to turn into chemical energy in all photosynthetic organisms. The visible

absorption of pigments facilitate qualitative and quantitative analysis of the pigments in various solvents. [109]

The spectral characteristics of chlorophyll-*a'* in aqueous methanol was studied by Boucher, Strain and Katz.[110] In their study, the phase behaviour of chlorophyll-*a'* in aqueous methanol was examined in terms of the composition of the solvent. In this study, visible absorption, circular dichroism (CD), fluorescence and resonance Raman spectroscopy, dynamic light-scattering measurements and electron microscopy were utilised.[111]

2.9.1 INFRARED SPECTROSCOPY

Infrared spectroscopic studies of chlorophyll-*a* have been the focus of many research papers.[57,59,109-116] Infrared spectra of chlorophyll-*a* and other chlorophyll derivatives in non-polar solvents in the 1600 – 1800 and 3000 – 3800 cm^{-1} region were studied. The infrared spectra were used to suggest structures of dimers, oligomers and chlorophyll-water adducts. The infrared spectra of metalloporphyrins in the region 4000 – 160 cm^{-1} of divalent metal complexes of chlorophyll were measured in the solid state and in solution, frequency shifts were linked to metal ligand coordinate bond strength. [115]

The infrared studies of monomeric and aggregated chlorophyll[110] and metalloporphyrins have been studied. [115] The mid and far-infrared spectra of chlorophylls-*a* and -*b*, methyl chlorophyllides-*a* and -*b*, dueteriochlorophyll-*a* and -*b*, pheophytins-*a* and *b*, and pheophobides-

a and -*b* were examined in the solid state and in solution in the region 667 – 160 cm^{-1}. [110]

In the region 4000 – 160 cm^{-1}, infrared spectra of divalent metals (Co, Ni, Cu, Zn, Pd, Cd and Mg) complexes of protoporphyrin(IX) dimethyl ester and hematoporphyrin(IX) dimethyl ester were measured in the solid state and in solution. A strong absorption near 350 cm^{-1} arises from a coupling of the metal-nitrogen stretch with a porphyrin skeletal deformation. [115]

Infrared studies of chlorophylls-*a* and -*b*, bacteriochlorophyll and pyrochlorophyll-*a* in non-polar solvents in the 1600 – 1800 cm^{-1} and 3000 – 3800 cm^{-1} regions have also been examined.
The infrared and nuclear magnetic resonance studies have provided evidence that the coordination number of magnesium in chlorophyll is always larger than 4, and that the coordination properties of magnesium are factors that determine the state of chlorophyll in solution.[112]

2.9.2 RAMAN SPECTROSCOPY

The Raman spectra of chlorophyll-*a* was studied by Diers *et al.*[117] The effect of peripheral substituents on the vibrational characteristics indicate that the Q_y electronic transitions of the chlorophyll aggregates have an out-of-plane character. [31]

The Soret excitation Raman spectra of chlorophyll-*a*, and several derivatives including copper-and-zinc substituted pheophytin were studied. Differences in the Raman spectra of metal substituted pheophytins suggest that chlorophyll-*a*, undergoes significant conformational changes with loss of an electron. Raman and infrared spectra of chlorophyll-*a* and metal-substituted pheophytins in the solid state and in solution have indicated that the frequencies of the metal-sensitive bands in the Raman and infrared spectra of metal-pheophytins have a linear function with metal-nitrogen distance.[31,117-119]

2.9.3 ULTRAVIOLET-VISIBLE SPECTROSCOPY

Spectrophotometric determination of chlorophylls and pheophytins in plant extracts were carried out to determine quantitatively chlorophyll-*a*, chlorophyll-*b*, pheophytin-*a*, pheophytin-*b*, total chlorophyll, total pheophytins and percent retention of chlorophylls in 80% acetone. The chlorophylls and pheophytins used for the determination of the specific absorptivities were extracted from spinach.[10,14,59]

Chromatographic methods were used to separate the chlorophylls on a sugar column, while the pheophytins were prepared from purified chlorophyll by adding one drop of concentrated hydrochloric acid to 20 cm^3 of chlorophyll solution. The chromatographic column was eluted with 0.4% propyl alcohol in petroleum ether.[59,120]

Spectroscopic determination of pheophytins in the 400 – 700nm range was carried out with the use of tetracyanoethylene to remove carotenoids, which interfere with the measurement.[85,104] This study was based on the fact that extracts of plant material containing the chlorophylls and pheophytins always contain carotenoids, which have absorption maxima in the 400 – 500 nm range.[104]

The chlorophylls are chromophores in that they contain many conjugated double bonds (Figure 2.9). Ten conjugated double bonds are contained in the tetrapyrrole ring of chlorophyll-*a*, these double bonds are delocalised giving rise to the resonance structure shown in Figure 2.10. [1,7,18]

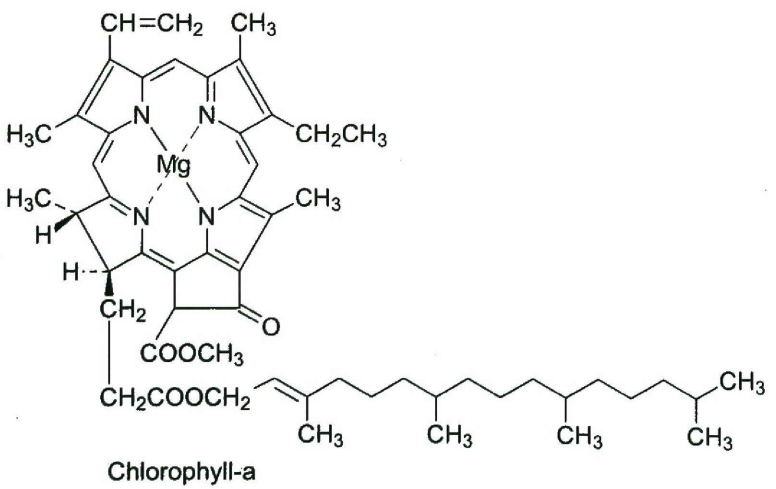


Figure 2.9 Chlorophyll-*a* showing conjugated double bonds.

When the tetrapyrrole absorbs energy, an electron from the conjugated system is elevated to a higher orbital. This is a singlet state orbital electron, since a single electron is present in this orbital. [38]

The energy required for this singlet state excitation in chlorophyll is low because the higher the conjugation, the lower the energy required.

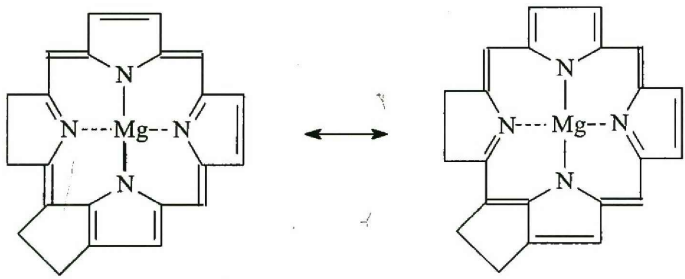


Figure 2.10 Resonance structure of chlorophyll-*a*

This light absorption by the conjugated system of the tetrapyrrole ring is influenced by the phytyl side chain.[18] The spectra of chlorophyll-*a* has two main absorption maxima showing that chlorophyll has two main excitation states which are known as first and second singlets.[59]

The function of the phytyl group may be to anchor chlorophyll in the liquid crystalline lipid matrix of the plant.[3,7,10] The main function of magnesium may be to adjust the redox potentials of the ground and excited state chlorophyll to the proper operating values for photosynthesis. Magnesium may also be involved in the binding of chlorophyll to the membrane.

2.9.4 MASS SPECTROMETRY

Several methods of analysis have been employed in the determination of the mass spectra and fragmentation pattern of chlorophyll.[93,121-130] The method of field desorption was employed by Dougherty *et al* [121]

for the *in vivo* and *in vitro* studies of chlorophyll-chlorophyll and chlorophyll-water interactions to provide a better understanding of the function of chlorophyll in photosynthesis.

Hunt and coworkers[122] used californium-252 plasma desorption mass spectrometry method in the study of chlorophyll-*a* systems. Chlorophyll extracted from spinach and complexed with lanthanum(III) was determined by electrospray ion mass spectrometry.[123] The mass spectra of chlorophyll and lanthanum(III) pheophytin and the fragmentation scheme presented indicate that electrospray ion mass spectrometry is a good method for the analysis of the chemical composition of chlorophyll.

Studies of chlorophyll have shown that the chlorophyll dimer ion peak in plasma desorption mass spectrometry (PDMS) is found at *m/z* 1787. Intense fragmentation is also observed leading to loss of one phytyl and two phytyl groups at *m/z* 1509 and *m/z* 1236.[122,124] Another peak of interest is that of chlorophyllide at *m/z* 614. (893.5 – 278.6). the aforementioned peaks are assigned as follows:

Chla.chla = (893.5 x 2 = 1787)

Chla.chla – phytyl (1787 – 278.6 = 1508)

Chla.chla – 2 phytyl [1787 – 2 x 278.6 = 1230]

Another chlorophyll study with deuterium using plasma desorption mass spectrometry,[124] states that shifts due to deuterium are found at *m/z* 481 for a chlorophyll derivative with formula $C_{30}H_{25}N_4OMg$, and

at *m/z* 414 for another fragment of chlorophyll at $C_{25}H_{18}N_4OMg$. Multi-photon ionisation mass spectrometry (MPI-MS),[125] of chlorophyll gives a molecular peak for chlorophyll at *m/z* 892. At *m/z* 908, there is 10-hydroxychlorophyll-*a*, an oxidation product formed during extraction. The main fragmentation corresponds to the loss of the phytyl chain as indicated by the signal at *m/z* 614. [123,126]

Field desorption mass spectrometry (FD-MS) of chlorophyll yielded the following fragmentations: chlorophyll-*a* at *m/z* 892; pheophytin-*a* at *m/z* 870. [127]

Phe-*a* – water at *m/z* 852.

Phe-*a* + methanol at *m/z* 902

Chla + Mg at *m/z* 916

Chla – Mg + water at *m/z* 886 and a dihydrate chlorophyll (chla + 2 water) at *m/z* 929.

Wang and coworkers,[123] in their study of chlorophyll and Lanthanum(III) pheophytin complex, used electrospray ion mass spectrometry (ESI-MS). The ESI-MS spectra do not show the signal for chlorophyll at a mass-to-charge value of 892 or 893. A small signal at *m/z* 871.3 could be attributed to pheophytin. They have rather indicated dimerized chlorophyll-*a* as chla.H_2O.chla.H_2O with two molecules of water. [123,126] In their fragmentation analysis, they have indicated that the signal at *m/z* 1176 is due to [chla.H_2O.chla.H_2O – 2(COOphytyl) – H^+] = 1823 – 644 – 1 = 1178

Regarding the electrospray mass spectral analysis, Benoit Schoefs [126] commented that the chlorophylls have long presented special analytical challenges to mass spectrometry because of their high molar masses, low volatility, and thermal instability. The chlorophylls (chlorophyll-*a*, chlorophyll-*b* and chlorophyll-*c*) therefore provide only pyrrolitic fragments in electron impact (EI) mass spectra.[126] Similarly for pheophytins, only a weak molecular ion peak is observed in EI MS.

2.10 METAL MACROCYCLES

Metal complexes of macrocyclic rings are common in biological systems with haem, chlorophyll, vitamin B_{12} and coenzymes.[38] Metal porphyrins and chlorophylls with a central metal atom other than magnesium have been synthesized and studied.[10,38,45]

Metals such as copper and zinc have a high binding affinity for the porphyrin ring even higher than that of the native complex for magnesium.[89,131] The binding of these metals to the pheophytin and pheophorbide causes a re-greening of the metallochlorophyll.[89] Zinc porphyrins are widely used as surrogates for chlorophyll in photosynthetic model systems and molecular photonic devices.[25,28]

The energies of the Q_y band is almost independent of the metal while that of the Q_x band depends on the central metal atom as well as the presence of additional axial ligands leads to spectral variations.[130] These metal-substituted systems demonstrate high stability and are

acid resistant. This stability is observed in their extreme reluctance to undergo exchange and replacement reactions in solution.[131]

Metallochlorophylls in which the magnesium atom at the centre of the tetrapyrrole ring has been replaced by other metals have been studied. Silver replacement of magnesium in chlorophyll and bacteriochlorophyll were carried out and studied.[132]
The behaviour of metallochlorophylls are valuable in that they provide information about the contribution of the metal to the various properties and functions of chlorophyll.[57]

The compleation of a chlorophyll/porphyrin molecule in solution is believed to consist of the following steps: (a) deformation of the tetrapyrrole ring, (b) outer-sphere association of the solvated metal ion and tetrapyrrole, (c) exchange of a solvent molecule with the first pyrrolenine nitrogen atom, (d) chelate-ring closure with the expulsion of more solvent molecules, (e) first deprotonation of a pyrrole nitrogen and (f) second deprotonation of the other nitrogen, which will lead to the formation of the metallochlorophyll or metalloporphyrin.[109]

The spectroscopic as well as the chromatographic characteristics of mercury-substituted chlorophyll was found to suggest that both the pheophytin and mercury(II) form a complex in a ratio of 1:1.
Lanthanum(III) complex of chlorophyll-*a* was synthesized and studied in methanol and acetic acid. Ultraviolet-visible and variable temperature MCD spectral analysis were carried out.[123,133]

2.11 KINETIC STUDIES

Kinetic studies of the equilibration of freshly prepared samples of chlorophylls *a*, *a'* and *b* in solvents such as tetrahydrofuran and pyridine, showed that the half-life time for chlorophyll-*a*, to reach equilibrium is about two hours at 30°C.[10]

The rate of pheophytinization of zinc bacteriochlorophyll-*a* and magnesium bacteriochlorophyll-*a* in acidified acetone solution has been studied by Kobayashi *et al.*[58] The rate of pheophytinization was observed to be a pseudo first order reaction. A chlorophyll-*a* type species is more susceptible to pheophytinization than bacteriochlorophyll-*a* type species probably due to the M-H coordination bonds in the chlorin ring being weaker than those in the bacteriochlorophyll ring. However, no work has been reported on the rate of the reaction of metallochlorophylls in any solution.

2.12 MECHANISMS OF INORGANIC OXIDATION-REDUCTION REACTIONS IN OCTAHEDRAL COMPLEXES

Inorganic oxidation-reduction reactions involving the transfer of at least one electron from a reducing agent to an oxidizing agent are widely used in analytical procedures and are important in many biological processes.

The change in oxidation state of the reducing agent and the oxidizing agent in a reaction could also be classified as either complementary or non-complementary. [134-138]

An oxidation-reduction reaction involving chromium and silver (equation [2.3]) or zinc and copper (equation [2.4]) could be represented as follows:

$$Cr^{2+} + Ag^{+} \rightarrow Ag + Cr^{3+} \qquad [2.3]$$

$$Zn + Cu^{2+} \rightarrow Cu + Zn^{2+} \qquad [2.4]$$

There are examples of a complementary stoichiometric oxidation-reduction reaction.

When the oxidizing agent and reducing agent undergo different net changes in oxidation state, a non-complementary stoichiometric reaction has taken place. (e.g Equations [2.5] and [2.6]):

$$2Cr^{2+} + T\ell^{3+} \rightarrow 2Cr^{3+} + T\ell^{+} \qquad [2.5]$$

$$Zn + 2Fe^{3+} \rightarrow Zn^{2+} + 2Fe^{2+} \qquad [2.6]$$

Complementary reactions have been observed to be faster than non-complementary reactions. This is not a universal observation but the mechanistic rationale for this observation is based on the fact that reactions take place in bimolecular steps.

2.13 INNER SPHERE AND OUTER-SPHERE MECHANISM

The determination of the type of mechanism involved in a reaction requires the application of kinetics. The kinetic features of a reaction could be employed in determining if a reaction proceeds by an "inner-sphere electron transfer" or an "outer-sphere electron transfer" process. [138]

2.13.1 INNER SPHERE

Inner-sphere electron transfer requires that the oxidant and reductant be firmly bonded during the act of electron transfer and that a bridge is formed by at least one ligand that is common to the coordination sphere of the oxidant and reductant through which the electron is transmitted.

$$L_5M^{III}X + M^{II}Y_6 \rightarrow \{L_5M^{III}—X—M^{II}Y_5\} \rightarrow \text{Products} \qquad [2.7]$$

In equation [2.7], —X— is a bridging ligand formed in the transition state by one of the metals in order to form the intermediate or transition state. Electron transfer could therefore occur through the bridging ligand.

Taube and co-workers[138] first demonstrated this mechanism in a system that exploited substitution lability and inertness. [30,122] Table 2.1 shows the spin state and lability/inertness of both cobalt and chromium ions.

Table 2.1 Spin states of cobalt and chromium

Complex	Spin state	Labile/Inert
Cobalt(II)	High spin d^7	Labile
Chromium (II)	High spin d^4	Labile
Cobalt(III)	Low spin d^6	Inert
Chromium(III)	Low spin d^3	Inert

The above combination allowed the reaction products to establish definitely an inner-sphere mechanism for the reaction of chromium and cobalt complexes shown in Figure 2.11.

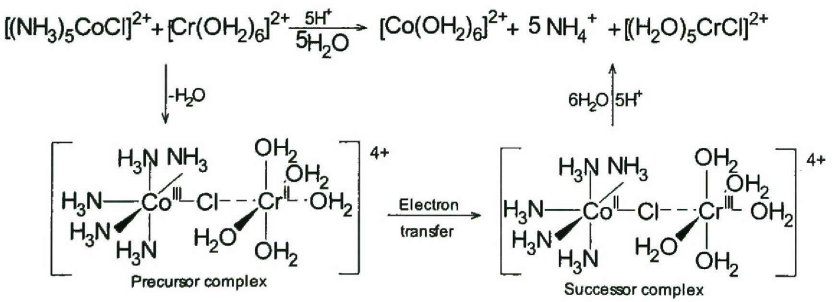


Figure 2.11 Electron-transfer process in a cobalt complex

The above scheme was crucial in establishing that an inner-sphere electron transfer occurred.

A wide range of bridging ligands are known. These include halide, pseudohalide, hydroxide and carboxylate ions. Ammonia cannot act as a bridging ligand because it does not have a second unshared pair of

electron, which is necessary for simulating bonding to the oxidizing and reducing centres.

2.13.2 OUTER-SPHERE

In an outer-sphere electron transfer, the interaction between the oxidant and the reductant at the time of electron transfer is small and it occurs through the process with the coordination sphere of the oxidant and reductant remaining intact during the electron transfer.

$$M^{III}L_6 + M^{II}Y_6 \rightarrow (L_5M^{III}L)(YM^{II}Y_5) \rightarrow M^{II}L_6 + M^{III}Y_6 \qquad [2.8]$$

In this situation, equation [2.8], an electron tunnelling mechanism takes place. A mechanistic decision between the inner- and outer-sphere possibilities is often based on whether or not the reaction rate corresponds reasonably to the predictions of the outer-sphere theory.

2.13.3 FRANCK-CONDON RESTRICTION

Electron transfer processes must satisfy the Frank-Condon restrictions, which arise in principle from the fact that the act of electron transfer takes place within a time of about 10^{-15}s. This means that the atomic nuclei remain frozen in position during the act of electron transfer. Consider the reactions below:

$$\underset{t_{2g}^6 e_g^1}{[Co(phen)_3]^{2+}} + \underset{t_{2g}^6}{[Co(phen)_3]^{3+}} \rightleftharpoons \underset{t_{2g}^6}{[Co(phen)_3]^{3+}} + \underset{t_{2g}^6 e_g^1}{[Co(phen)_3]^{2+}} \qquad [2.9]$$

$$\underset{t_{2g}^5 e_g^2}{Co(NH_3)_n^{2+}} + \underset{t_{2g}^6}{Co(NH_3)_6^{3+}} \rightleftharpoons \underset{t_{2g}^6}{Co(NH_3)_n^{3+}} + \underset{t_{2g}^5 e_g^2}{Co(NH_3)_6^{2+}} \qquad [2.10]$$

In the first example, equation [2.9], an electron is transferred from the e_g orbital of cobalt(III) to that of cobalt(III) while in the second example equation [2.10], there is electron transfer as well as change of spin state. [134-138]

It is convenient to start with cobalt(II) because cobalt(II) complexes undergo substitution reactions very rapidly as they are kinetically labile, whereas reactions of cobalt(III) complexes are very slow since these are kinetically inert.

Many oxidizing agents are able to oxidize cobalt(II) to cobalt(III) in the presence of suitable ligands but only a few are convenient to use.

- ⇒ Oxidizing agents such as potassium manganate(VII), ($KMnO_4$) potassium chromate (VI), ($K_2Cr_2O_7$) introduce to the reaction ions that are not easily separated.
- ⇒ Oxygen and hydrogen peroxide (H_2O_2) do not introduce foreign metal ions to the reaction mixture.
- ⇒ Another type of suitable oxidizing agent is one whose reduction product is insoluble and can be removed by filtration, e.g. PbO_2 → Pb^{2+} removed as insoluble $PbC\ell_2$.

CHAPTER THREE

EXPERIMENTAL

3.1 REAGENTS

3.1.1 ACETONE

Acetone used in all experiments was obtained from UnivAR Saarchem Merck Chemical (Pty) Ltd and was redistilled before use. Acetone solutions (80%) were prepared from the redistilled acetone.

3.1.2 PETROLEUM ETHER (60 – 80)°C

Petroleum ether used in all experiments was obtained from UnivAR Saarchem Merck Chemical (Pty) Ltd and twice redistilled before use.

3.1.3 n-PROPANOL

The Propanol used in all extraction was obtained from UnivAR Saarchem Merck chemical (Pty) Ltd and used without further purification.

3.1.4 DIETHYL ETHER

Diethyl ether was obtained from UnivAR Saarchem Merck Chemical (Pty) Ltd and twice distilled before use.

3.1.5 SILICA GEL

The silica gel used for chromatographic separation of extracted pigments was 60M (0.04 – 0.063mm, 230 – 400 mesh Astm) and obtained from Merck Chemicals.

3.1.6 OTHER CHEMICALS

All the remaining chemicals were obtained from Fluka Chemie AG, Unilab and UnivAR Saarchem Merck Chemical (Pty) Ltd and used without further purification.

3.2 EXTRACTION OF CHLOROPHYLL

3.2.1 ALUMINA COLUMN METHOD (METHOD 1)

Spinach leaves (20g) were crushed using a mortar and pestle. A pinch of washed sand (acid washed) was added to aid the crushing of the leaves. When the leaves were finely crushed, 80% aqueous acetone (20ml) was added and the leaves crushed further until a fine paste was obtained. To the fine paste or slurry obtained, another portion of acetone (20ml) was added and the slurry filtered.

Three portions of acetone (20ml) were used to wash the mortar and pestle into the funnel. The filtrate was treated with sodium sulphate crystals (1g) to remove water and after filtering off the sodium sulphate; it was transferred to a separating funnel. Petroleum ether (60-80°C) (50ml) was then added to the mixture and shaken lightly. The acetone layer (lower layer) was separated and discarded.

The petroleum ether layer of the whole chlorophyll extract was then shaken with aqueous methanol (60-40 v/v) (2x30ml) and the lower aqueous layer discarded.

A (10 ml) portion of the chlorophyll extract in the petroleum ether layer was then purified by passing it through a chromatography column packed with finely divided alumina as stationary phase. Toluene was used as the initial mobile phase to elute the column. A yellow carotene layer was eluted. After eluting the yellow carotene layer, a second mobile phase, a mixture of n-butanol, ethanol and water in the ratio (3:1:1) was then used to elute the column. The chlorophyll-*a* band was collected. Acidification of the eluent with a few drops of dilute hydrochloric acid to yielded pheophytin.
This method is summarized in the flow chart in Figure 3.1.

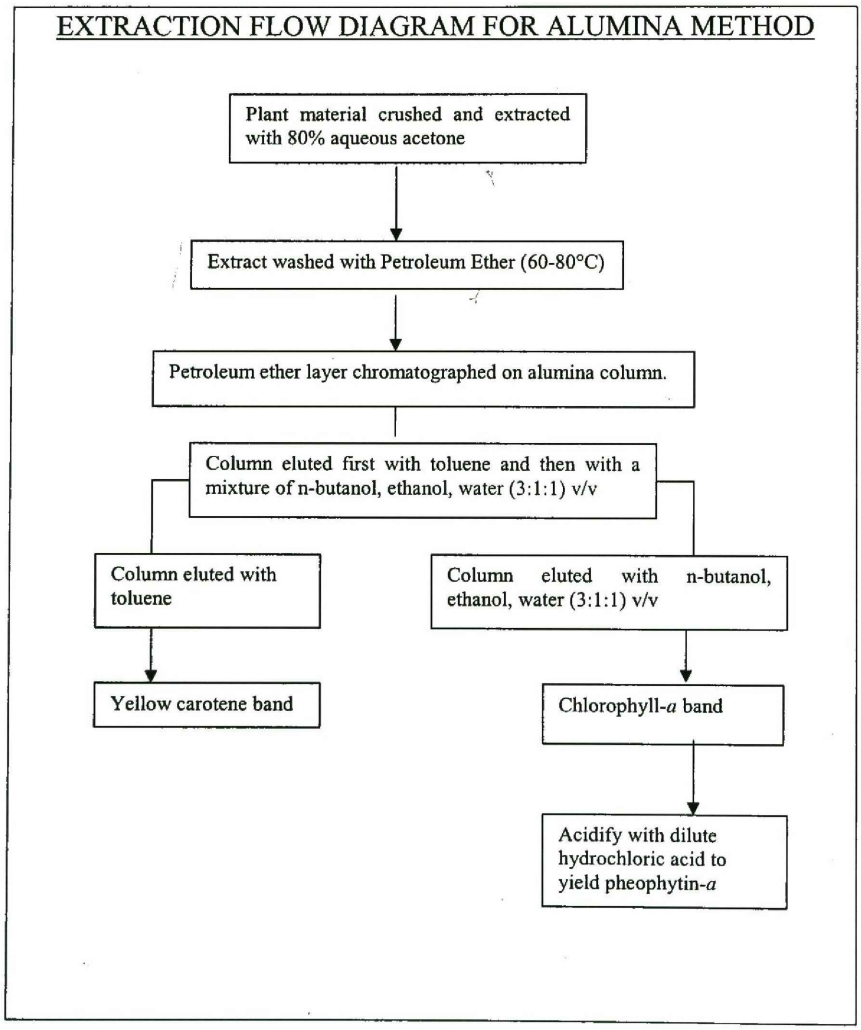


Figure 3.1 Extraction of chlorophyll using the alumina method

3.2.2 SILICA GEL COLUMN METHOD (METHOD 2)

Spinach leaves (20 g) were crushed using a mortar and pestle. A pinch of washed sand (acid washed) was added to aid the crushing of the leaves. When the leaves were finely crushed, 80% aqueous acetone (20ml) was added and the leaves crushed further until a fine paste was obtained. To the fine paste or slurry obtained, another portion of acetone (20ml) was added and the slurry filtered.

Three portions of acetone (20 ml) were used to wash the mortar and pestle into the funnel. The filtrate was treated with sodium sulphate crystals (1 g) to remove water and after filtering off the sodium sulphate; it was transferred to a separating funnel. Petroleum ether (60-80°C) (50 ml) was then added to the mixture and shaken lightly. The acetone layer (lower layer) was separated and discarded. The petroleum ether layer of the whole chlorophyll extract was then shaken with aqueous methanol (60-40 v/v) (2x30 ml) and the lower aqueous layer discarded.

A (10 ml) portion of the chlorophyll extract in the petroleum ether layer was then purified by passing it through a chromatography column packed with finely divided silica gel as stationary phase. Toluene was used as the initial mobile phase to elute the column. The yellow carotene layer was eluted.

After eluting the yellow carotene layer, a second mobile phase, a mixture of n-butanol, ethanol and water in the ratio (3:1:1) was then used to elute the column. The chlorophyll-*a* band was collected.

Acidification of the eluent with a few drops of glacial acetic acid yielded pheophytin.

The silica gel column method is summarized in a flow diagram in Figure 3.2.

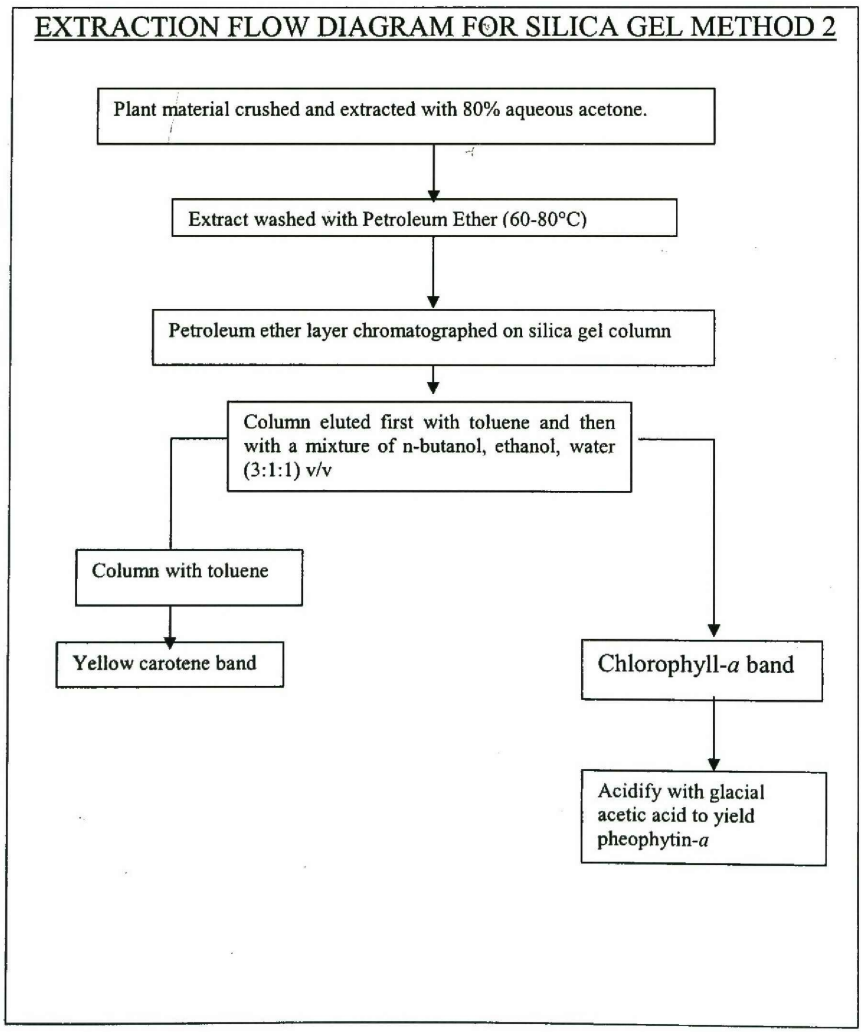


Figure 3.2 Extraction of chlorophyll using the silica gel method 2

3.2.3 IMPROVED SILICA GEL COLUMN METHOD (METHOD 3)

Spinach leaves (20 g) were again crushed in a mortar and pestle as done previously. A pinch of washed sand (acid washed) was added to aid with the crushing of the leaves. When the leaves were finely crushed, 80% aqueous acetone (20 ml) was added and the leaves crushed further until a fine paste was obtained. To the fine paste or slurry obtained, another portion of acetone (20 ml) was added and the slurry filtered.

Three portions of 80% aqueous acetone (20 ml) were used to wash the mortar and pestle into the funnel. The filtrate was treated with sodium sulphate crystals (1 g) to remove water and after filtering off the sodium sulphate; it was transferred to a separating funnel. Petroleum ether (60-80°C) (50 ml) was then added to the mixture and shaken lightly. The acetone layer (lower layer) was separated. The acetone layer was combined and concentrated using a rotary evaporator and washed again with petroleum ether and the lower acetone layer analyzed for chlorophyll content and discarded.

The petroleum ether layer of the whole chlorophyll extract was then shaken with aqueous methanol (60-40 v/v) (2x30 ml). The lower aqueous layer was washed with petroleum ether to recover any chlorophyll then analysed and discarded.

All the petroleum ether extracts were then collected concentrated in a rotary evaporator then separated by column chromatography on a

silica gel stationary phase. Petroleum ether and n-propanol (0.4 %) were used as the mobile phases to separate chlorophyll-*a* from other plant components.

Acidification of the chlorophyll-*a* band with a few drops of glacial acetic acid yielded pheophytin-*a*.

The improved silica gel method is summarized in the flow diagram in Figure 3.3.

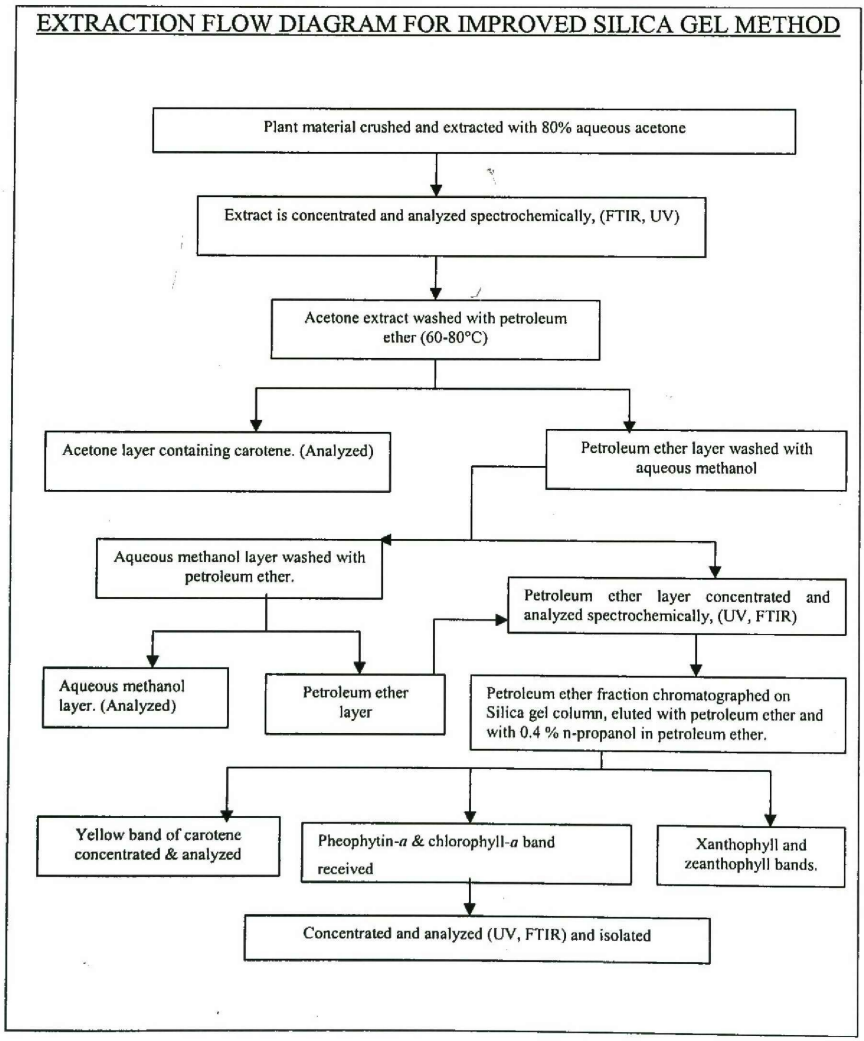


Figure 3.3 Extraction of chlorophyll using improved silica gel (method 3)

3.2.4 WINTER EXTRACTION METHOD (METHOD 4)

The difficulty experienced by previous workers[139] in extracting chlorophyll from spinach leaves in winter led to our exploration of a new method for the extraction of chlorophyll from spinach during the winter months using diethyl ether.

Spinach leaves (20 g) were crushed and extracted with 80% aqueous acetone as previously described. Several washings of the extracts were then combined and concentrated using a rotary evaporator. The concentrated extract was then washed with light petroleum ether (60-80°C) and separated with a separating funnel. This procedure was repeated three times. The petroleum ether layer (yellowish in colour) was then analysed in the ultraviolet and visible region of the spectrum before being discarded.

The acetone layer was also analyzed by UV-visible spectroscopy. It was then washed with 40ml of diethyl ether several times. The diethyl ether extracts were combined and concentrated, and then separated on a silica gel chromatography column (203 – 400 mm).

The column was first eluted with diethyl ether, which removed the yellow carotenoids and then again eluted with a mixture of diethyl ether and n-propanol (0.4%) to obtain chlorophyll-*a*.
The winter extraction method is summarized in the flow diagram in Figure 3.4.

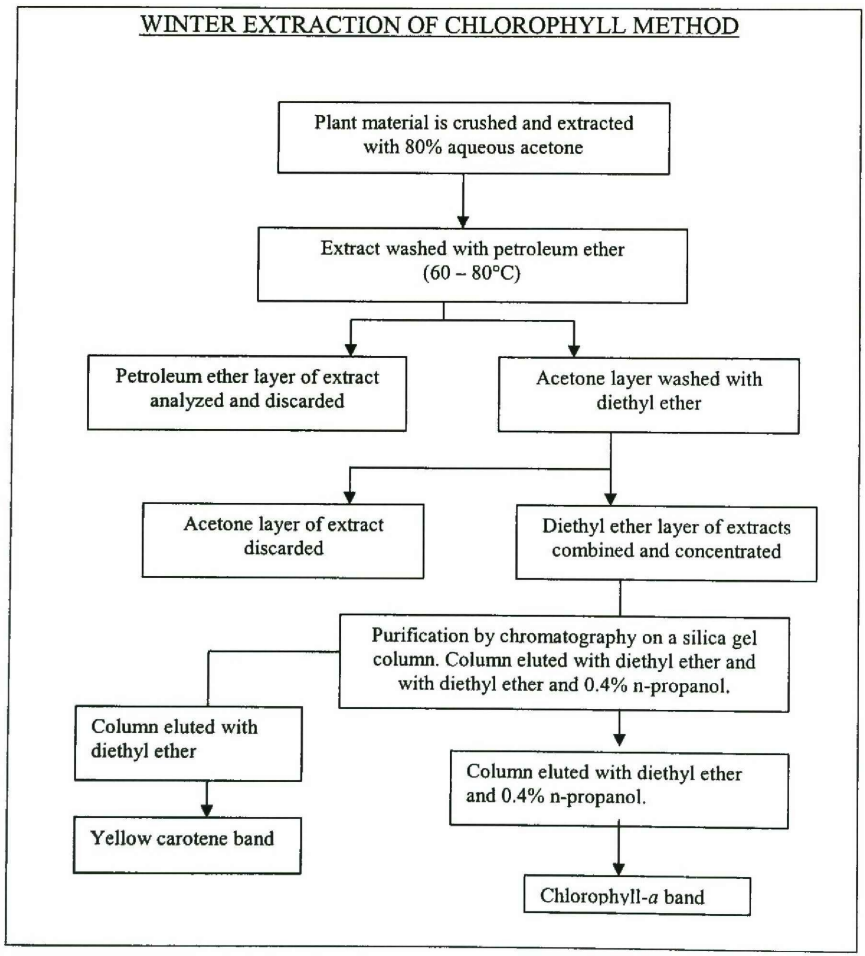


Figure 3.4 Extraction of chlorophyll using winter extraction method

3.3 PRECAUTIONS TAKEN DURING EXTRACTION

Spinach leaves used throughout this research were fresh young leaves, which had not undergone any visible degradation and were without blemish.

The midribs and major veins of the young leaves were removed before the leaves were crushed in a mortar with pestle. Crushing and extraction of chlorophyll was done in dimlight or in the dark to avoid photo-oxidation of the chlorophyll.

Ultraviolet-visible and infrared spectroscopic analyses of the extracts in solution were carried out at the end of each stage of the extraction.

3.4 CHARACTERIZATION OF CHLOROPHYLL

3.4.1 ULTRAVIOLET-VISIBLE ABSORPTION SPECTRA

The UV-visible absorption spectra of freshly prepared solutions of the chlorophyll extracts were measured in a 1-cm quartz cell using a Unicam SP 8700 spectrophotometer and a Varian Cary 50 ultraviolet-visible spectrophotometer. Measurements were made from 300 to 800 nm.

Tables 4.1(a), 4.12(a) and 4.18(a) summarizes the positions of λ_{max} & ϵ_{max} in appropriate solvents while the spectra are displayed in Figures 4.1 - 4.17.

3.4.2 DETERMINATION OF CHLOROPHYLL AND PHEOPHYTIN CONTENT

The determination of the total chlorophyll and pheophytin content is frequently required in plant analysis. Fresh spinach leaf tissues were extracted and measured immediately.

Measurements of chlorophyll-*a* and pheophytin-*a* were made by direct determination of the absorbance in the range 300 – 800 nm.
The concentrations of total chlorophyll, chlorophyll-*a*, chlorophyll-*b* as well as pheophytin-*a* were calculated using equations [3.1 - 3.6] as outlined on pages 24 and 25.

$$\text{Total chlorophyll (mg/L)} = 20.2\ A_{645} + 8.02\ A_{663} \quad [3.1]$$

$$\text{Chlorophyll-}a\text{ (mg/L)} = 12.7\ A_{663} - 2.69\ A_{645} \quad [3.2]$$

$$\text{Chlorophyll-}b\text{ (mg/L)} = 22.9\ A_{645} - 4.68\ A_{663} \quad [3.3]$$

$$\text{Total pheophytin (mg/L)} = 6.75\ A_{666} + 26.03\ A_{655} \quad [3.4]$$

$$\text{Pheophytin-}a\text{ (mg/L)} = 20.15\ A_{666} - 5.87\ A_{655} \quad [3.5]$$

$$\text{Pheophytin-}b\text{ (mg/L)} = 31.90\ A_{655} - 13.40\ A_{666} \quad [3.6]$$

The spectrophotometric determination of chlorophyll-*a* and -*b* and pheophytin-*a* and -*b* in a mixture assumes that neither pigment influences the specific absorption of the other. The concentration of chlorophyll-*a* obtained in various methods is summarized in Table 4.17.

3.4.3 INFRARED SPECTRA

Infrared spectra of nujol mull of complexes between potassium bromide cells were measured with a Nicolet Impact 410 Fourier transform infrared spectrophotometer from 4000 - 500 cm^{-1}. The relevant absorption peaks are collected in Table 5.5 while the spectra are displayed in Figure 4.26 - 4.29.

3.4.4 MASS SPECTROMETRY

Mass spectral analysis was carried out on a Finnigan LCQ deca electron ion mass spectrometer at the analytical chemistry laboratory of the University of Botswana. The spectra are displayed in Figure 4.36 - 4.39 while the *m/z* ratios of relevant absorption peaks are given in Tables 5.2 and 5.3.

3.5 REMOVAL OF MAGNESIUM

Magnesium is easily removed from chlorophyll to obtain pheophytin. In this thesis the removal of magnesium from chlorophyll is referred to as demetallation.

In this process, a chlorophyll solution in petroleum ether or diethyl ether (20 ml) obtained from the chromatographic column was demetallated by the addition of 5 cm^3 of acetic acid. A change in colour from green to olive green was observed. The removal of magnesium from chlorophyll is represented by equation [3.7].

$$C_{55}H_{72}N_4O_5Mg + 2H^+ \rightarrow C_{55}H_{74}N_4O_5 + Mg^{2+} \quad [3.7]$$

Figure 3.5 is a structural representation of the demetallation.

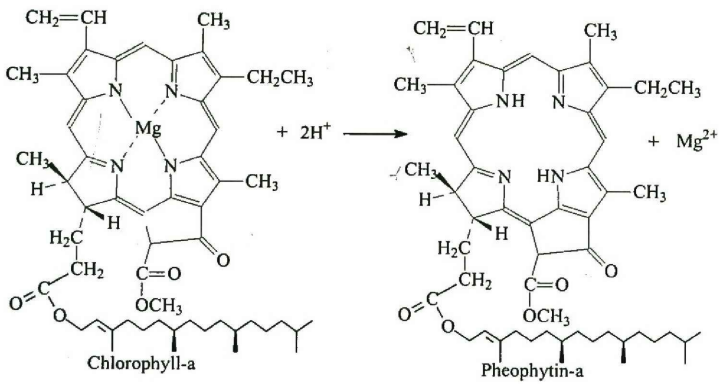


Figure 3.5 Demetallation of chlorophyll-*a* to give pheophytin-*a*.

3.6 INSERTION OF METAL ION INTO PHEOPHYTIN

3.6.1 COBALT INSERTION

Cobalt(II) acetate (8.85 g) was dissolved in 500 ml of glacial acetic acid to make a 0.1 mol/dm^3 solution of cobalt(II) acetate. This solution was then heated on a hot plate and reacted with 20 cm^3 of a 0.15 mol/dm^3 solution of the pheophytin solution in glacial acetic acid. The mixture was then heated mildly for 5 minutes then allowed to cool.

When cold, the cobalt(II) pheophytin-*a* complex formed was passed through a cation exchange column packed with amberlite IR-120 cation ion exchanger. The column was packed in a 50 cm^3 burette with internal diameter of 1.075 cm and eluted with 50 cm^3 of glacial acetic acid. The solution of the cobalt(II) pheophytin-*a* complex was then

concentrated and crystallized from glacial acetic acid. The crystals were then washed with water to remove unreacted metal acetate before recrystallization from diethyl ether. Crystals of cobalt(II) pheophytin-*a* complex were then analyzed by elemental analysis, electrospray ion mass spectrometry and ultraviolet-visible and infrared spectroscopies. A yield of 81.6% was obtained.

3.6.2 COPPER INSERTION

Copper(II) acetate (9.1 g) was dissolved in 500 ml of glacial acetic acid to make a 0.1 mol/dm^3 solution of copper(II) acetate. This solution (15 cm^3) was then heated on a hot plate and reacted with 20 cm^3 of a 0.15 mol/dm^3 solution of the pheophytin solution in glacial acetic acid. The mixture was then heated mildly for 5 minutes then allowed to cool.

When cold, the copper(II) pheophytin-*a* complex was passed through a cation exchange column packed with amberlite IR-120 cation ion exchanger. The column was packed in a 50 cm^3 burette with internal diameter of 1.075 cm and eluted with 50 cm^3 of glacial acetic acid. The solution of the copper(II) pheophytin-*a* complex was then concentrated and crystallized. The crystals were washed with water to remove unreacted copper(II) acetate before recrystallization from diethyl ether. Crystals of copper(II) pheophytin-*a* complex were then analysed by elemental analysis and ultraviolet-visible and infrared spectroscopies. A yield of 77.4% was obtained

3.6.3 ZINC INSERTION

Zinc acetate (9.15 g) was dissolved in 500 ml of glacial acetic acid to make a 0.1 mol/dm^3 solution of zinc acetate. This solution (15 cm^3) was then heated on a hot plate and reacted with 20 cm^3 of a 0.15 mol/dm^3 solution of the pheophytin solution in glacial acetic acid. The mixture was then heated mildly for 5 minutes then allowed to cool.

When cold, the zinc pheophytin-*a* complex was passed through a cation exchange column packed with amberlite IR-120 cation ion exchanger. The column was packed in a 50 cm^3 burette with internal diameter of 1.075 cm and eluted with 50 cm^3 of glacial acetic acid. The solution of the zinc pheophytin-*a* complex was then concentrated and crystallized. The crystals were washed with water to remove unreacted zinc acetate before recrystallization from diethyl ether. Crystals of zinc pheophytin-*a* complex crystals obtained were then analyzed by elemental analysis and UV-visible and infrared spectroscopies. A yield of 65.3% was obtained.

3.6.4 NICKEL INSERTION

Nickel(II) acetate (8.85 g) was dissolved in 500ml of glacial acetic acid to make a 0.1 mol/dm^3 solution of nickel(II) acetate. This solution (15 cm^3) was then heated on a hot plate and reacted with 20 cm^3 of a 0.15 mol/dm^3 solution of the pheophytin solution in glacial acetic acid. The mixture was then heated mildly for 5 minutes then allowed to cool.

When cold, the nickel(II) pheophytin-*a* complex was passed through a cation exchange column packed with amberlite IR-120 cation ion exchanger. The column was packed in a 50 cm^3 burette with internal diameter of 1.075 cm and eluted with 50 cm^3 of glacial acetic acid. The solution of the nickel(II) pheophytin-*a* complex was then concentrated and crystallized. The crystals were washed with water to remove unreacted nickel(II) acetate before recrystallization from diethyl ether. Crystals of nickel(II) pheophytin-*a* complex crystals obtained were then analysed by elemental analysis and UV-visible and infrared spectroscopies. A yield of 75.3% was obtained.

3.6.5 CHROMIUM INSERTION

Chromium(III) chloride (8.35 g) was dissolved in 250ml of dimethylformamide to make a 0.1 mol/dm^3 solution of chromium(III) chloride. This solution (15 cm^3) was then heated on a hot plate and reacted with 20 cm^3 of a 0.15 mol/dm^3 solution of the pheophytin solution in glacial acetic acid. The mixture was then heated mildly for 5 minutes then allowed to cool.

When cold, the chromium(III) pheophytin-*a* complex formed was passed through a cation exchange column packed with amberlite IR-120 cation ion exchanger. The column was packed in a 50 cm^3 burette with internal diameter of 1.075 cm and eluted with 50 cm^3 of glacial acetic acid. The solution of the chromium(III) pheophytin-*a* complex was then concentrated and crystallized. The crystals were washed with

water to remove unreacted chromium(III) chloride before recrystallization from diethyl ether. Crystals of chromium(III) pheophytin-*a* complex were then analyzed by elemental analysis and UV-visible and infrared spectroscopies. A yield of 71.8% was obtained.

3.7 CHARACTERIZATION OF METAL PHEOPHYTIN COMPLEXES

3.7.1 ULTRAVIOLET-VISIBLE SPECTROSCOPY

The electronic absorption spectra of freshly prepared solutions of the metal pheophytin complexes were measured in a 1 cm quartz cell using a Unicam SP 8700 spectrophotometer. The spectra are displayed in Figures 4.18 - 4.23.

3.7.2 INFRARED SPECTROSCOPY

Infrared spectra of metal pheophytin complexes were measured with a Nicolet 410 Impact Fourier transform infrared spectrophotometer. The infrared spectra are displayed in Figures 4.29 - 4.31.

3.7.3 MASS SPECTROMETRY

The mass spectrum of the cobalt(II) pheophytin-*a* complex was measured with a Finnigan Electrospray ionization mass spectrometer. Mass spectra of the cobalt(II) pheophytin-*a* complex are displayed in Figure 4.36 to 4.37.

3.7.4 ELEMENTAL ANALYSES

The elemental analyses of the metal pheophytin complexes were performed at the Instrumental Analysis Laboratory of the University of Cape Town. The microanalytical results are displayed in Figures 4.38 - 4.42 and summarized in Table 4.25.

3.8 PROCEDURE FOR KINETIC STUDY OF THE REDOX REACTION OF COBALT(II) PHEOPHYTIN-a COMPLEX

A spectrophotometric procedure was employed to study the reaction of the cobalt(II) pheophytin-*a* complex with the hexaaquachromium(III) cation. In this method, a solution of cobalt(II) pheophytin-*a* in 0.1 M hydrochloric acid was made and allowed to equilibrate at room temperature. A solution of chromium(III) chloride, 0.01 M in 0.1 M hydrochloric acid was also made and allowed to equilibrate at the same temperature. The two solutions were then mixed and quickly transferred to a 1 cm quartz cell in a thermostated compartment of the UV-visible spectrophotometer.

The UV-visible absorption spectrum 300 nm – 800 nm was then scanned at specific time intervals. Maintenance of isosbestic point throughout the entire reaction was an indication of a simple reaction involving two species in equilibrium. Addition of zinc dust shifted the equilibrium back to the starting material indicating that the change in spectrum was due to the reduction reaction. Following this preliminary study, the wavelength corresponding to a maximum

absorbance change between the substance and the product was chosen and fixed. The change in absorbance at this fixed wavelength was then recorded as a function of time.

3.9 COMPUTATION OF RATE CONSTANTS AND ACTIVATION PARAMETERS.

In the present work, all the reactions studied were over 96% complete and the observed rate constants were obtained from plots of $\ln[(A_t-A_\infty)/(A_0-A_\infty)]$ against time,

where

A_t is the absorbance at time t,

A_0 is the absorbance at time 0 and

A_∞ is the absorbance at time infinity.

The Arrhenius parameters were obtained from the Arrhenius equation, equation [3.8].[134-136]

$$k = Ae^{-\frac{E_a}{RT}} \qquad [3.8]$$

where:

k is the rate constant

A is the pre-exponential factor.

E_a is the activation energy

R is the ideal gas constant

T is absolute temperature

The above equation could be transformed to a more convenient form by taking the logarithm of both sides to yield equation [3.9] below.

$$\ln k = \ln A - \frac{E_a}{RT} \qquad [3.9]$$

This equation implies that the logarithm of the rate constant is a linear function of the reciprocal of the absolute temperature.

A plot of 1/T against ln*k* from equation [3.9], should give the activation energy (E_a) of the reaction from the equation.

E_a = -R x gradient [3.10]

The pre-exponential factor, A, could then be determined from the activation energy E_a from the equation: [134-136]

$$\ln A = \ln k + \frac{E_a}{RT} \qquad [3.11]$$

3.10 COMPUTATION OF THE AMOUNT OF CHLOROPHYLL-*a* AND PHEOPHYTIN-*a*.

Estimation of the concentration of chlorophyll-*a* and pheophytin-*a* in extracts were calculated from the absorbances at pre-determined wavelengths which depend on the solvent (see pages 24 and 25) used in the extraction.[1,3,19,59] In the spectra where these absorption peaks are not recorded by the spectrophotometer, the absorbance at such wavelengths were set and read from the instrument. Such absorption bands are not included in the tables provided.

CHAPTER FOUR

RESULTS

4.1 EXTRACTION OF CHLOROPHYLL

4.1.1 ALUMINA METHOD (METHOD 1)

The chlorophyll-*a*, carotene and pheophytin-*a* fractions obtained from this chromatographic separation were analyzed spectrophotometrically in the ultraviolet-visible region of the spectrum. The spectra are displayed in Figures 4.1, 4.2 and 4.3, respectively.

A summary of the wavelengths of maximum absorption and the absorbances at these wavelengths for chlorophyll-*a*, carotene and pheophytin-*a* is given in Tables 4.1(a), 4.2 and 4.3(a).

The concentrations of total chlorophyll, chlorophyll-*a*, chlorophyll-*b*, total pheophytin and pheophytin-*a* in mg/L obtained are in Tables 4.1(b) and 4.3(b).

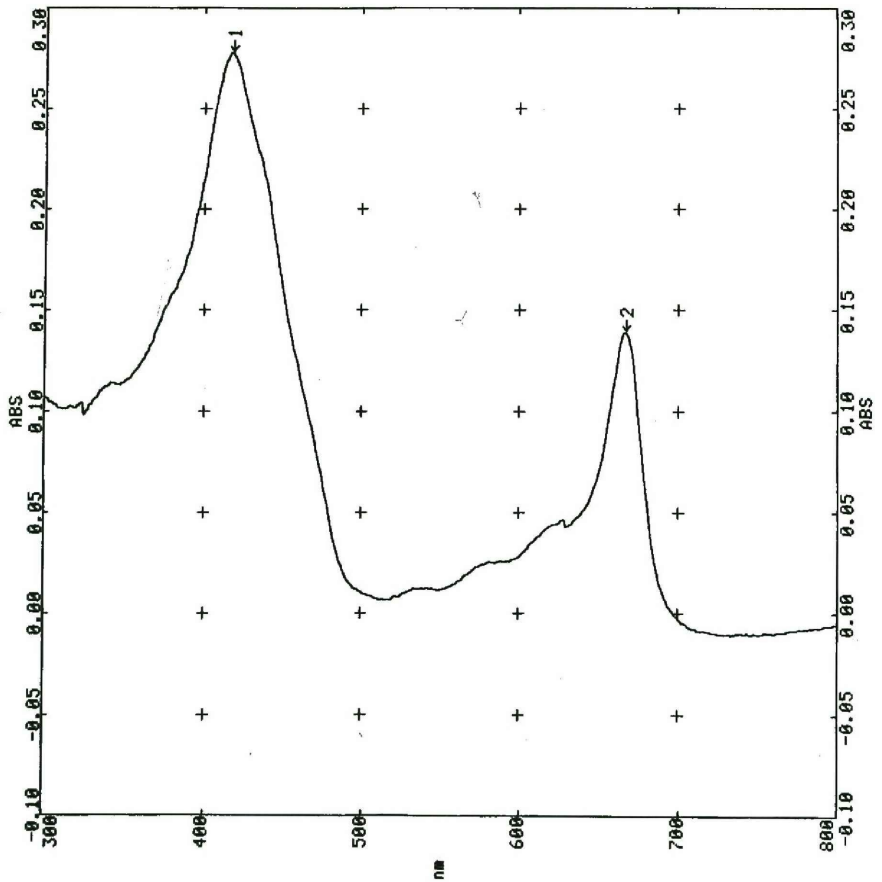


Figure 4.1. Electronic spectrum of chlorophyll extract in petroleum ether on alumina stationary phase.

Table 4.1(a) Absorption bands obtained from alumina

Peaks	Wavelength (nm)	Absorbance	Molar extinction coefficient (ϵ) (cm^{-1} mol^{-1} dm^3)
1	417	0.278	9270
2	645	0.05	
3	663	0.125	
4	667	0.139	4630

Table 4.1(b) Concentration of chlorophyll from alumina stationary phase

Total chlorophyll (mg/L)	20.2 x 0.05 + 8.02 x 0.125	= 2.013
Chlorophyll-*a* (mg/L)	12.7 x 0.125 – 2.69 x 0.05	= 1.453
Chlorophyll-*b* (mg/L)	22.9 x 0.05 – 4.68 x 0.125	= 0.560

In 80% acetone,[19,59]

total chlorophyll (mg/L) = $20.2D_{645} + 8.02D_{663}$

chlorophyll-a (mg/L) = $12.7D_{663} - 2.69D_{645}$

chlorophyll-b (mg/L) = $22.9D_{645} - 4.68D_{663}$

where D_{645} and D_{663} are the absorbances at the specified wavelengths.

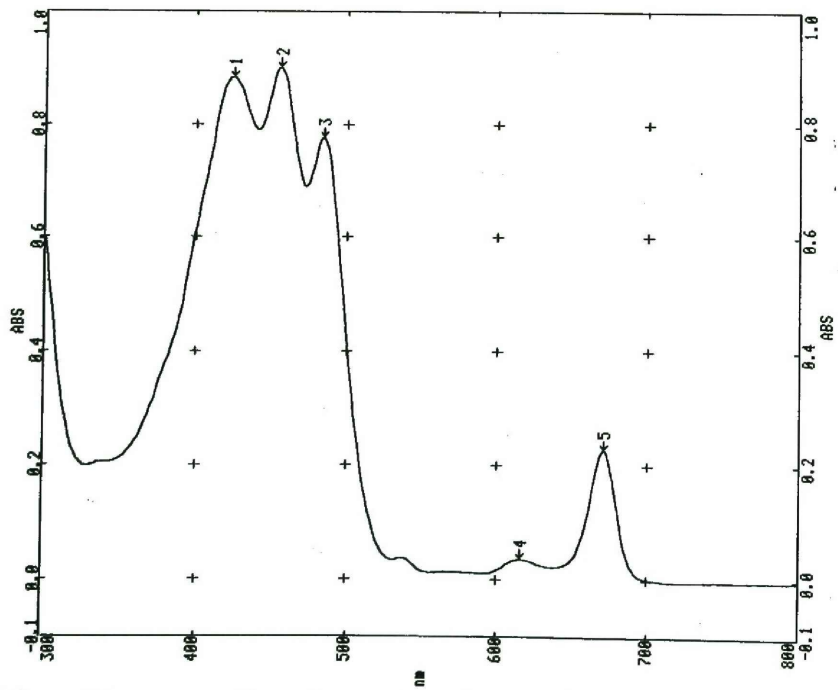


Figure 4.2 Absorption spectrum of carotene layer from alumina chromatographic column in petroleum ether.

Table 4.2 Absorption bands from carotene layer of extract in petroleum ether.

Peaks	Wavelength (nm)	Absorbance
1	424	0.883
2	455	0.899
3	484	0.776
4	616	0.036
5	671	0.228

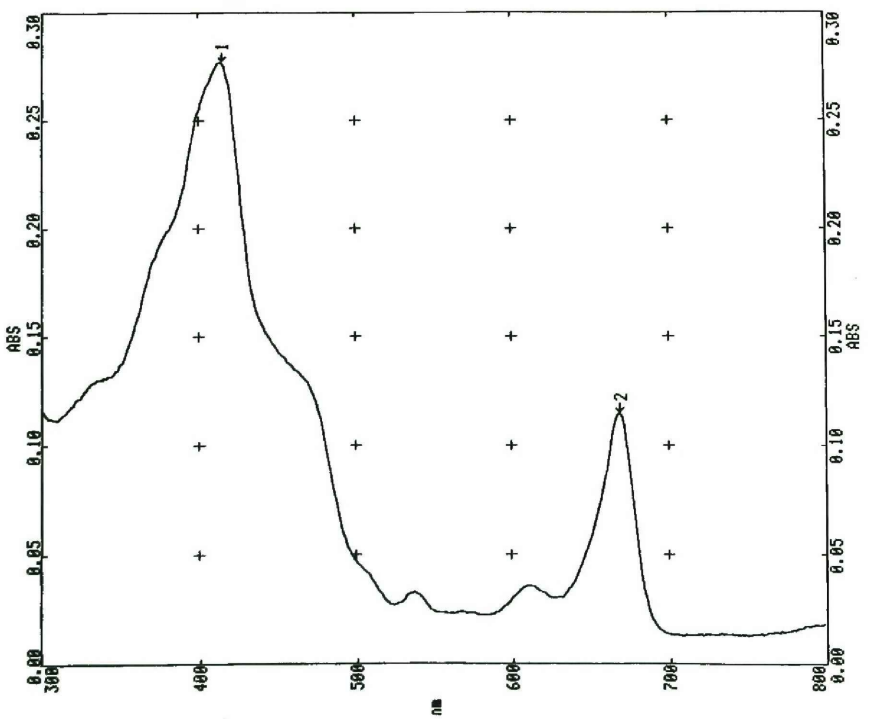


Figure. 4.3 Electronic spectrum of chlorophyll extract in petroleum ether from alumina stationary phase column acidified with dilute hydrochloric acid (pheophytin).

Table 4.3(a) Absorption bands of pheophytin extract on alumina column.

Peaks	Wavelength (nm)	Absorbance
1	415	0.277
2	655	0.078
3	666	0.113
4	669	0.115

Table 4.3(b) Concentration of pheophytin on alumina column

Total pheophytin (mg/L)	6.75 x 0.113 + 26.03 x 0.078	= 2.793
Pheophytin-*a* (mg/L)	20.15 x 0.113 – 5.87 x 0.078	= 1.819

In 80% acetone,[19,59]

total pheophytin (mg/L) $= 6.75D_{666} + 26.03D_{655}$

pheophytin-*a* (mg/L) $= 20.15D_{666} - 5.87D_{655}$

where D_{655} and D_{666} are the absorbances at the specified wavelengths.

4.1.2 SILICA GEL METHOD (METHOD 2)

The chlorophyll-*a*, carotene and pheophytin-*a* fractions obtained in this chromatographic separation, were analyzed spectrophotometrically in the ultraviolet-visible region of the spectrum. The spectra are displayed in Figures 4.4, 4.5 and 4.6, respectively.

A summary of the wavelengths of maximum absorption and the absorbances at these wavelengths for chlorophyll-*a*, carotene and pheophytin-*a* is given in Tables 4.4(a), 4.5 and 4.6(a).

The concentrations of total chlorophyll, chlorophyll-*a* and chlorophyll-*b* in mg/L in petroleum ether are shown in Table 4.4(b).

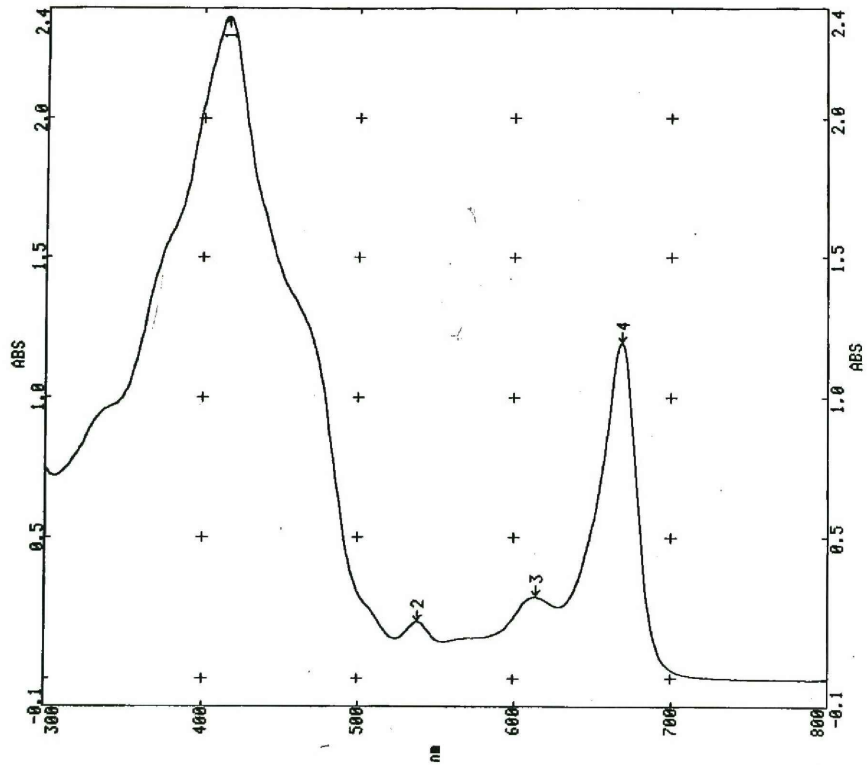


Figure. 4.4 Electronic spectrum of chlorophyll extract in petroleum ether obtained from silica gel chromatographic column.

Table 4.4(a) Absorption band of chlorophyll extract from silica gel column.

Peaks	Wavelength (nm)	Absorbance
1	415	2.371
2	539	0.203
3	614	0.291
4	645	0.35
5	663	0.93
6	669	1.195

Table 4.4(b) Concentration of chlorophyll from silica gel column

Total chlorophyll (mg/L)	20.2 x 0.35 + 8.02 x 0.93	= 14.529
Chlorophyll-*a* (mg/L)	12.7 x 0.93 – 2.69 x 0.35	= 10.870
Chlorophyll-*b* (mg/L)	22.9 x 0.35 – 4.68 x 0.93	= 3.663

In 80% acetone,[1,19,59]

total chlorophyll (mg/L) = $20.2D_{645} + 8.02D_{663}$

chlorophyll-a (mg/L) = $12.7D_{663} - 2.69D_{645}$

chlorophyll-b (mg/L) = $22.9D_{645} - 4.68D_{663}$

where D_{645} and D_{663} are the absorbances at the specified wavelengths.

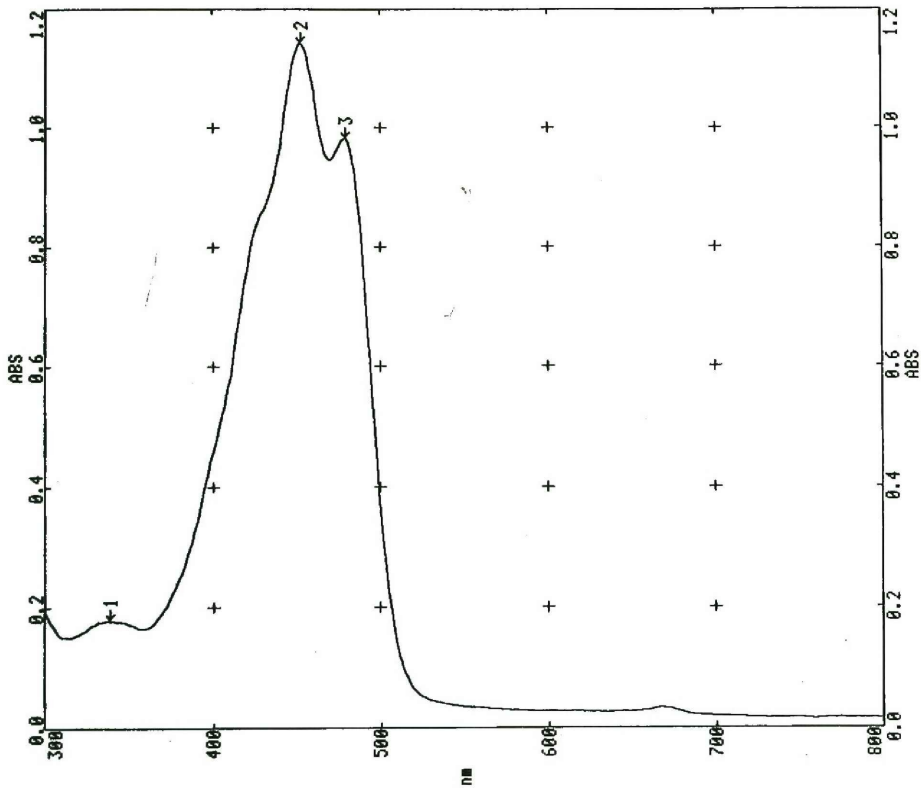


Figure 4.5 Absorption spectrum of carotene layer in petroleum ether on silica gel chromatographic column.

Table 4.5 Absorption bands of carotene layer from silica gel stationary phase

Peaks	Wavelength (nm)	Absorbance
1	338	0.178
2	452	1.142
3	478	0.981

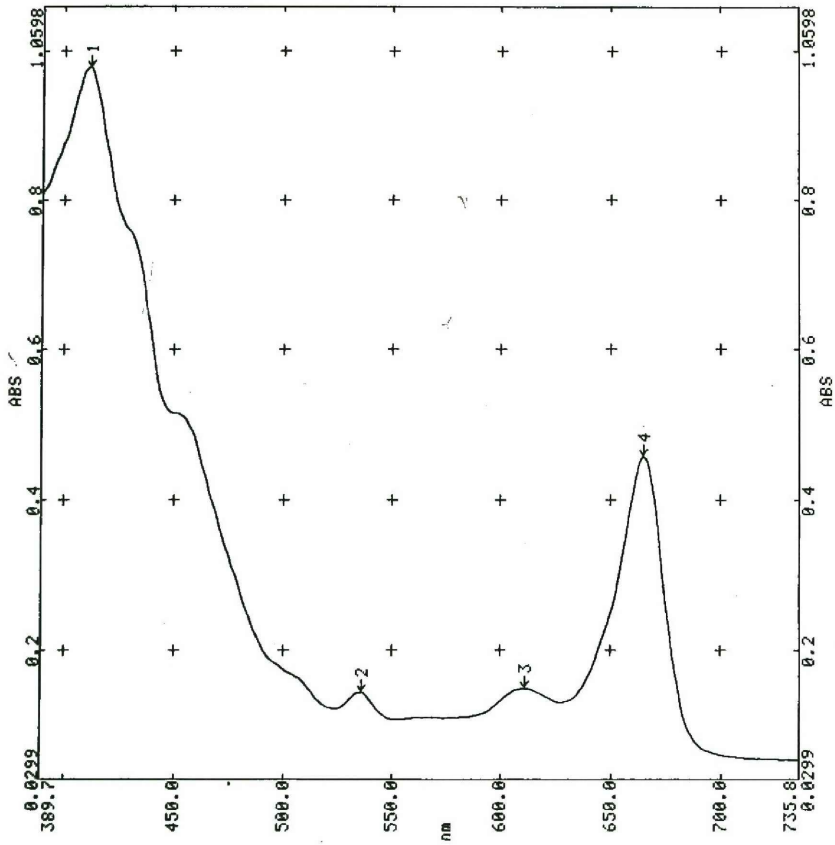


Figure 4.6 Electronic spectrum of chlorophyll extract in petroleum ether from silica gel stationary phase column acidified with glacial acetic acid, (pheophytin).

Table 4.6 Absorption bands of pheophytin from silica gel column in petroleum ether.

Peaks	Wavelength (nm)	Absorbance
1	411.8	0.978
2	536.0	0.145
3	611.2	0.150
4	665.3	0.458

4.1.3 IMPROVED SILICA GEL METHOD (METHOD 3)

The spectra of the whole extract in 80% aqueous acetone produced several absorption bands [Figure 4.7, Table 4.7(a)], which on further chromatographic separation produced chlorophyll-*a*. The ultraviolet-visible spectrum of the acetone layer of the extract after washing with petroleum ether is shown in Figure 4.8.

The carotene, chlorophyll-*a* and pheophytin-*a* fractions obtained in this chromatographic separation, were analysed spectrophotometrically in the ultraviolet-visible region of the spectrum. The spectra obtained for the carotene, chlorophyll-*a* and pheophytin-*a* fractions are displayed in Figures 4.9, 4.10 and 4.11, respectively.

A summary of the wavelengths of maximum absorption and the absorbances at these wavelengths for carotene, chlorophyll-*a* and pheophytin-*a* is given in Tables 4.9, 4.10(a) and 4.11(a). The concentrations of total chlorophyll, chlorophyll-*a*, chlorophyll-*b* and pheophytin-*a* in mg/L obtained are in Table 4.10(b) and 4.11(b).

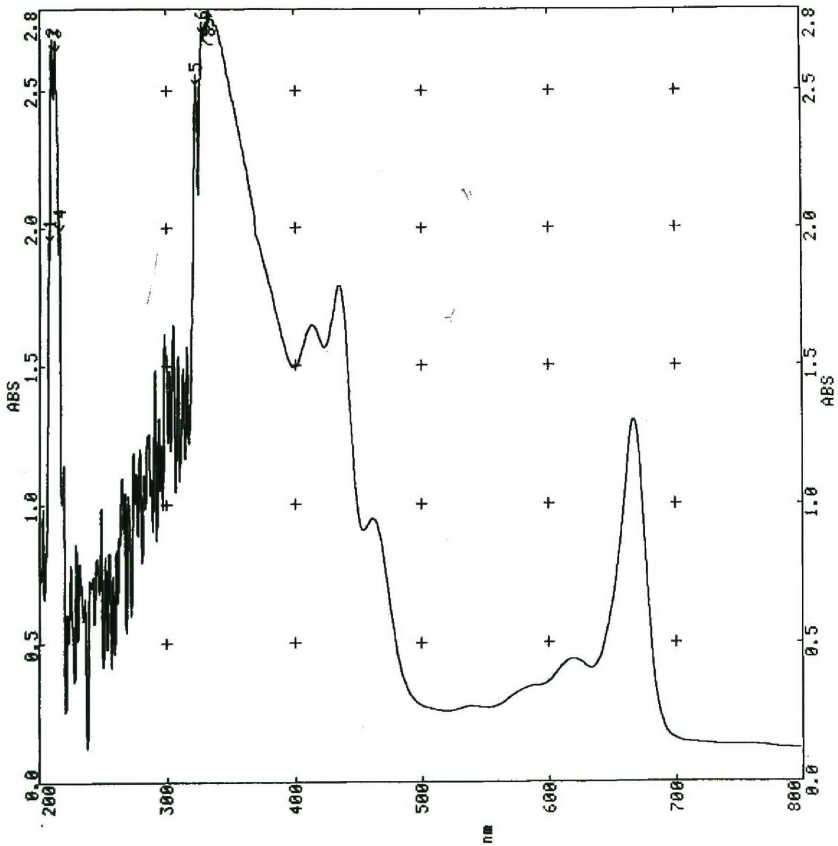


Figure 4.7 Absorption spectrum of whole extract in 80% aqueous acetone

Table 4.7(a) Absorption bands of whole chlorophyll extract

Peaks	Wavelength (nm)	Absorbance
1	208	1.950
2	210	2.649
3	213	2.643
4	217	1.989
5	323	2.517
6	328	2.710
7	645	0.47
8	663	1.08

Table 4.7(b) Concentration of chlorophyll in whole extract

Total chlorophyll (mg/L)	20.2 x 0.47 + 8.02 x 1.08	= 18.156
Chlorophyll-*a* (mg/L)	12.7 x 1.08 – 2.69 x 0.47	= 12.452
Chlorophyll-*b* (mg/L)	22.9 x 0.47 – 4.68 x 1.08	= 5.709

In 80% acetone,[1,19,59]

total chlorophyll (mg/l) = $20.2D_{645} + 8.02D_{663}$

chlorophyll-a (mg/l) = $12.7D_{663} - 2.69D_{645}$

chlorophyll-b (mg/g) = $22.9D_{645} - 4.68D_{663}$

where D_{645} and D_{663} are the absorbances at the specified wavelength.

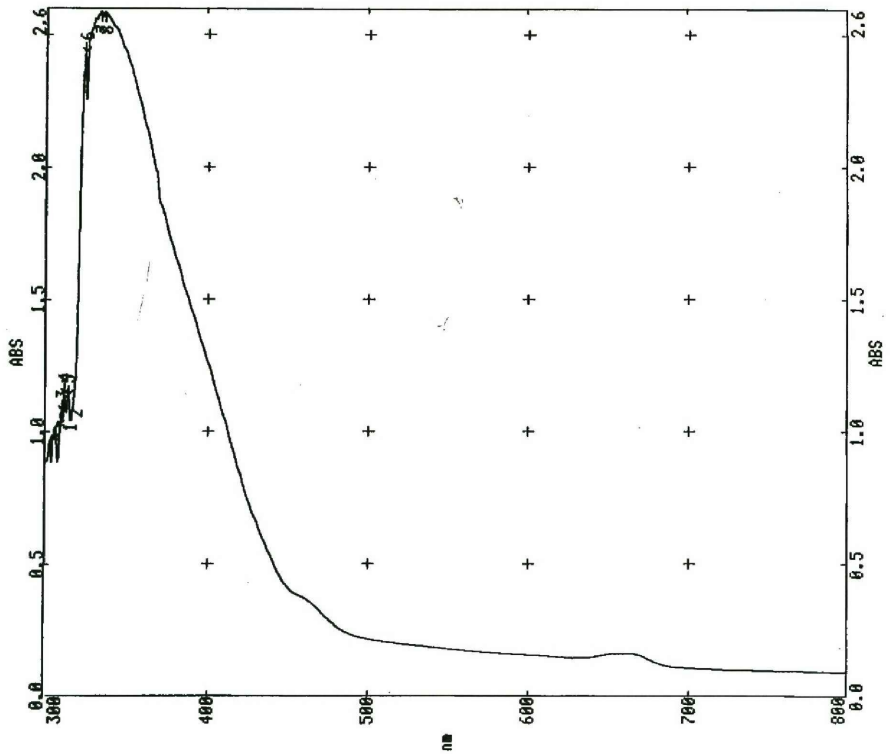


Figure 4.8 Absorption spectrum of acetone layer of extract after washing with petroleum ether (60-80°C).

Table 4.8(a) Absorption bands in acetone layer

Peaks	Wavelength (nm)	Absorbance
1	302	0.963
2	306	1.016
3	310	1.074
4	311	1.142
5	314	1.132
6	324	2.427
7	645	0.115
8	663	0.124

Table 4.8(b) Concentration of chlorophyll in acetone layer

Total chlorophyll (mg/L)	20.2 x 0.115 + 8.02 x 0.124	= 3.318
Chlorophyll-*a* (mg/L)	12.7 x 0.124 – 2.69 x 0.115	= 1.266
Chlorophyll-*b* (mg/L)	22.9 x 0.115 – 4.68 x 0.124	= 2.053

In 80% acetone,[1,19,59]

total chlorophyll (mg/l) = $20.2D_{645} + 8.02D_{663}$

chlorophyll-a (mg/l) = $12.7D_{663} - 2.69D_{645}$

chlorophyll-b (mg/g) = $22.9D_{645} - 4.68D_{663}$

where D_{645} and D_{663} are the absorbances at the specified wavelengths.

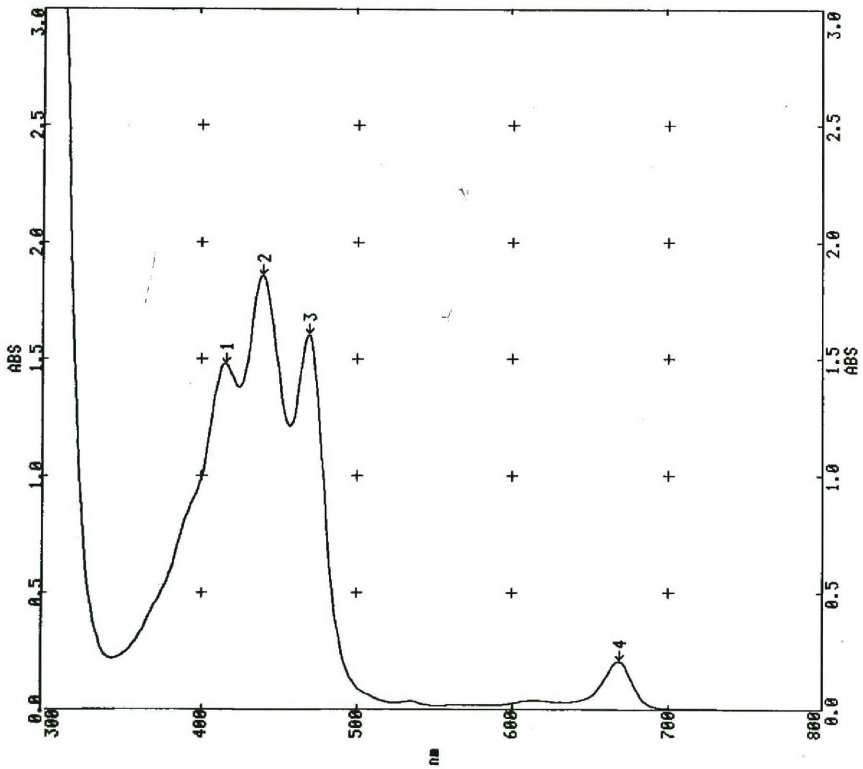


Figure 4.9 Absorption spectrum of carotene layer of extract in petroleum ether.

Table 4.9 Absorption bands from carotene layer in petroleum ether.

Peaks	Wavelength (nm)	Absorbance
1	415	1.479
2	439	1.854
3	469	1.603
4	669	0.287

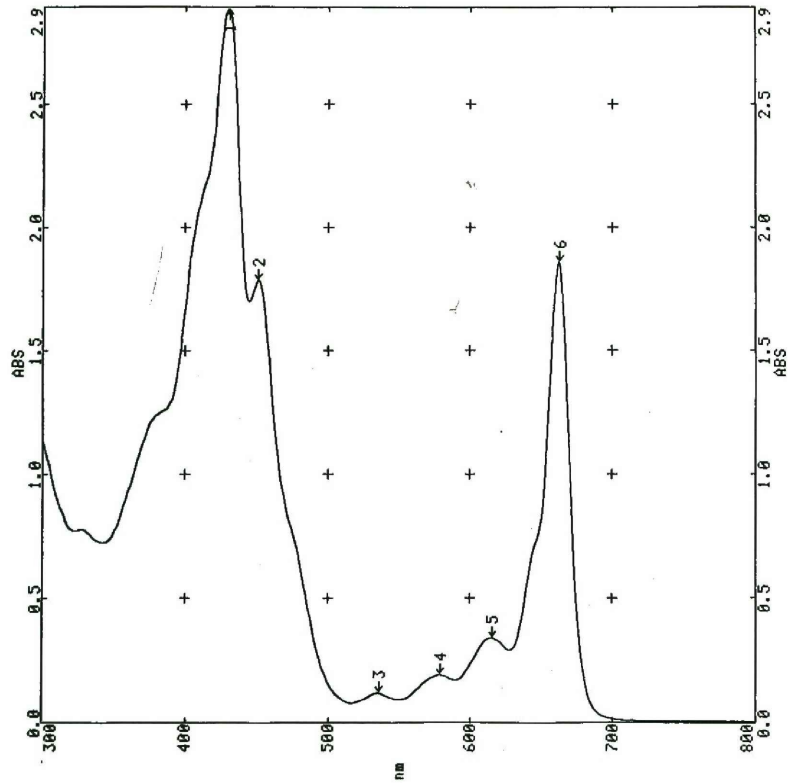


Figure 4.10 Absorption spectrum of chlorophyll-*a* in petroleum ether on a silica gel column in petroleum ether.

Table 4.10(a) Absorption bands of chlorophyll-*a* in petroleum ether

Peaks	Wavelength (nm)	Absorbance
1	430	2.894
2	451	1.786
3	536	0.121
4	579	0.191
5	616	0.340
6	645	0.600
7	663	1.856

Table 4.10(b) Concentration of chlorophyll in petroleum ether

Total chlorophyll (mg/L)	20.2 x 0.600 + 8.02 x 1.856	= 27.005
Chlorophyll-*a* (mg/L)	12.7 x 1.856 – 2.69 x 0.600	= 21.957
Chlorophyll-*b* (mg/L)	22.9 x 0.600 – 4.68 x 1.856	= 5.054

In 80% acetone,[10,19,59]

total chlorophyll (mg/L) = $20.2D_{645} + 8.02D_{663}$

chlorophyll-a (mg/L) = $12.7D_{663} - 2.69D_{645}$

chlorophyll-b (mg/L) = $22.9D_{645} - 4.68D_{663}$

where D_{645} and D_{663} are the absorbances at the specified wavelengths.

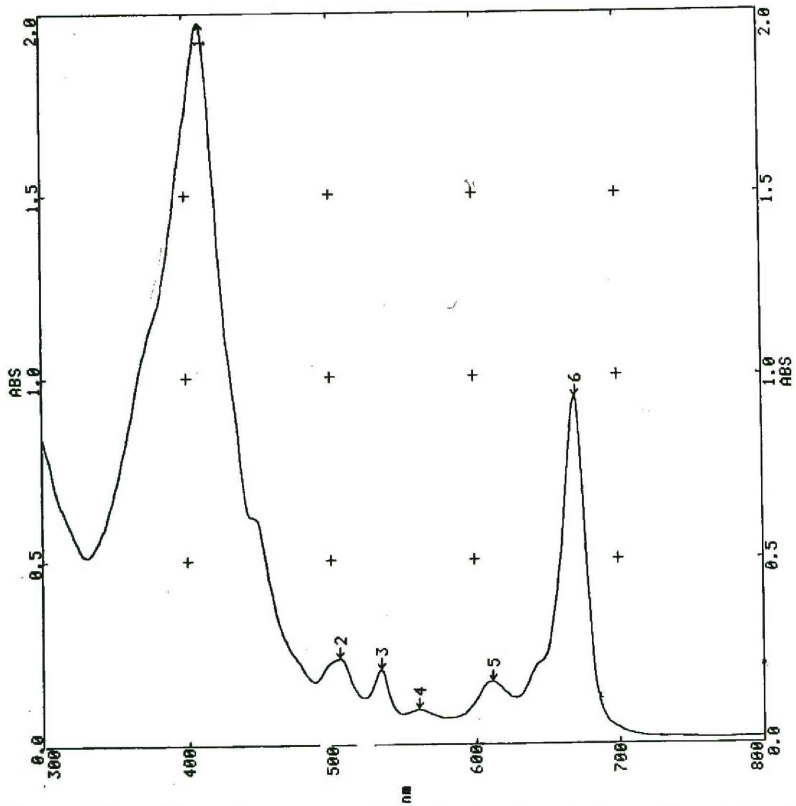


Figure 4.11 Absorption spectra of pheophytin-*a* in petroleum ether obtained by acidification with glacial acetic acid.

Table 4.11(a) Absorption bands of pheophytin in petroleum ether

Peaks	Wavelength (nm)	Absorbance
1	411	1.976
2	506	0.234
3	535	0.203
4	562	0.095
5	613	0.171
6	655	0.333
7	666	0.679
8	671	0.941

Table 4.11(b) Concentration of pheophytin in petroleum ether

Total pheophytin (mg/L)	6.75 x 0.679 + 26.03 x 0.333	= 13.251
Pheophytin-*a* (mg/L)	20.15 x 0.679 – 5.87 x 0.333	= 11.727

total pheophytin (mg/L) $= 6.75D_{666} + 26.03D_{655}$

pheophytin-*a* (mg/L) $= 20.15D_{666} - 5.87D_{655}$

where D_{655} and D_{666} are the absorbances at the specified wavelengths.

4.1.4 WINTER EXTRACTION METHOD (METHOD 4)

The absorption spectrum of the whole chlorophyll extract in 80% aqueous acetone produced several absorption bands (Figure 4.12), which on further chromatographic separation produced chlorophyll-*a* (Figure 4.16).

The spectrum of the acetone layer of the extract after washing with petroleum ether and the spectrum of the petroleum ether washings are shown in Figures 4.13 and 4.14, respectively.

The chlorophyll-*a* and pheophytin-*a* fractions obtained in this chromatographic separation were analysed spectrophotometrically in the ultraviolet-visible region of the spectrum. The spectra obtained for the chlorophyll-*a* (before and after purification) and pheophytin-*a* fractions are displayed in Figures 4.15, 4.16 and 4.17, respectively.

A summary of the wavelengths of maximum absorption and the absorbances at these wavelengths for chlorophyll-*a*, carotene and

pheophytin-*a* is given in Tables 4.16(a), 4.14 and 4.18(a), respectively.

The concentrations of total chlorophyll, chlorophyll-*a*, chlorophyll-*b* and pheophytin-*a* in mg/L obtained are in Tables 4.16(b) and 4.18(b)

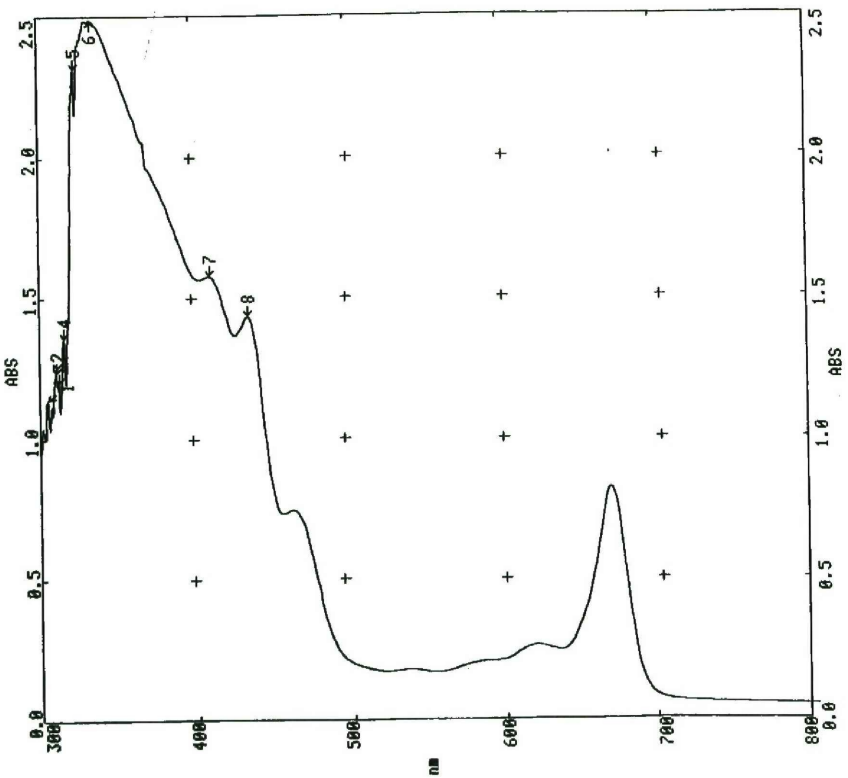


Figure 4.12 Absorption spectrum of whole chlorophyll extract in 80% acetone during winter.

Table 4.12(a) Absorption band of whole chlorophyll during winter

Peaks	Wavelength (nm)	Absorbance
1	305	1.143
2	311	1.237
3	313	1.201
4	316	1.356
5	324	2.313
6	335	2.492
7	410	1.575
8	434	1.432
9	645	0.273
10	663	0.609

Table 4.12(b) Concentration of chlorophyll in acetone layer during winter

Total chlorophyll (mg/L)	20.2 x 0.273 + 8.02 x 0.609	= 10.399
Chlorophyll-*a* (mg/L)	12.7 x 0.609 – 2.69 x 0.273	= 7.000
Chlorophyll-*b* (mg/L)	22.9 x 0.273 – 4.68 x 0.609	= 3.402

In 80% acetone,[10,19,59]

total chlorophyll (mg/l) = $20.2D_{645} + 8.02D_{663}$

chlorophyll-a (mg/l) = $12.7D_{663} - 2.69D_{645}$

chlorophyll-b (mg/g) = $22.9D_{645} - 4.68D_{663}$

where D_{645} and D_{663} are the absorbances at the specified wavelengths.

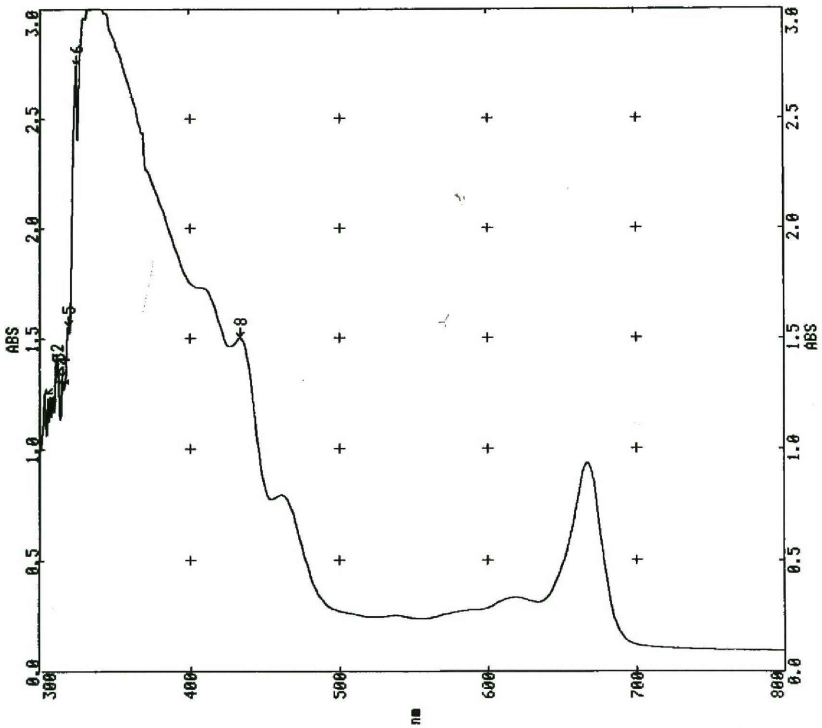


Figure 4.13 Absorption spectrum of acetone layer of whole chlorophyll extract after washing with petroleum ether.

Table 4.13(a) Absorption bands of whole chlorophyll in petroleum ether

Peaks	Wavelength (nm)	Absorbance
1	302	1.246
2	311	1.385
3	312	1.345
4	315	1.328
5	319	1.557
6	324	2.744
7	332	>3.0
8	433	1.501
9	645	0.370
10	663	0.834

Table 4.13(b) Concentration of chlorophyll in petroleum ether

Total chlorophyll (mg/L)	20.2 x 0.370 + 8.02 x 0.834	= 14.163
Chlorophyll-*a* (mg/L)	12.7 x 0.834 – 2.69 x 0.370	= 9.597
Chlorophyll-*b* (mg/L)	22.9 x 0.370 – 4.68 x 0.834	= 4.570

In 80% acetone,[10,19,59]

total chlorophyll (mg/L) = $20.2D_{645} + 8.02D_{663}$

chlorophyll-*a* (mg/L) = $12.7D_{663} - 2.69D_{645}$

chlorophyll-*b* (mg/L) = $22.9D_{645} - 4.68D_{663}$

where D_{645} and D_{663} are the absorbances at the specified wavelengths.

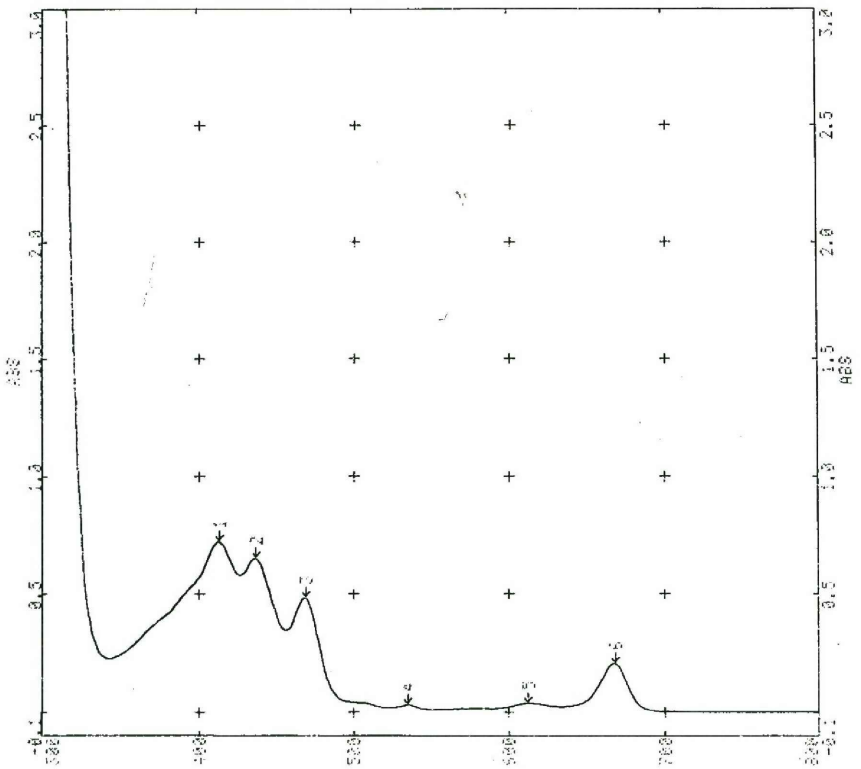


Figure 4.14 Absorption spectrum of petroleum ether fraction of extract during winter showing the presence of carotenoids and less chlorophyll.

Table 4.14(a) Absorption bands of chlorophyll in petroleum ether during winter

Peaks	Wavelength (nm)	Absorbance
1	413	0.722
2	436	0.650
3	469	0.483
4	535	0.030
5	613	0.036
6	645	0.025
7	663	0.136
8	668	0.204

Total chlorophyll (mg/L)	20.2 x 0.025 + 8.02 x 0.136	= 1.596
Chlorophyll-*a* (mg/L)	12.7 x 0.136 – 2.69 x 0.025	= 1.66
Chlorophyll-*b* (mg/L)	22.9 x 0.025 – 4.68 x 0.136	= -0.064

Table 4.14(b) Concentration of chlorophyll extract during winter

In 80% acetone,[10,19,59]

total chlorophyll (mg/L) = $20.2D_{645} + 8.02D_{663}$

chlorophyll-*a* (mg/L) = $12.7D_{663} - 2.69D_{645}$

chlorophyll-*b* (mg/L) = $22.9D_{645} - 4.68D_{663}$

where D_{645} and D_{663} are the absorbances at the specified wavelength.

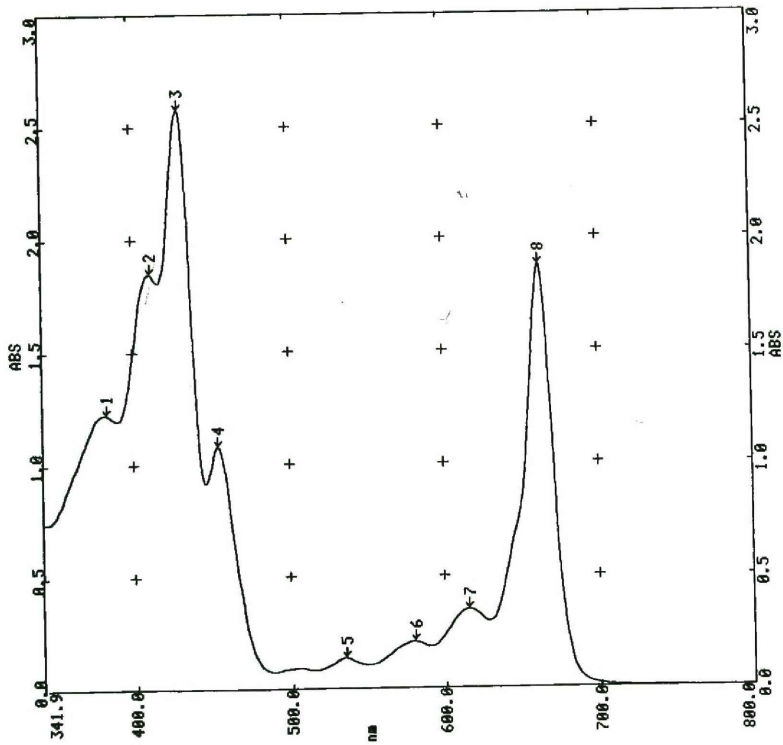


Figure 4.15 Absorption spectra of chlorophyll-*a* in diethyl ether before purification on a silica gel chromatographic column.

Table 4.15(a) Absorption bands of chlorophyll in diethyl ether

Peaks	Wavelength (nm)	Absorbance
1	382	1.225
2	412	1.845
3	431	2.577
4	454	1.078
5	536	0.137
6	581	0.209
7	616	0.350
8	642.5	0.532
9	660	1.501
10	663	1.871

Table 4.15(b) Concentration of chlorophyll-*a* in diethyl ether before purification

Total chlorophyll (mg/L)	7.12 x 1.5 + 16.8 x 0.532	= 19.618
Chlorophyll-*a* (mg/L)	9.93 x 1.5 – 0.78 x 0.532	= 14.480
Chlorophyll-*b* (mg/L)	17.6 x 0.532 – 2.8 x 1.5	= 5.163

In diethyl ether [10,14,19,59]

Total chlorophyll (mg/L) = $7.12D_{660} + 16.8D_{642.5}$

chlorophyll-*a* (mg/L) = $9.93D_{660} - 0.78D_{642.5}$

chlorophyll-*b* (mg/L) = $17.6D_{642.5} - 2.8D_{660}$

where $D_{642.5}$ and D_{660} are the absorbances at the specified wavelengths.

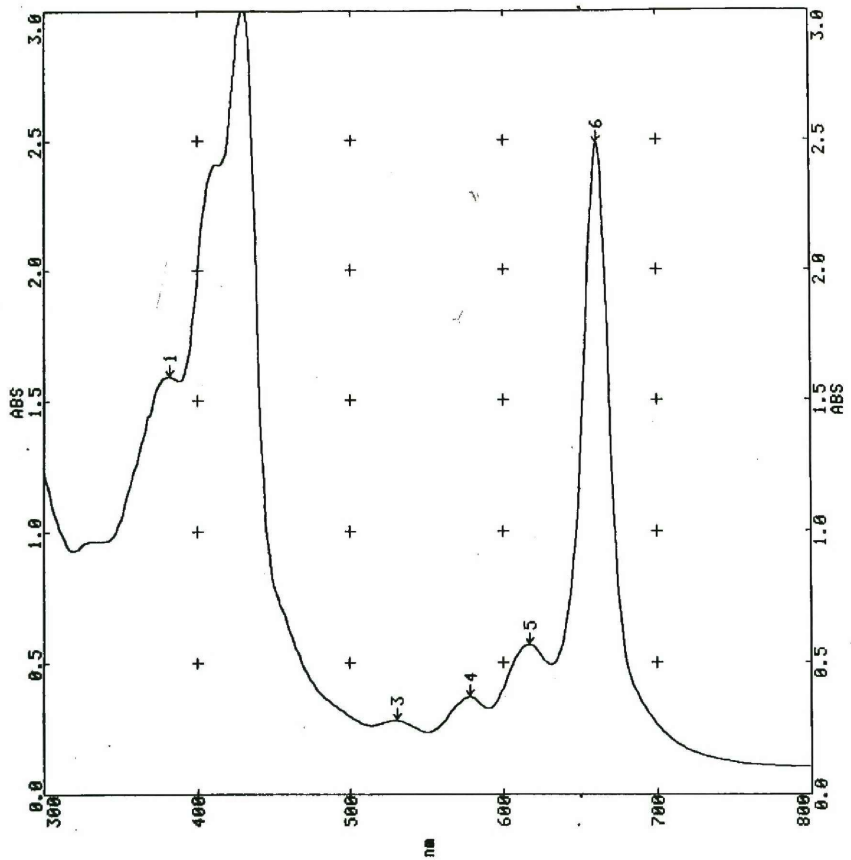


Figure 4.16 Absorption spectrum of chlorophyll-*a* in diethyl ether after purification on a silica gel chromatographic column.

Table 4.16(a) Absorption bands of chlorophyll-*a* in diethyl ether.

Peaks	Wavelength (nm)	Absorbance
1	382	1.592
2	429	3.000
3	530	0.280
4	579	0.369
5	618	0.567
6	642.5	0.636
7	660	2.116
8	661	2.406

Table 4.16(b) Concentration of chlorophyll in diethyl ether after purification.

Total chlorophyll (mg/L)	7.12 x 2.116 + 16.8 x 0.636	= 25.751
Chlorophyll-*a* (mg/L)	9.93 x 2.116 – 0.78 x 0.636	= 20.516
Chlorophyll-*b* (mg/L)	17.6 x 0.636 – 2.8 x 2.116	= 5.269

In diethyl ether [10,19,59]

Total chlorophyll (mg/L) = $7.12D_{660} + 16.8D_{642.5}$

chlorophyll-*a* (mg/L) = $9.93D_{660} - 0.78D_{642.5}$

chlorophyll-*b* (mg/L) = $17.6D_{642.5} - 2.8D_{660}$

where $D_{642.5}$ and D_{660} are the absorbances at the specified wavelengths.

4.1.5 SUMMARY OF QUANTITIES OF CHLOROPHYLL EXTRACTED USING DIFFERENT METHODS

Table 4.17 is a summary of the relative quantities of chlorophyll extracted by the various methods of extraction employed in this research work.

Table 4.17 Summary of the relative quantities of chlorophyll extracted, using different solvents.

Extraction method	**Quantity of chlorophyll-*a* extracted (mg/L)**
Alumina column method (method 1) (pages 54 – 56)	1.453 (petroleum ether)
Silica gel column method (method 2) (pages 57 and 58)	10.870 (petroleum ether)
Improved silica gel column method (method 3) (pages 59 – 61)	21.957 (diethyl ether)
Winter extraction method (method 4) (pages 62 and 63)	20.516 (diethyl ether)

4.2 DEMETALLATION OF CHLOROPHYLL-*a*

Chlorophyll-*a* extract in petroleum ether (60-80°C) or diethyl ether was demetallated to form pheophytin-*a* by reacting the extract with an acid such as dilute hydrochloric acid or glacial acetic acid. The colour of the chlorophyll-*a* solution immediately changed from green to olive green. The pheophytin-*a* solution obtained was then analyzed by ultraviolet-visible and infrared spectroscopies in the regions 300 – 800 nm and 500 – 4000 cm^{-1}, respectively.

The ultraviolet-visible spectra of pheophytin-*a* obtained for the different extraction methods show absorption bands around 410, 506, 534, 562, 607 and 666 nm (Figures 4.11 and 4.17). the absorptions vary slightly with different solvents (petroleum ether versus diethyl ether).

The infrared spectra of pheophytin-*a* in petroleum ether obtained show major absorption bands at 2731 1931, 1617, 1523, 1378, 1029, 765 and 689 cm^{-1} (Figure 4.26).

The electrospray ionization mass spectrum of the pheophytin-*a* indicates a peak at *m/z* 593.2 and a 100% relative abundance (Figure 4.32).

Tables 4.12(a) and 4.18(a) show the wavelengths of maximum absorption and the absorbances at these wavelengths of the pheophytin-*a*. Tables 4.12(b) to 4.18(b) show the concentrations of total pheophytin and pheophytin-*a* in mg/L obtained in this analysis.

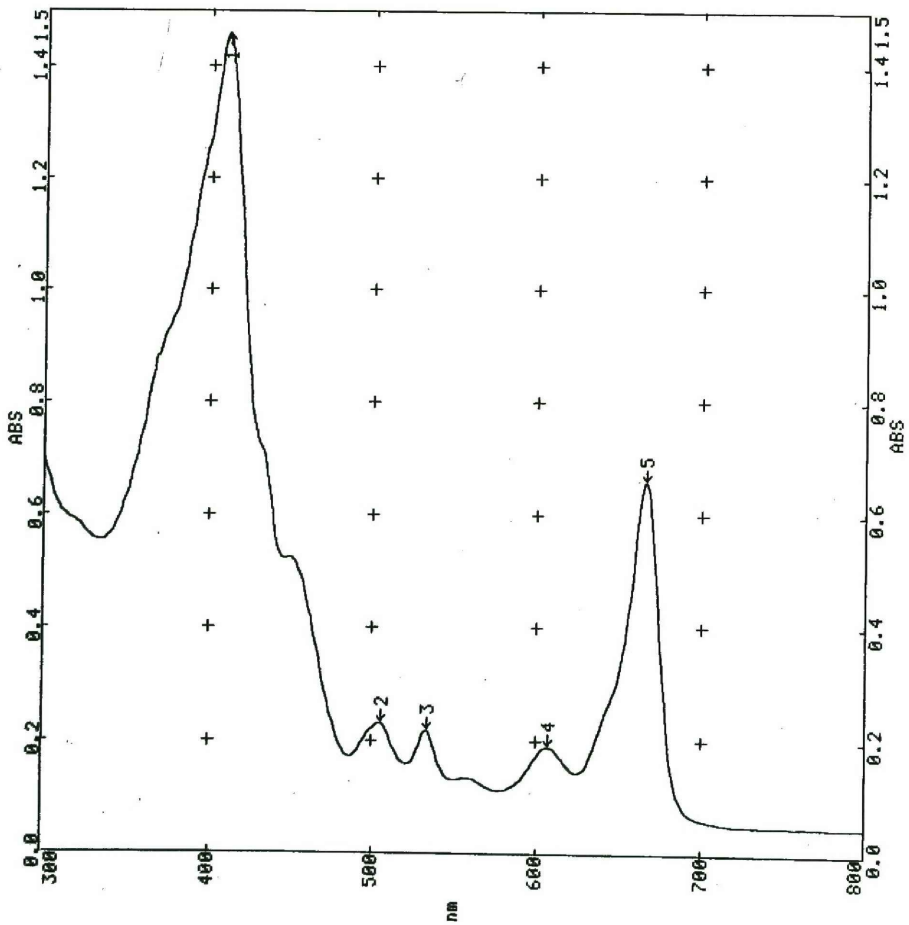


Figure 4.17 Absorption spectrum of pheophytin-*a* in diethyl ether after purification on a silica gel chromatographic column.

Table 4.18(a) Absorption band of pheophytin-*a* in diethyl ether after

Peaks	Wavelength (nm)	Absorbance
1	410	1.459
2	506	0.233
3	534	0.220
4	607	0.190
5	655	0.403
5	666	0.659

Table 4.18(b) Concentration of pheophytin-*a* in diethyl ether

Total pheophytin (mg/L)	6.75 x 0.659 + 26.03 x 0.403	= 14.938
Pheophytin-*a* (mg/L)	20.15 x 0.659 – 5.87 x 0.403	= 10.913

Total pheophytin (mg/L) $= 6.75D_{666} + 26.03D_{655}$

Pheophytin-*a* (mg/L) $= 20.15D_{666} - 5.87D_{655}$

where D_{655} and D_{666} are the absorbances at the specified wavelengths.

4.3 COMPLEXATION OF PHEOPHYTIN-*a*

Complexation of pheophytin-*a* with the metal ions cobalt(II), copper(II), chromium(III), nickel(II), and zinc were carried out. The metal pheophytin complexes were characterized by UV-visible and infrared spectroscopies.

Ultraviolet-visible spectra of these metal complexes were found to have mainly two absorption bands one between 407 and 430 nm and the other between 590 and 650 nm (Figures 4.18 – 4.23) The ultraviolet-visible spectra of these metal pheophytin complexes were compared with the ultraviolet-visible spectrum of copper chlorophyllin trisodium salt (Merck) Figure 4.19.

The infrared spectra of these metal pheophytin complexes in nujol show major absorption bands at the carbonyl stretching frequency at about 1700 cm^{-1}.

The mass spectrum analyzes of the cobalt(II) pheophytin-*a* (Figure 4.36) shows a peak with *m/z* ratio 648.66 and a relative abundance of 85 %.

The ultraviolet-visible, infrared and mass spectra of the metal pheophytin complexes are displayed in Figures 4.18 – 4.23, 4.24 – 4.31 and 4.32 – 4.37, respectively.

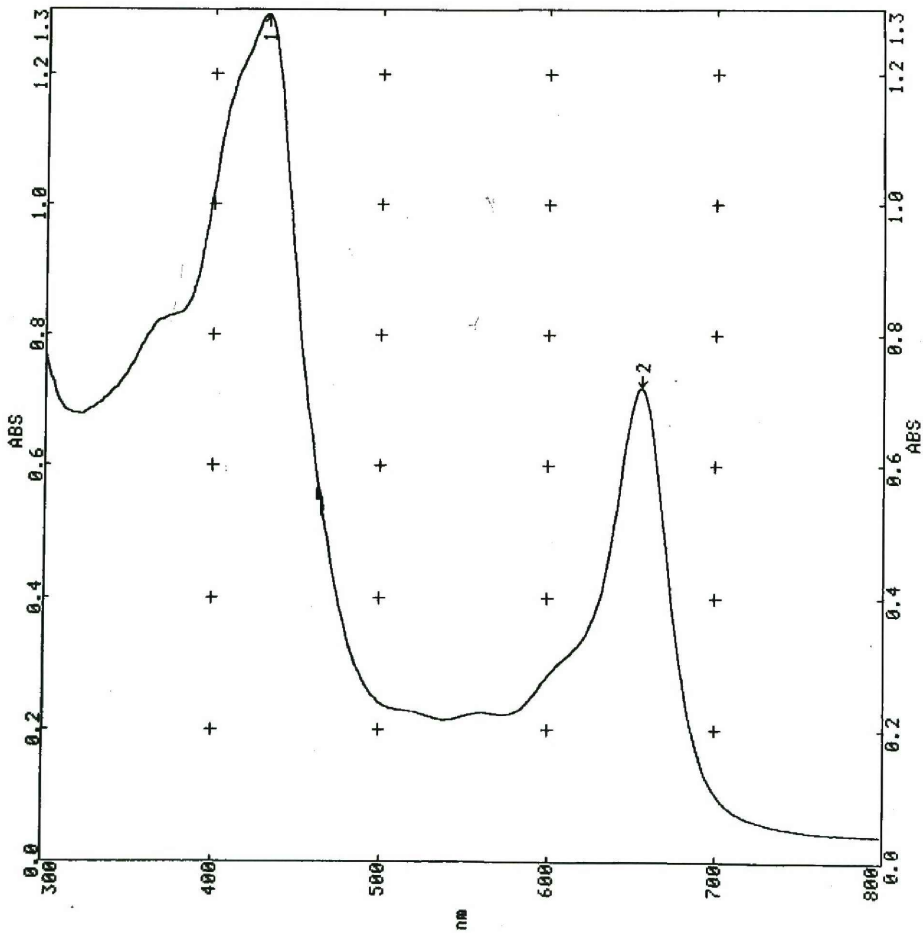


Figure 4.18 Absorption spectrum of cobalt(II) pheophytin-*a* (Cophe) complex deionised with amberlite IR-120.

Table 4.19 Absorption band of cobalt(II) pheophytin-*a*

Peaks	Wavelength (nm)	Absorbance
1	431	1.293
2	656	0.719

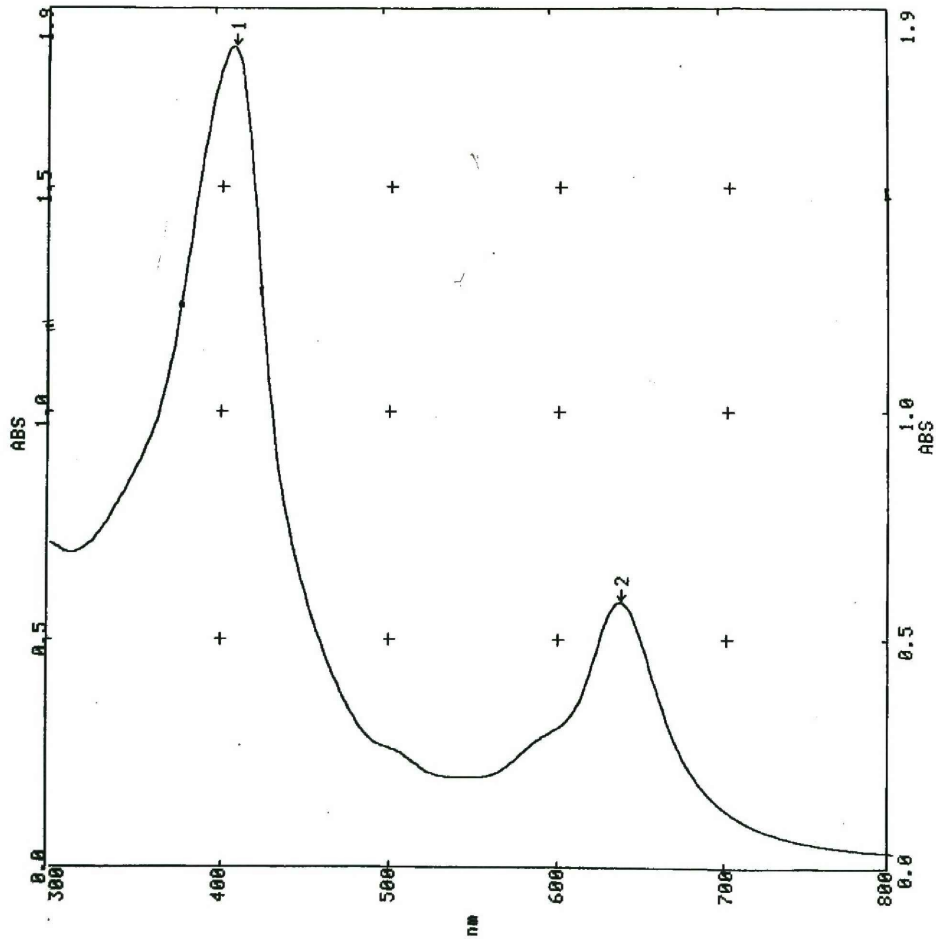


Figure 4.19 Absorption spectrum of chlorophillin coppered trisodium (Na_3Cuphe) salt in water.

Table 4.20 Absorption bands of coppered chlorophillin trisodium salt

Peaks	Wavelength (nm)	Absorbance
1	407	1.813
2	637	0.582

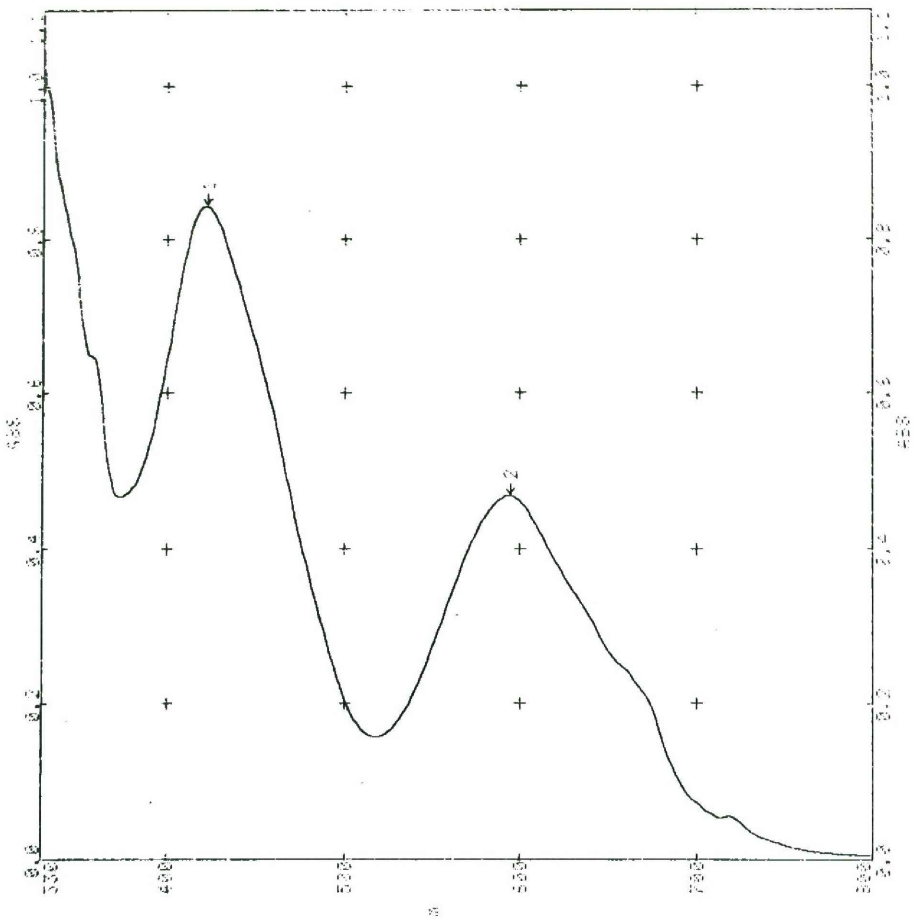


Figure 4.20 Absorption spectrum of Chromium(III) pheophytin-*a* (Crphe) complex deionised with amberlite IR-120.

Table 4.21 Absorption bands of chromium(III) pheophytin-*a*.

Peaks	Wavelength (nm)	Absorbance
1	422	0.843
2	594	0.465

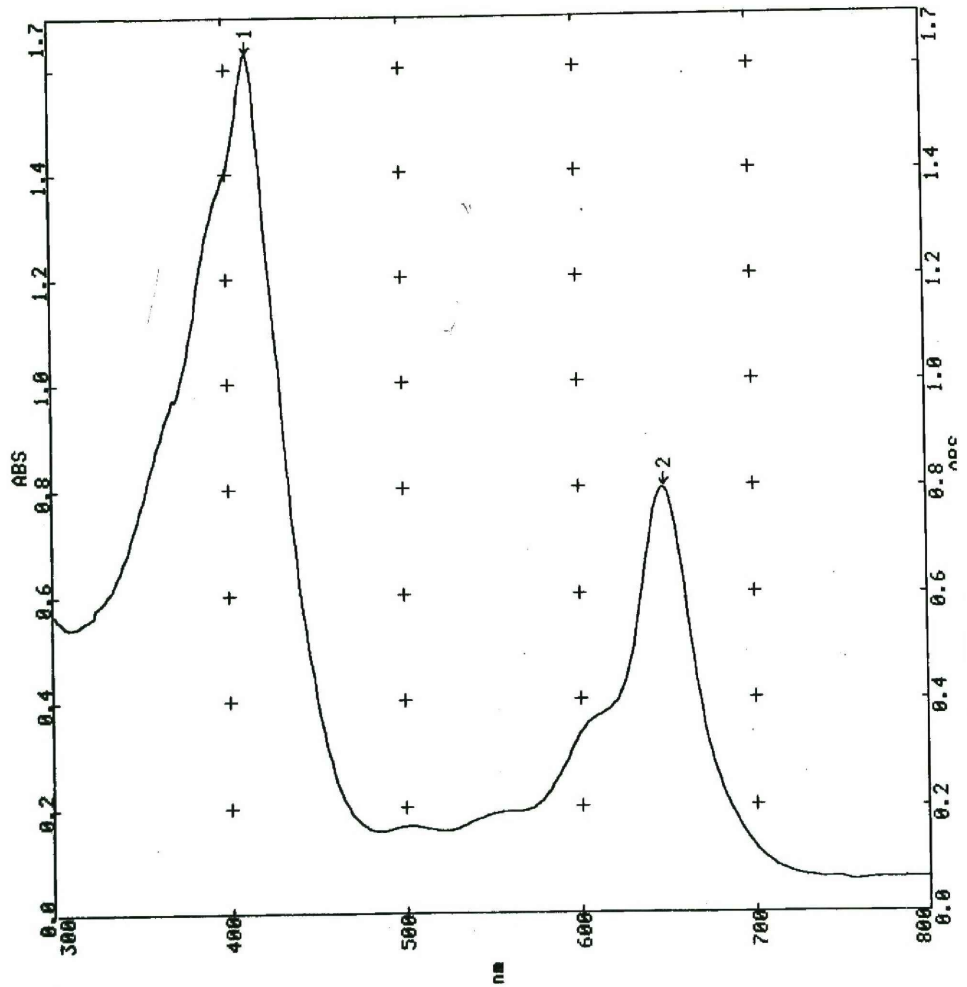


Figure 4.21 Absorption spectrum of Copper(II) pheophytin-*a* (Cuphe) complex deionised with amberlite IR-120.

Table 4.22 Absorption band of in copper(II) pheophytin-*a*.

Peaks	Wavelength (nm)	Absorbance
1	412	1.629
2	649	0.797

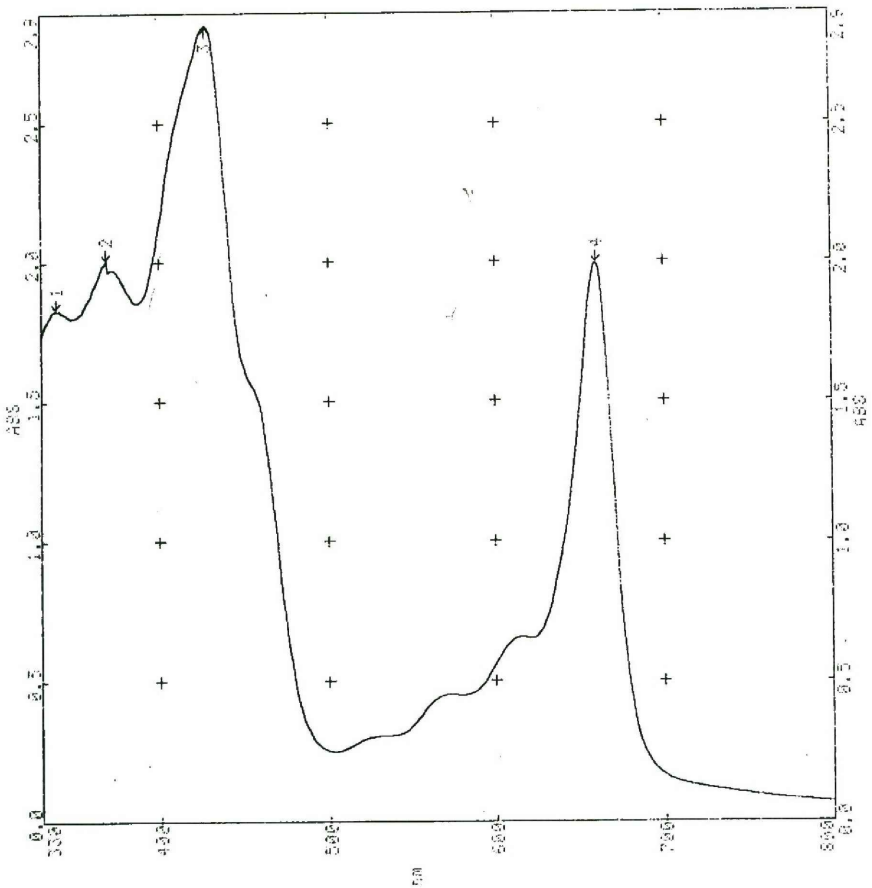


Figure 4.22 Absorption spectrum of Zinc pheophytin-*a* (Znphe) complex deionised with amberlite IR-120.

Table 4.23 Absorption bands of zinc pheophytin-*a*

Peaks	Wavelength (nm)	Absorbance
1	339	1.630
2	369	2.004
3	428	2.856
4	660	1.986

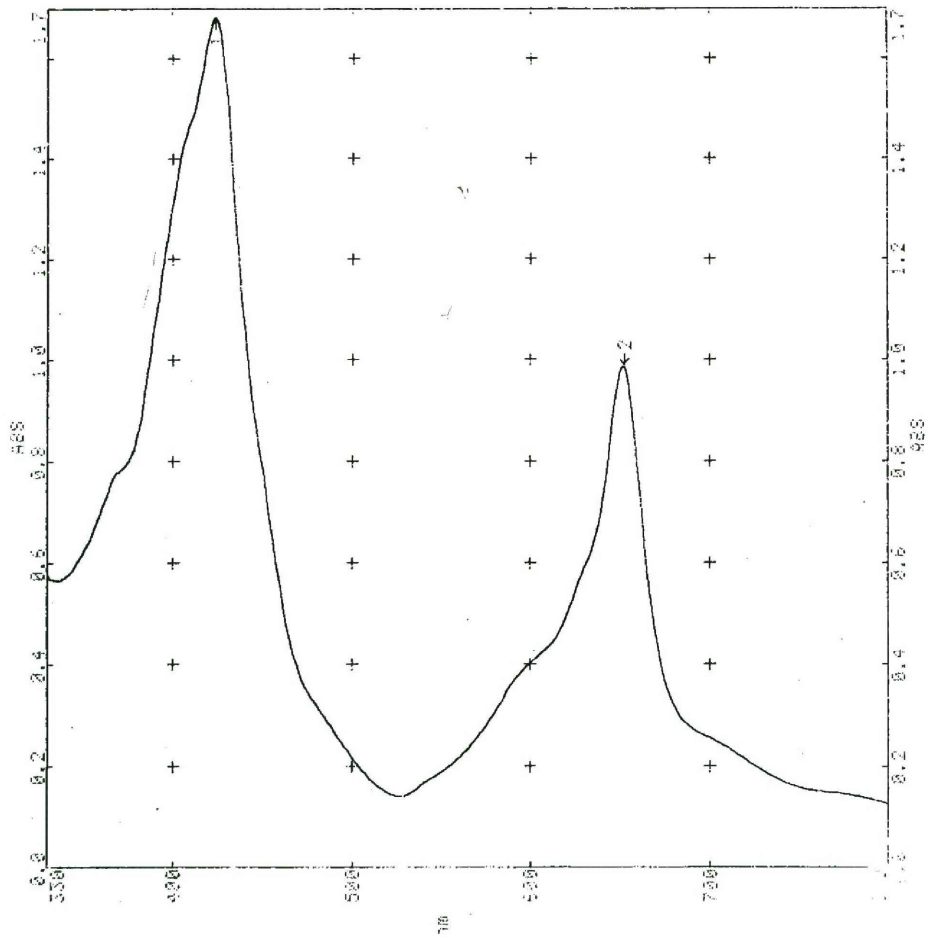


Figure 4.23 Absorption spectra of Nickel(II) pheophytin-*a* (Niphe) complex deionised with amberlite IR-120.

Table 4.24 Absorption bands of nickel(II) pheophytin-*a*

Peaks	Wavelength (nm)	Absorbance
1	423	1.682
2	652	0.935

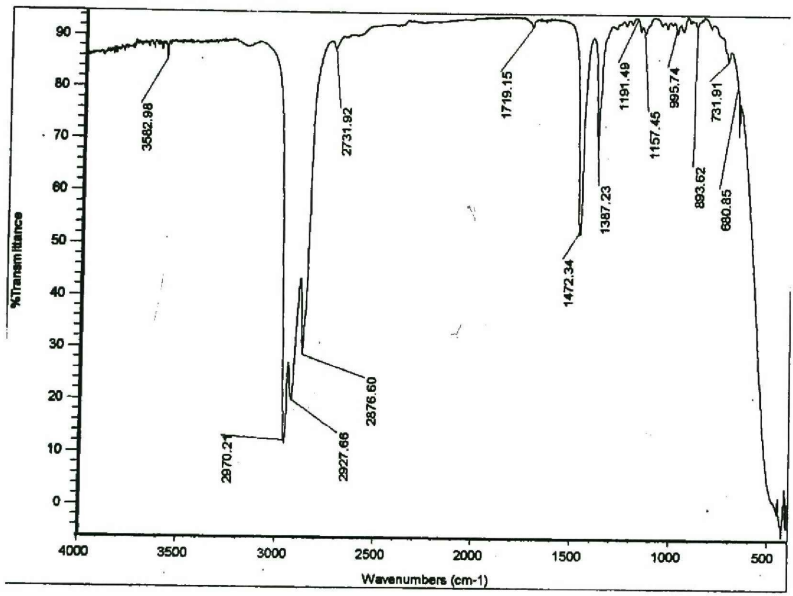


Figure 4.24 Infrared spectrum of chlorophyll-*a* in petroleum ether.

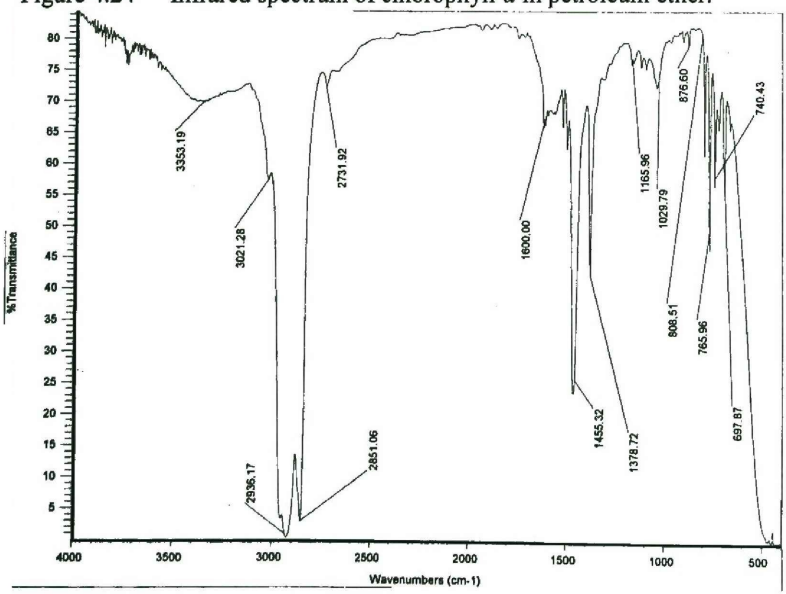


Figure 4.25 Infrared spectrum of chlorophyll-*a* in diethyl ether.

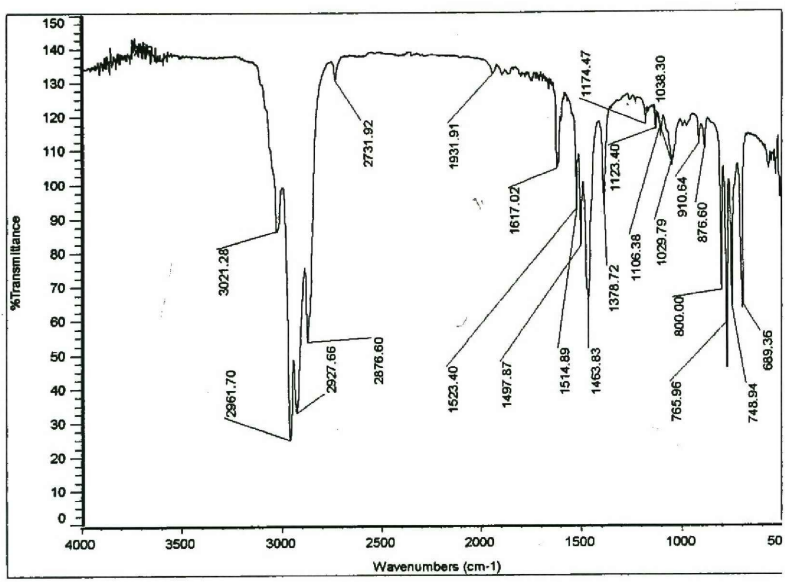


Figure 4.26 Infrared spectrum of pheophytin in petroleum ether without nujol.

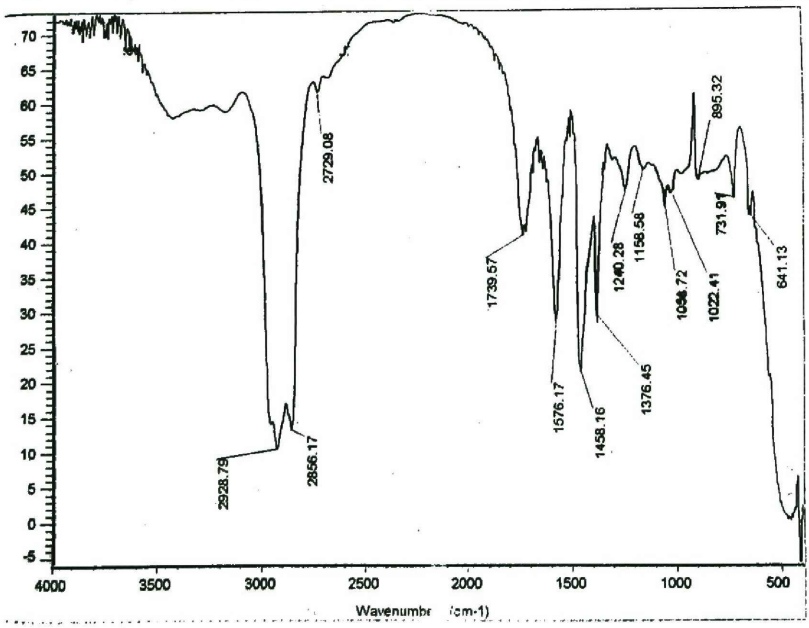


Figure 4.27 Infrared spectrum of cobalt(II) pheophytin-*a* complex.

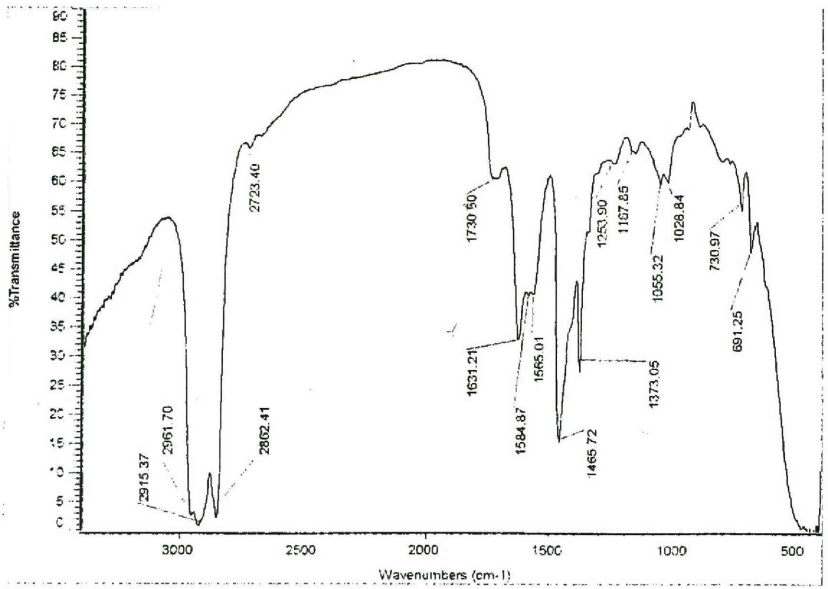


Figure 4.28 Infrared spectrum of copper(II) pheophytin-*a* complex

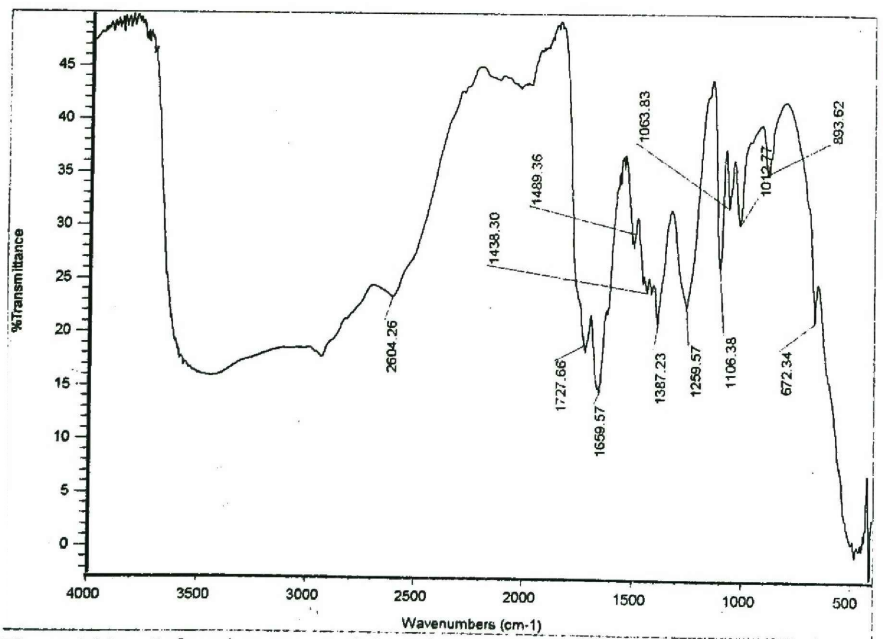


Figure 4.29 Infrared spectrum of chromium(III) pheophytin-*a* complex

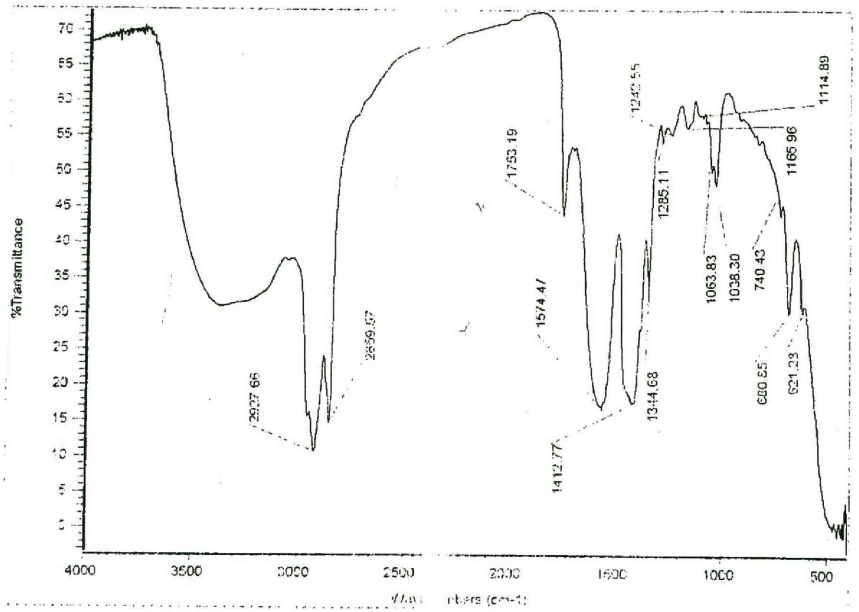


Figure 4.30 Infrared spectrum of nickel(II) pheophytin-*a* complex.

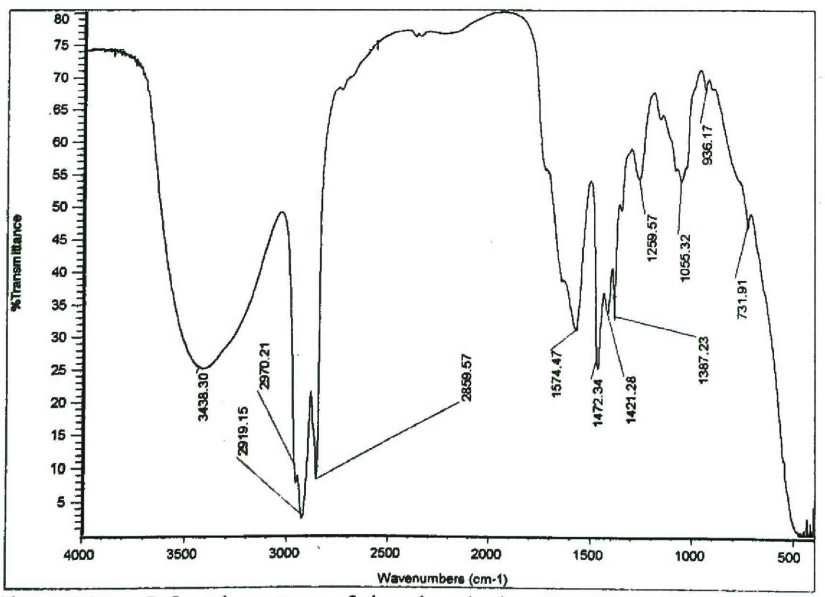


Figure 4.31 Infrared spectrum of zinc pheophytin-*a* complex

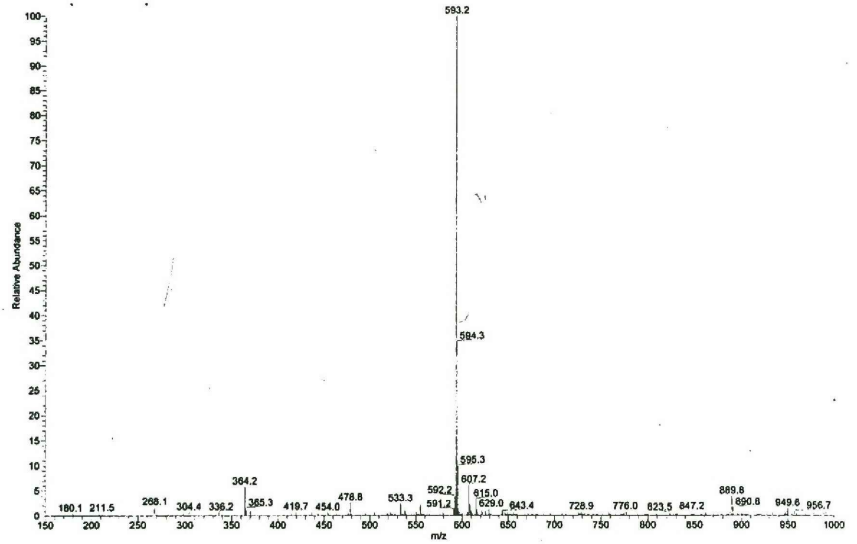


Figure 4.32 Electrospray ionization mass spectrum of pheophytin-*a* (*m/z* 150 – 1000)

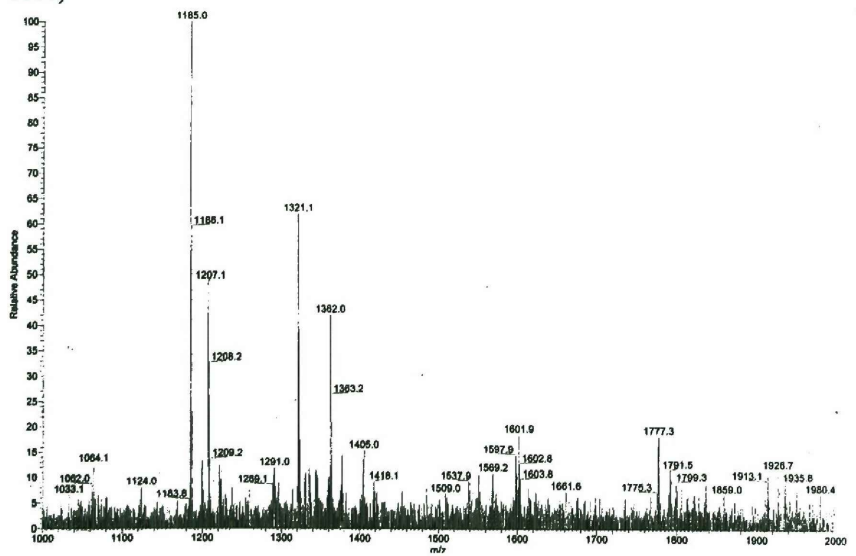


Figure 4.33 Electrospray ionization mass spectrum of pheophytin-*a* (*m/z* 1000 – 2000)

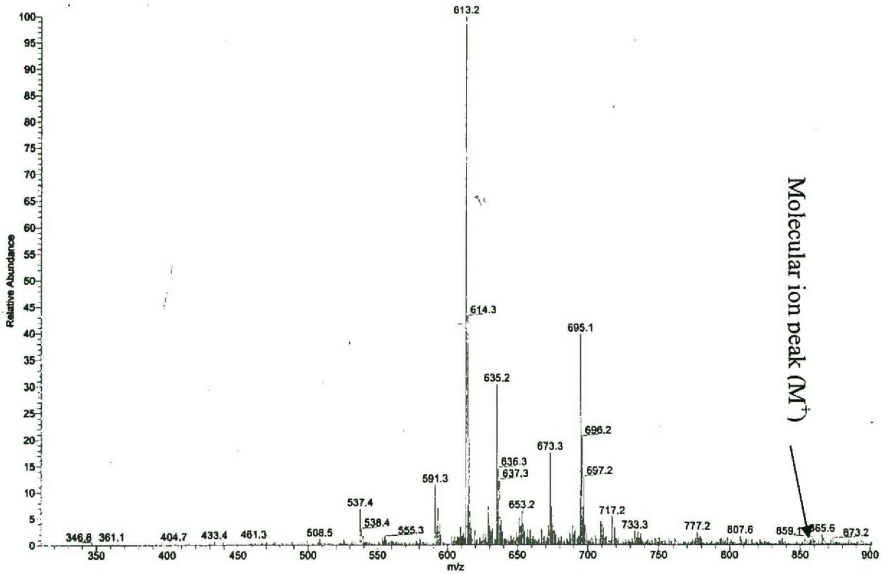


Figure 4.34 Electrospray ionization mass spectrum of chlorophyll-*a* (*m/z* 350 – 900)

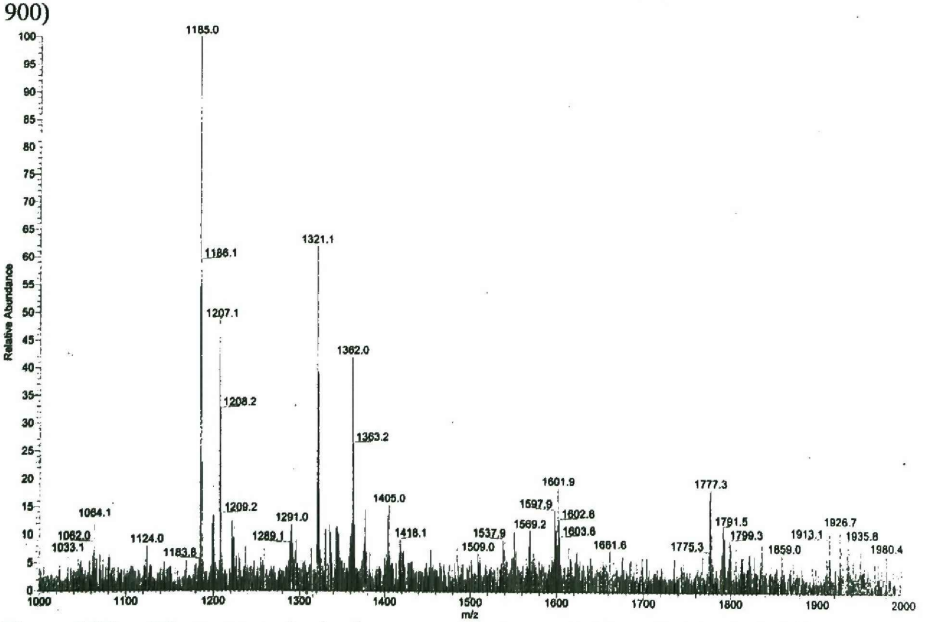


Figure 4.35 Electrospray ionization mass spectrum of chlorophyll-*a* (*m/z* 1000 – 2000)

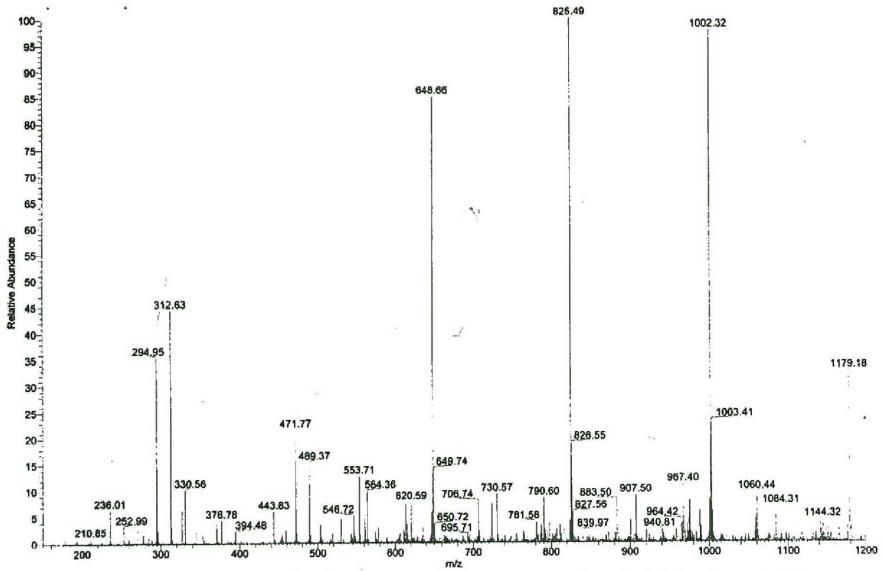


Figure 4.36 Electrospray ionization mass spectrum of cobalt(II) pheophytin-*a* complex. (*m/z* 200 – 1200)

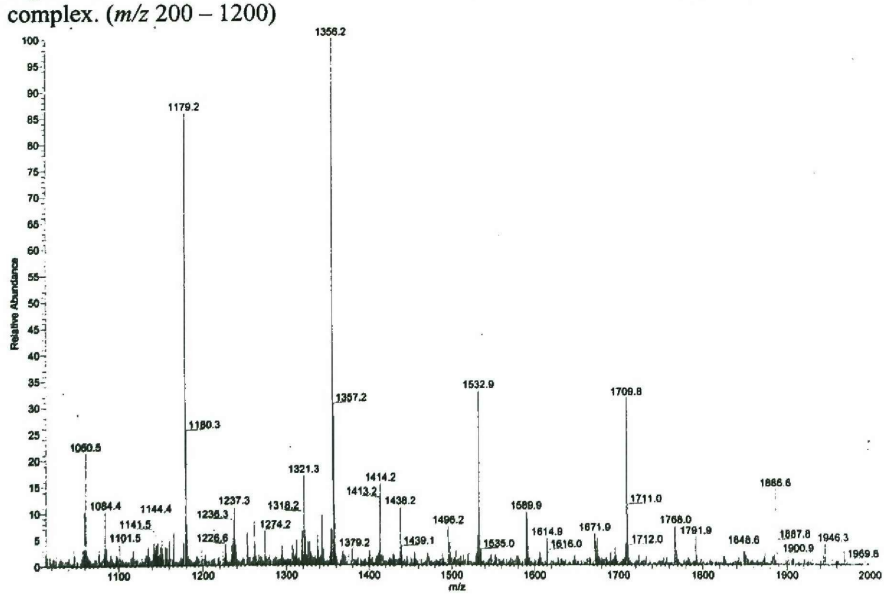


Figure 4.37 Electrospray ionization mass spectrum of cobalt(II) pheophytin-*a* complex. (*m/z* 1100 – 2000)

4.4 ELEMENTAL ANALYSES

Elemental analyses of the isolated metal pheophytin complexes (percentages of carbon, hydrogen and nitrogen in the various complexes) produced results that are in agreement with the formulations of the complexes.

The percentage composition of carbon, hydrogen and nitrogen in the various metal complexes are shown in Figures 4.38 – 4.42 and in Table 4.25.

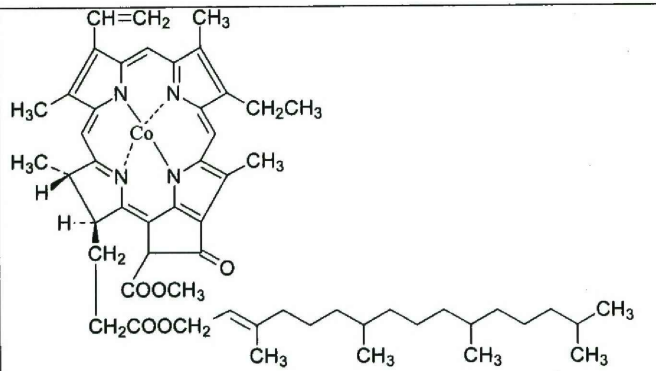
Name	Cobalt(II) pheophytin-*a* (Cophe)		
Formula	$C_{55}H_{72}N_4O_5Co$		
Relative Molecular Mass	928.13		
Structure			
ELEMENTAL ANALYSIS (%)			
	C	H	N
Found	70.93	7.98	5.90
Calculated	71.18	7.82	6.04

Figure 4.38 Elemental analysis of cobalt(II) pheophytin-*a* (Cophe)

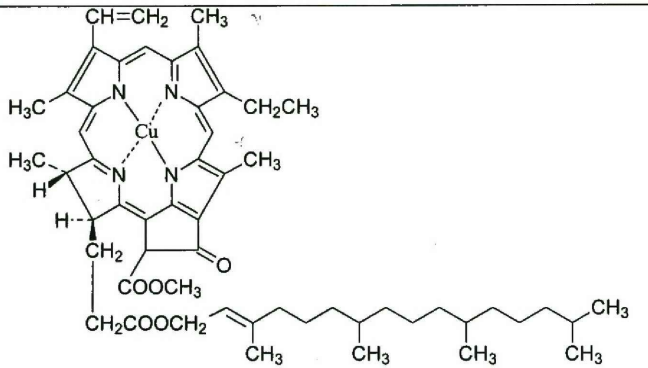
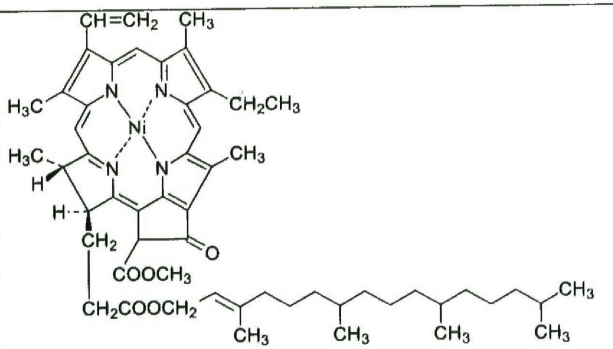
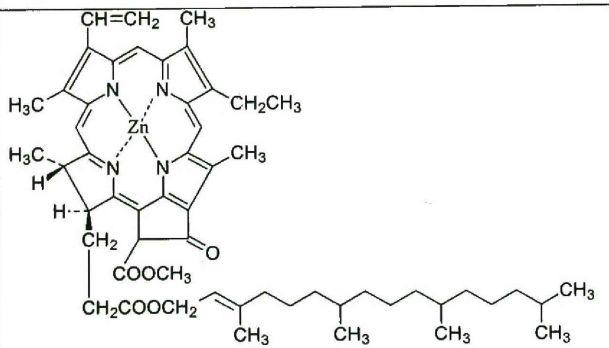
Name	Copper(II) pheophytin-*a* (Cuphe)		
Formula	$C_{55}H_{72}N_4O_5Cu$		
Relative Molecular Mass	932.75		
Structure			
ELEMENTAL ANALYSIS (%)			
	C	H	N
Found	70.56	7.91	5.77
Calculated	70.82	7.78	6.01

Figure 4.39 Elemental analysis of copper(II) pheophytin-*a* (Cuphe)

Name	Nickel(II) pheophytin-*a* (Niphe)
Formula	$C_{55}H_{72}N_4O_5Ni$
Relative Molecular Mass	927.89
Structure	

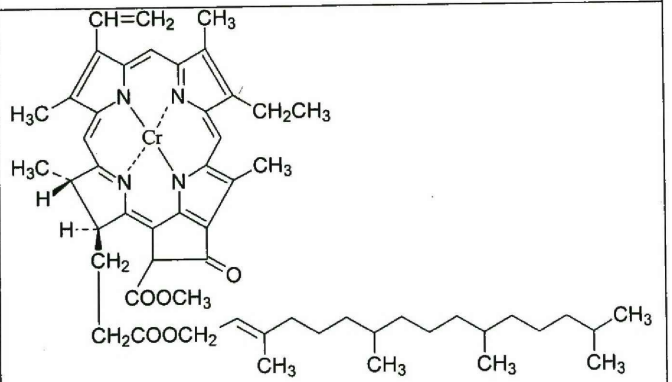
ELEMENTAL ANALYSIS (%)			
	C	H	N
Found	71.40	7.95	5.79
Calculated	71.19	7.82	6.04

Figure 4.40 Elemental analysis of nickel(II) pheophytin-*a* (Niphe)

Name	Zinc pheophytin-*a* (Znphe)
Formula	$C_{55}H_{72}N_4O_5Zn$
Relative Molecular Mass	934.58
Structure	

ELEMENTAL ANALYSIS (%)			
	C	H	N
Found	70.54	8.01	6.15
Calculated	70.68	7.77	5.99

Figure 4.41 Elemental analysis of zinc pheophytin-*a* (Znphe)

Name	Chromium(III) pheophytin-*a* (Crphe)
Formula	$C_{55}H_{72}N_4O_5Cr\ C\ell$
Relative Molecular Mass	956.70
Structure	

ELEMENTAL ANALYSIS (%)			
	C	H	N
Found	69.28	7.79	5.99
Calculated	69.05	7.60	5.86

Figure 4.42 Elemental analysis of chromium(II) pheophytin-*a* (Crphe)

Table 4.25 Summary of percentage composition by mass of carbon, hydrogen and nitrogen in metal pheophytin complexes.

Pheophytin Complex		**C (%)**	**H (%)**	**N (%)**
Cophe	Found Calculated	70.93 71.18	7.98 7.82	5.90 6.04
Cuphe	Found Calculated	70.56 70.82	7.91 7.78	5.77 6.01
Znphe	Found Calculated	70.54 70.68	8.01 7.77	6.15 5.99
Niphe	Found Calculated	71.40 71.19	7.95 7.82	5.79 6.04
[Crphe]Cℓ	Found Calculated	69.28 69.05	7.79 7.60	5.99 5.86

4.5 KINETICS OF OXIDATION OF COBALT(II) PHEOPHYTIN-*a* BY HEXAAQUACHROMIUM(III) CATION

Preliminary repetitive scanning of the ultraviolet-visible spectral region during oxidation of the cobalt(II) pheophytin-*a* complex (Cophe) by hexaaquachromium(III) cation, ($[Cr(H_2O)_6]^{3+}$) in 0.1 mol/dm^3 hydrochloric acid solution gave well-defined isosbestic points at 323, 442.3, 519.2 and 608.8 nm for more than 2 half-lives of the reaction. The spectral changes at different temperatures are shown in Figures 4.43 - 4.45.

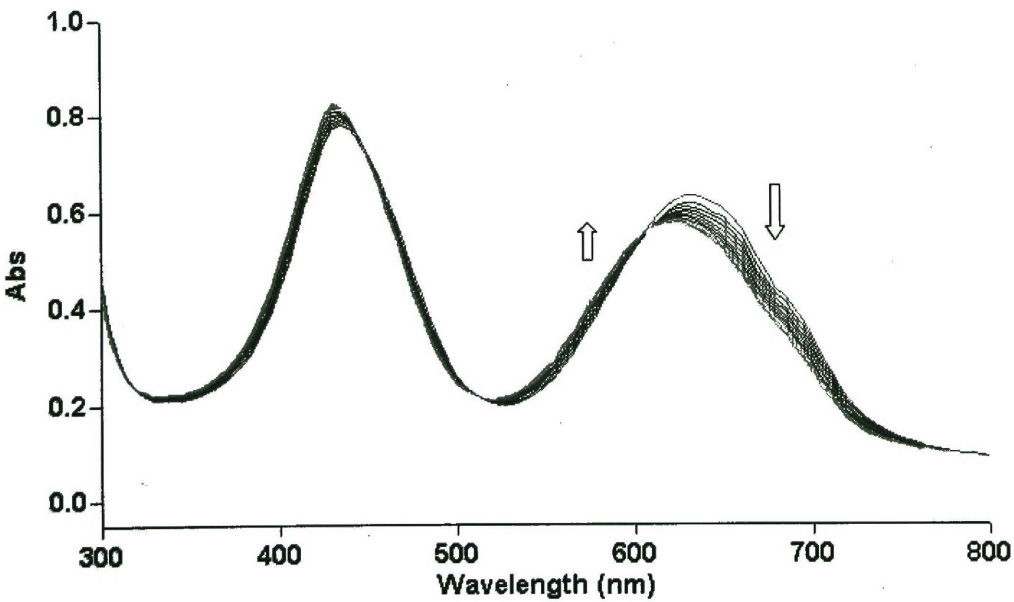


Figure 4.43 Spectral changes during the reaction of Cophe and ($[Cr(H_2O)_6]^{3+}$) in (0.1 mol/dm^3) hydrochloric acid solution at 5-minute intervals and at 313 K.

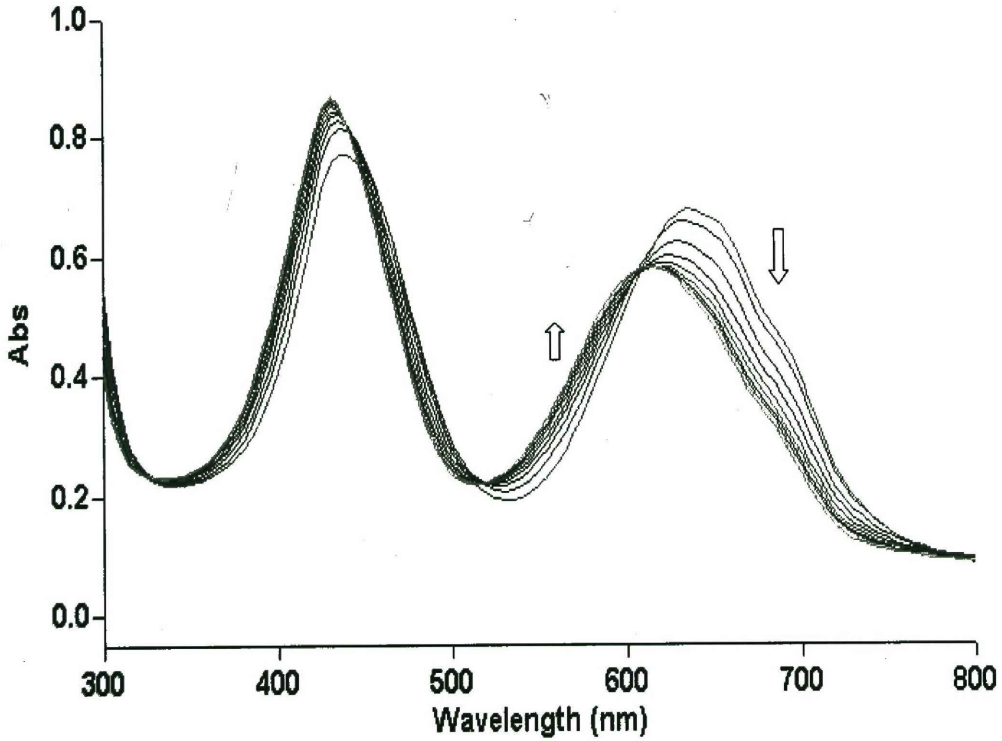


Figure 4.44 Spectral changes during the reaction of Cophe and ($[Cr(H_2O)_6]^{3+}$) in (0.1 mol/dm^3) hydrochloric acid solution at 10-minute intervals and at 323 K

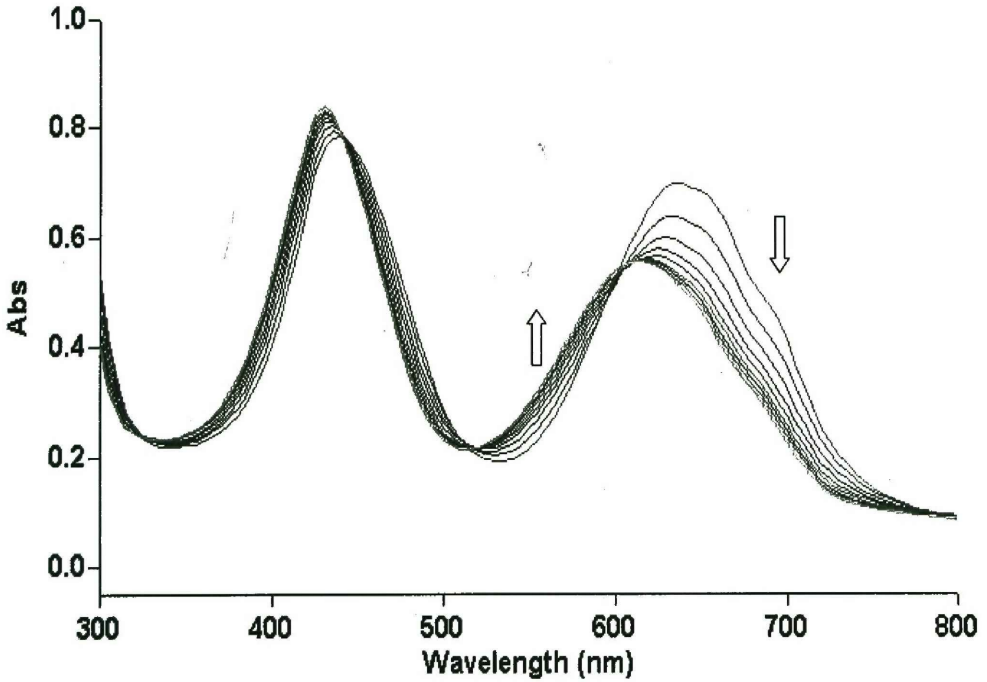


Figure 4.45 Spectral changes during the reaction of Cophe and ($[Cr(H_2O)_6]^{3+}$) in (0.1 mol/dm^3) hydrochloric acid solution at 20-minute intervals and at 333 K

The kinetics of the oxidation of cobalt(II) pheophytin-*a* was then followed at a fixed wavelength (630 nm) and the first order rate constants were obtained from plots of

$\ln[(A_t - A_\infty)/(A_0 - A_\infty)]$ versus time in minutes.

A_t = Absorbance at time t

A_0 = Absorbance at initial time

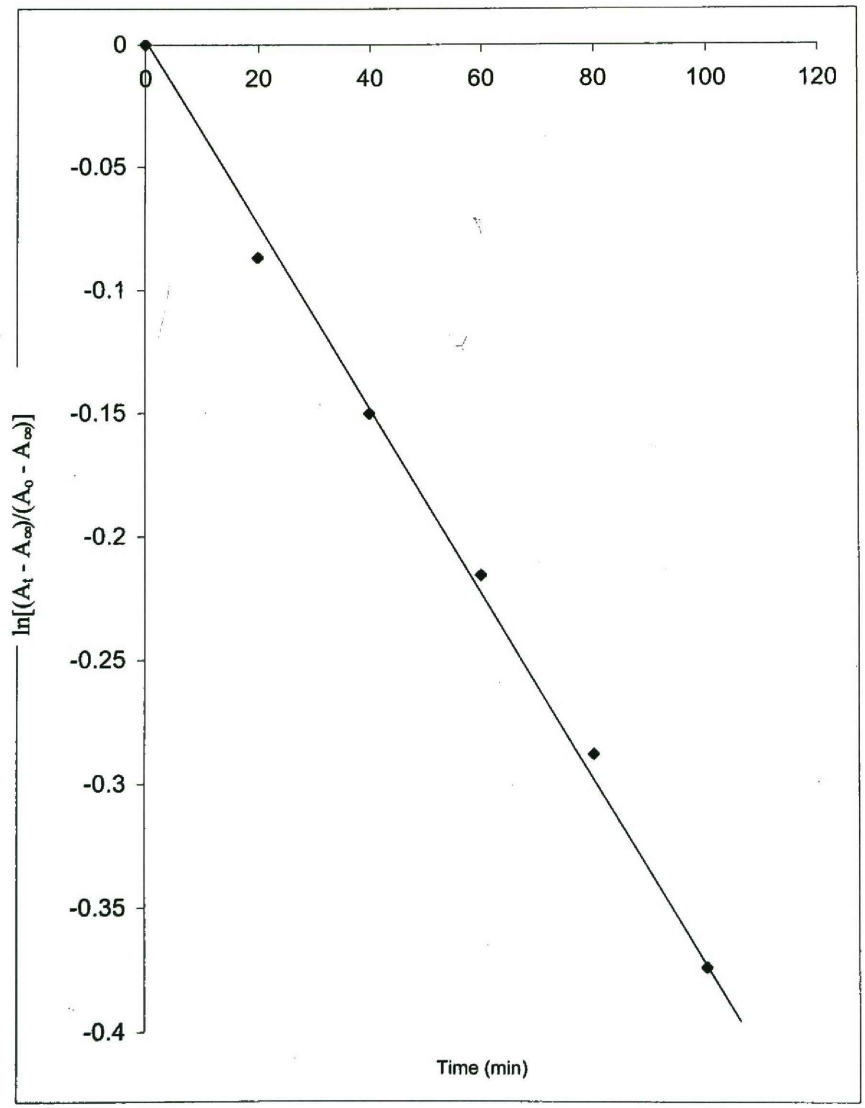
A_∞ = Absorbance at infinity

4.5.1 THE OXIDATION OF COBALT(II) PHEOPHYTIN-*a* BY HEXAAQUACHROMIUM(III) CATION AT 313 K

The kinetics of the oxidation of cobalt(II) pheophytin-*a* (Cophe: 6.45 x 10^{-5} mol/dm^3) with hexaaquachromium(III) cation ($([Cr(H_2O)_6]^{3+}$): 0.01 mol/dm^3) in hydrochloric acid (0.1 mol/dm^3) solution was then followed at a fixed wavelength of 630 nm, where the largest change in absorption was observed. Kinetic plots at 313 K are displayed in Figures 4.50 and 4.51.

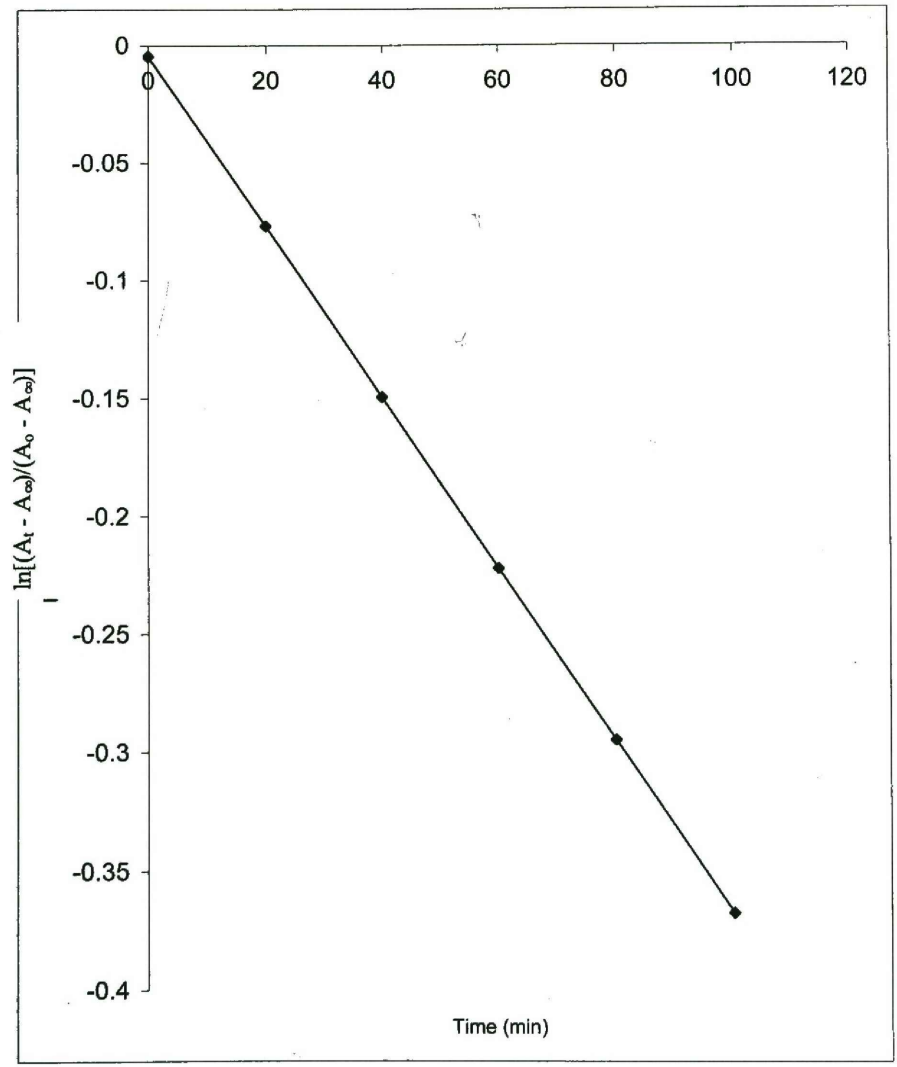
Table 4.26 Kinetic results for the oxidation of cobalt(II) pheophytin-*a* by hexaaquachromium(III) cation.

Time (minutes)	**Absorbance**	$(A_t-A_\infty)/(A_0-A_\infty)$	$\ln[(A_t-A_\infty)/(A_0-A_\infty)]$	Least square plot
0	0.5959	1	0	-0.00456
20	0.5715	0.916724	-0.08695	-0.07716
40	0.555	0.86041	-0.15035	-0.14976
60	0.539	0.805802	-0.21592	-0.22236
80	0.5226	0.749829	-0.28791	-0.29496
100	0.5045	0.688055	-0.37389	-0.36756



Rate constant = 5.4×10^{-5} s^{-1}

Figure 4.46 A typical plot of the oxidation of cobalt(II) pheophytin-*a* [6.45×10^{-5} mol/dm^3] by hexaaquachromium(III) cation at 313 K



Rate constant = 6.1×10^{-5} s^{-1}

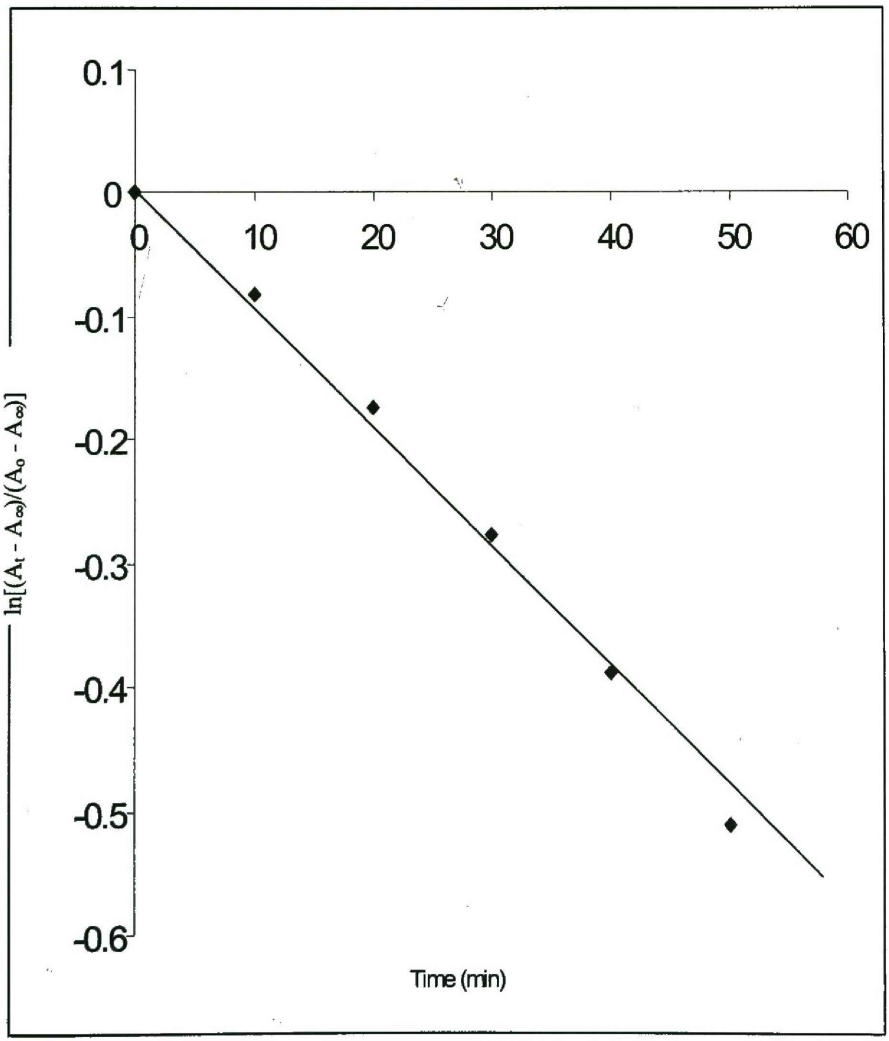
Figure 4.47 Least squares[141] kinetic plot for the oxidation of cobalt(II) pheophytin-*a* by hexaaquachromium(III) cation at 313 K

4.5.2 THE OXIDATION OF COBALT(II) PHEOPHYTIN-*a* BY HEXAAQUACHROMIUM(III) CATION AT 323 K

The Kinetics of the oxidation of cobalt(II) pheophytin-*a* (Cophe: 6.45 x 10^{-5} mol/dm^3) with hexaaquachromium(III) cation ($([Cr(H_2O)_6]^{3+}$): 0.01 mol/dm^3) in hydrochloric acid (0.1 mol/dm^3) solution was then followed at a wavelength of 630 nm. Kinetic plots at 323 K are displayed in Figures 4.48 and 4.49.

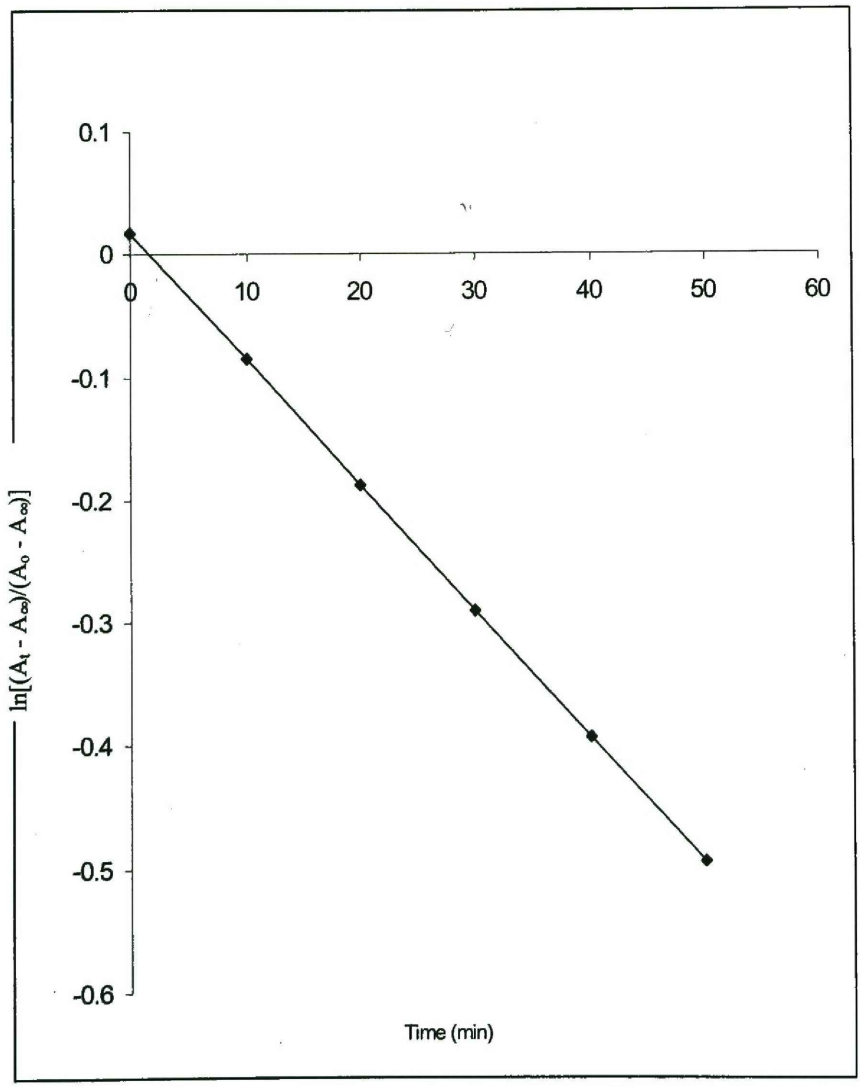
Table 4.27 Kinetic results for the oxidation of cobalt(II) pheophytin-*a* by hexaaquachromium(III) cation at 323 K

Time (minutes)	**Absorbance**	$(A_t-A_\infty)/(A_0-A_\infty)$	$\ln[(A_t-A_\infty)/(A_0-A_\infty)]$	Least squares plot
0	0.678	1	0	0.017128
10	0.6486	0.921621	-0.08162	-0.08527
20	0.6181	0.840309	-0.17399	-0.18767
30	0.5873	0.758198	-0.27681	-0.29007
40	0.5573	0.678219	-0.38828	-0.39247
50	0.5277	0.599307	-0.51198	-0.49487



Rate constant = 1.8×10^{-4} s^{-1}

Figure 4.48 A typical plot of the oxidation of cobalt(II) pheophytin-*a* [6.45×10^{-5} mol/dm^3] by hexaaquachromium(III) cation at 323 K



Rate constant = 1.7×10^{-4} s^{-1}

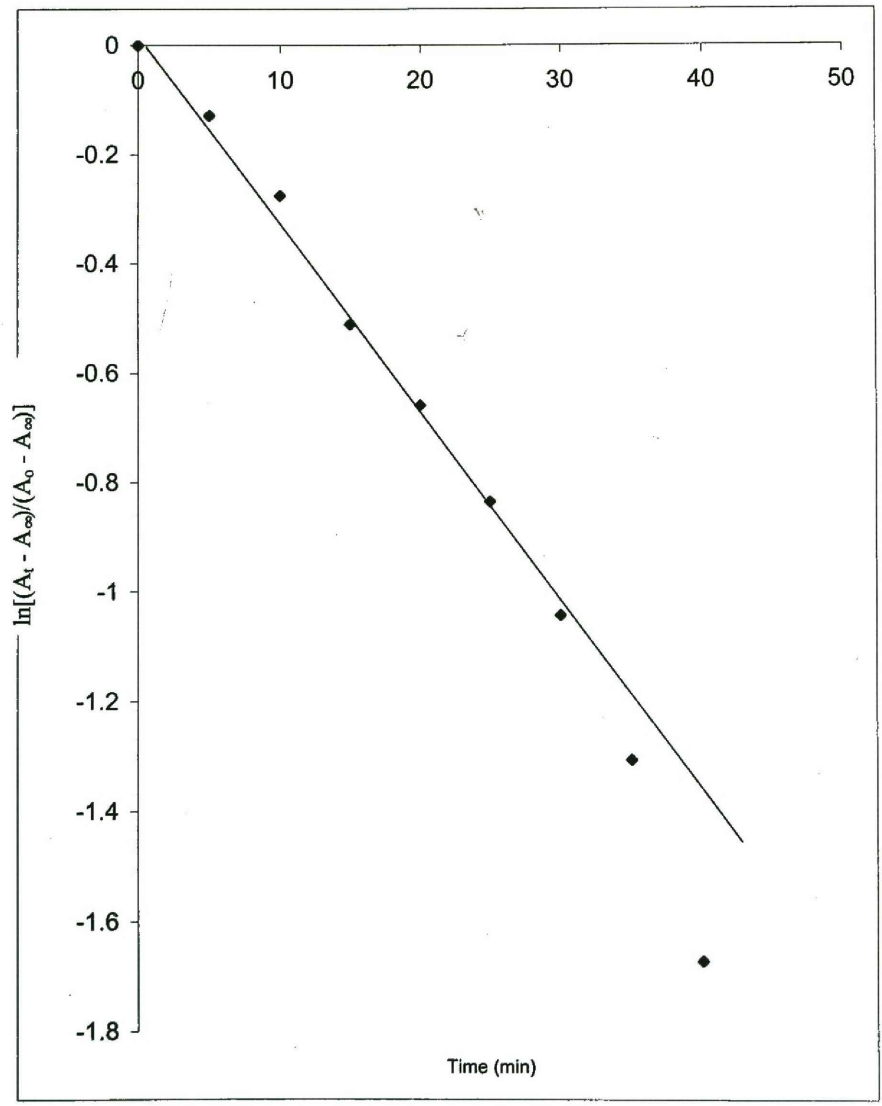
Figure 4.49 Least squares kinetic plot for the oxidation of cobalt(II) pheophytin-*a* by hexaaquachromium(III) cation at 323 K

4.5.3 THE OXIDATION OF COBALT(II) PHEOPHYTIN-*a* BY HEXAAQUACHROMIUM(III) CATION AT 333 K

Kinetics of the oxidation of cobalt(II) pheophytin-*a* (Cophe: 6.45 x 10^{-5} mol/dm^3) with hexaaquachromium(III) cation ($[Cr(H_2O)_6]^{3+}$): 0.01 mol/dm^3) in hydrochloric acid (0.1 mol/dm^3) solution was then followed at a wavelength of 630 nm. Kinetic plots at 333 K are displayed in Figures 4.50 and 4.51.

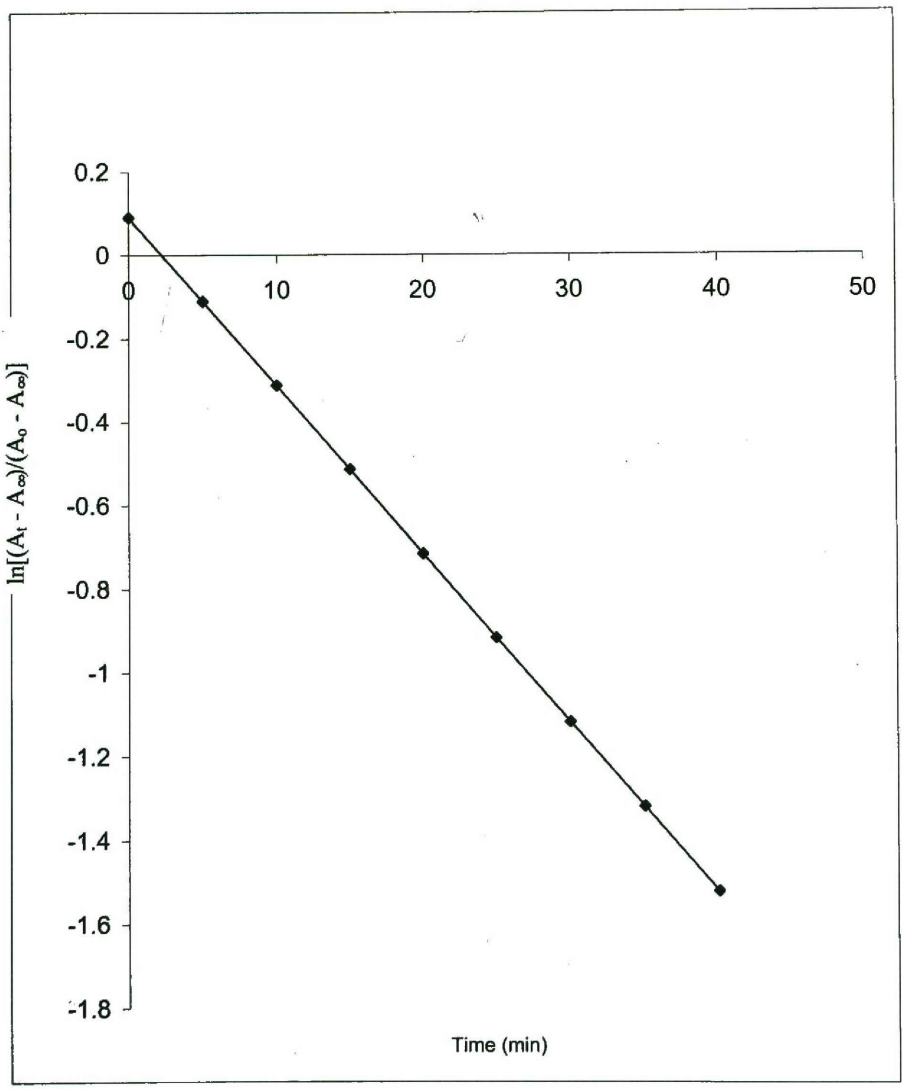
Table 4.28 Kinetic results for the reaction of cobalt(II) pheophytin-*a* by hexaaquachromium(III) cation.

Time (minutes)	**Absorbance**	$(A_t-A_\infty)/(A_o-A_\infty)$	$\ln[(A_t-A_\infty)/(A_o-A_\infty)]$	Least Squares
0	0.7333	1	-1.1E-16	0.090306
5	0.6813	0.879182	-0.12876	-0.11114
10	0.6293	0.758364	-0.27659	-0.31259
15	0.5607	0.598978	-0.51253	-0.51404
20	0.5253	0.516729	-0.66024	-0.71549
25	0.4893	0.433086	-0.83682	-0.91694
30	0.4544	0.351998	-1.04413	-1.11839
35	0.4193	0.270446	-1.30768	-1.31984
40	0.3837	0.187732	-1.67274	-1.52129



Rate constant = 5.9×10^{-4} s^{-1}

Figure 4.50 A typical plot of the oxidation of cobalt(II) pheophytin-*a* [6.45×10^{-5} mol/dm^3] by hexaaquachromium(III) cation at 333 K



Rate constant = 6.7×10^{-4} s^{-1}

Figure 4.51 Least squares kinetic plot for the oxidation of cobalt(II) pheophytin-*a* by hexaaquachromium(III) cation at 333 K

First order rate constants for the oxidation of cobalt(II) pheophytin-*a* (Cophe) by hexaaquachromium(III) cation ($[Cr(H_2O)_6]^{3+}$) at different temperatures.

Table 4.29 Table of calculated and best–fit (least squares) rate constants at different temperatures for the oxidation of cobalt(II) pheophytin-*a* by hexaaquachromium(III) cation.

Temperature (K)	**Rate Constant (s^{-1})**	**Least Square Rate Constant (s^{-1})**
313	5.4×10^{-5}	6.1×10^{-5}
313	7.9×10^{-5}	7.0×10^{-5}
323	1.8×10^{-4}	1.7×10^{-4}
323	1.7×10^{-4}	1.7×10^{-4}
323	1.8×10^{-4}	1.7×10^{-4}
333	5.9×10^{-4}	6.7×10^{-4}
333	5.2×10^{-4}	6.6×10^{-4}

4.5.4 ARRHENIUS PARAMETERS

Table 4.30 Kinetic results for the oxidation of cobalt(II) pheophytin-*a* by hexaaquachromium(III) cation.

Temperature (K)	Rate Constant (s^{-1})	$\frac{1}{T}$ (K)	ln K
313	5.4×10^{-5}	3.2×10^{-3}	-9.83
323	1.8×10^{-4}	3.1×10^{-3}	-8.62
333	5.9×10^{-4}	3.0×10^{-3}	-7.44

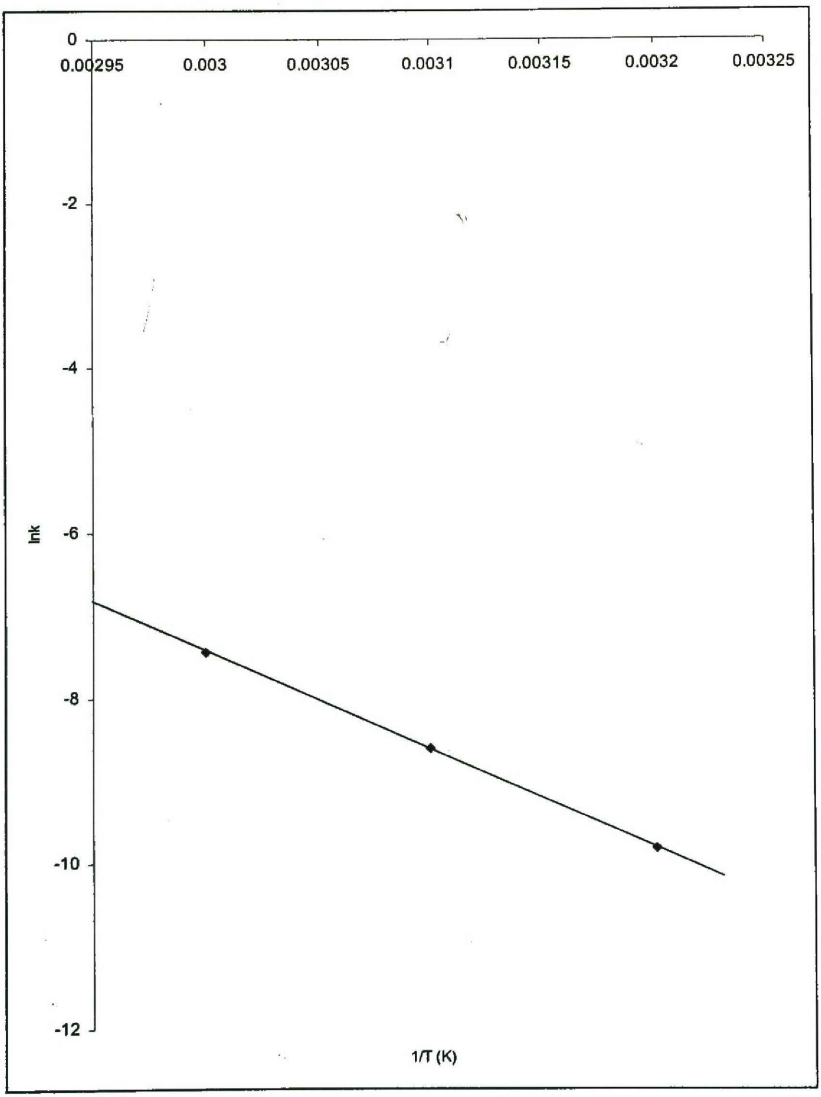


Figure 4.52 Temperature dependence of the first-order rate constant for the oxidation of Cophe by ($[Cr(H_2O)_6]^{3+}$)

Slope = -11950 K

E_a = -8.314 J ~~K~~$^{+}$ mol^{-1} x -11950 ~~K~~

E_a = 99352.3 J mol^{-1}

E_a = 99.35 kJmol^{-1}

From the equation

$$\ln A = \ln k + \frac{E_a}{RT}$$

At 40°C (313 K)

$$\ln A = -9.83 + \frac{99.35kJ/mol}{8.314J/Kmolx313K}$$

$\ln A = -9.79\ s^{-1}$

$A = 5.6 \times 10^{-5}\ s^{-1}$

CHAPTER FIVE

DISCUSSION

5.1 EXTRACTION

Several methods[10,59] of extraction of chlorophyll-*a* were employed and found unsatisfactory. These methods (alumina column method and silica gel column method) produced "chlorophyll-*a*" with absorption bands different from those observed by other researchers.[1,3,140] In addition, the amount of chlorophyll-*a* in the final extract was significantly low, indicating the presence of impurities. In an attempt to address the shortcomings of these methods, the silica gel method was modified to improve the quality and quantity of chlorophyll-*a* extracted.

5.1.1 THE ALUMINA COLUMN METHOD (METHOD 1)

The extract chromatographed on an alumina stationary phase with toluene and a mixture of *n*-butanol, ethanol and water (3:1:1 v/v) as mobile phases was unsuccessful. This was in contrast to research reports[59] of the use of alumina and toluene as stationary and mobile phases, respectively.

This procedure was unsatisfactory in the light of the shape of the absorption bands in the ultraviolet-visible spectra and concentrations of chlorophyll-*a* and pheophytin-*a* obtained at the end of the chromatographic separation [Figures 4.1 and 4.3; Tables 4.1(b) and 4.3(b)].

The concentration of total chlorophyll obtained from this chromatographic separation was 2.013 mg/L, which is relatively low. The low amount of chlorophyll-*a* and pheophytin-*a* obtained here indicates that there is a large amount of carotene, xanthophylls and other chlorophyll degradation products in the extract.

The extraction procedure employed in this method is shown in Figure 5.1.

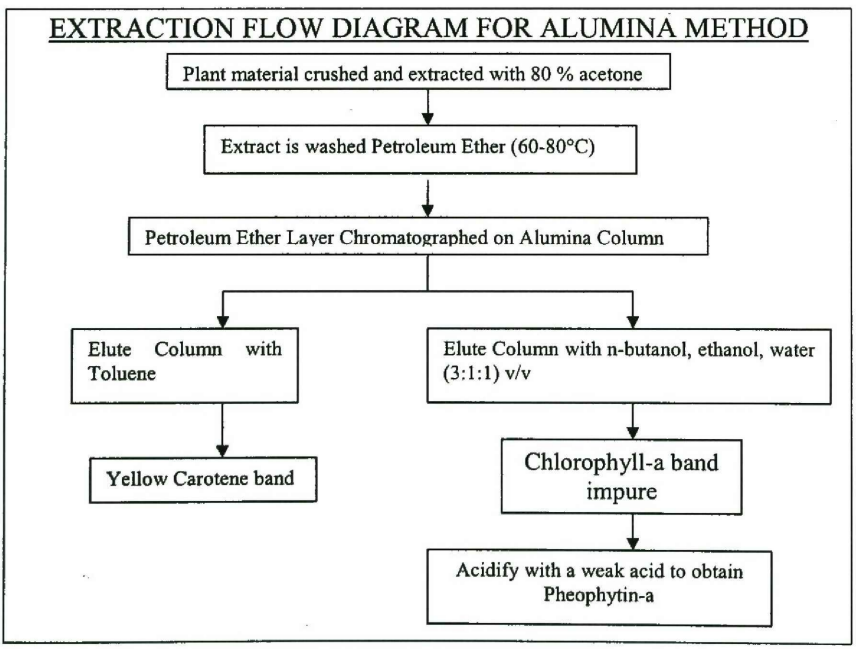


Figure 5.1 Extraction of chlorophyll using alumina column method (method 1)

5.1.2 SILICA GEL COLUMN METHOD (METHOD 2)

Silica gel was used as the stationary phase instead of alumina with toluene and *n*-butanol, ethanol and water (3:1:1 v/v) as mobile phases. This change resulted in absorption spectra with band shapes similar to those obtained in the alumina method, (Figures 4.3 and 4.4).

As in the case of the alumina column, this procedure was unsatisfactory in the light of the shape of the absorption bands in the ultraviolet-visible spectra and concentration of chlorophyll-*a* and pheophytin-*a* obtained at the end of the chromatographic separation. Figure 4.4, 4.6 and Table 4.4(b).

The concentration of total chlorophyll obtained in this chromatographic separation improved to 14.529 mg/L. However, the shape of the absorption bands in the ultraviolet-visible spectra is different to that reported in the literature.[3,12,140] The chlorophyll-*a* extract in the solvent system [*n*-butanol, ethanol and water (3:1:1 v/v)], was acidified with glacial acetic acid to give pheophytin-*a* in the expected colour, but could not be crystallized.

The extraction procedure employed in this method is summarized in the flow diagram shown in Figure 5.2.

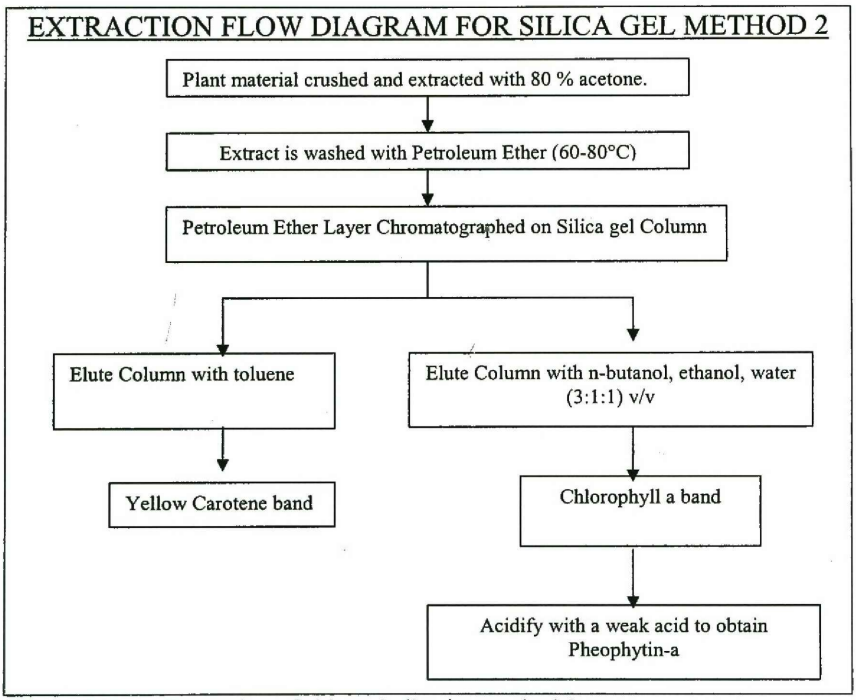


Figure 5.2 Extraction of chlorophyll using method 2

5.1.3 IMPROVED SILICA GEL COLUMN METHOD (METHOD 3)

Extraction of chlorophyll using the silica gel column method (Figure 5.2) was modified. This was because the shapes of the visible absorption bands of chlorophyll-*a* obtained from the previous methods (alumina method and silica gel method) were different from those reported in the literature.[3,12,59] The quantities of chlorophyll-*a* and pheophytin-*a* from the aforementioned methods of extraction were also significantly low compared to literature reports.

An improved silica gel column method was therefore developed and used.

In this modified silica gel column method, shown in Figure 5.3, the chlorophyll extract in the acetone was washed several times with petroleum ether and petroleum ether was used as the first mobile phase in the chromatographic column to elute carotene and carotenoids. A second mobile phase of petroleum ether and *n*-propanol was then used to elute chlorophyll-*a*.

The improvement in the extraction was such that the amount of total chlorophyll obtained in this modified method (27.005 mg/L) was higher than those obtained from the alumina column and the silica gel column (2.013 mg/L and 14.529 mg/L, respectively). The shape of the absorption bands and the wavelengths of absorption in this improved method (Figure 4.16) was in agreement with that obtained in literature reports.[3,12,19,140]

The advantage of this method in comparison to the other methods was that a liquid-liquid extraction procedure was used to obtain a good yield of chlorophyll. Due to several washings with petroleum ether and eluting the column with petroleum ether rather than with *n*-butanol, ethanol and water (3:1:1 v/v), carotenes, xanthophylls and other chlorophyll degradation products were greatly reduced.

Washing the methanol layer with petroleum ether several times helped to recover any chlorophyll that would otherwise have been lost. Washing the acetone layer and methanol layer with petroleum ether before chromatography, reduced the amount of carotene associated with the chlorophyll.

Carotenoids have been found[8,41,47,90,105,106] to mask the chlorophyll visible absorption spectra. Wilson and coworkers[104] used tetracyanoethylene to remove the visual carotenoids spectra from solutions of chlorophyll-*a* and pheophytin-*a*. Other researchers[41,47,90] have used HPLC methods to reduce the carotenoids content in chlorophyll. In order to improve on this in the absence of HPLC, diethyl ether was used in the extraction of chlorophyll (Figure 4.16). Several washings with the diethyl ether were employed before the extract was chromatographed on the silica gel stationary phase.

The chlorophyll-*a* and pheophytin-*a* obtained from this improved extraction process was much higher in quantity (Tables 4.10(b) &

4.11(b) and quality (Figures 4.10 & 4.11) compared to the previous methods. In addition, the absorption spectrum was very similar to those in the literature.[3,12,19,140]

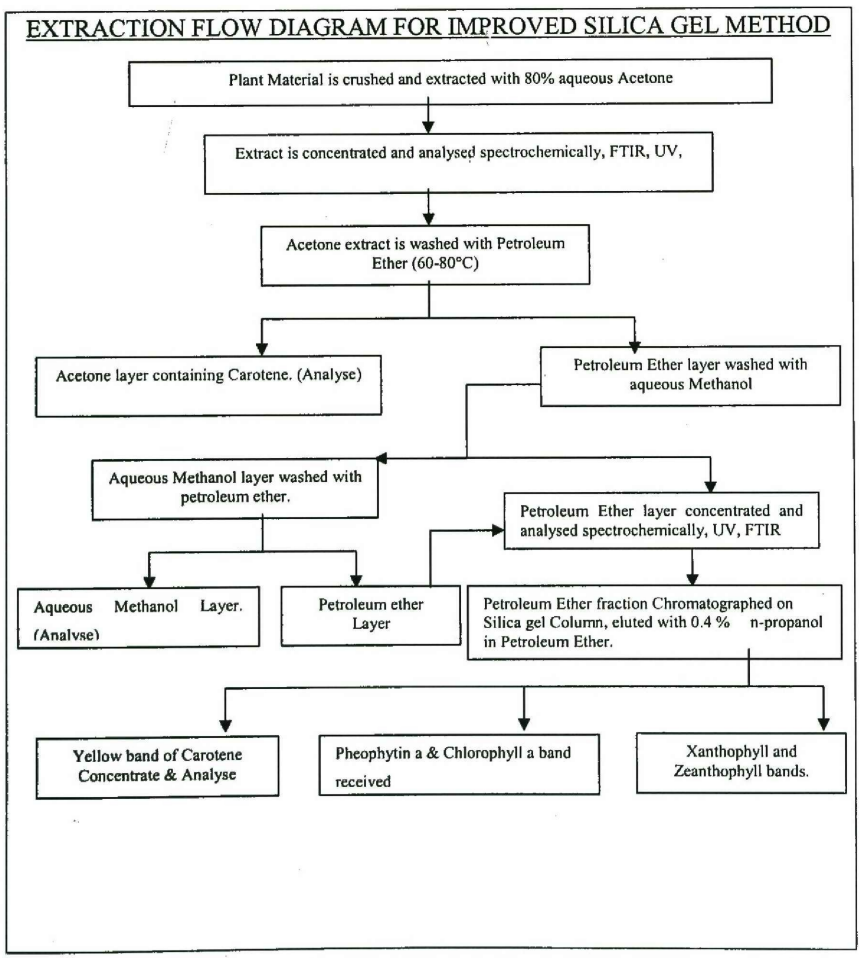


Figure 5.3 Extraction of chlorophyll using improved silica gel method 3

5.1.4 WINTER EXTRACTION METHOD (METHOD 4)

In the course of this work, it was noticed that spinach leaves extracted for chlorophyll during summer were easily extracted for chlorophyll using petroleum ether and diethyl ether and then purified by column chromatography.

In winter, however, it was observed that chlorophyll could not be extracted from spinach leaves using petroleum ether as was previously the case. Previous workers[139] have also described this difficulty in the extraction of chlorophyll. When extracted for chlorophyll with petroleum ether, the petroleum ether layer (Figure 4.14) was visibly yellowish showing that it was now richer in carotene and the carotenoids than in chlorophyll.

To overcome this apparent difficulty, after the spinach was extracted with 80% acetone and washed with petroleum ether several times, the acetone layer was then washed with diethyl ether (Figure 3.4). The petroleum ether fraction at this point removed most of the carotenoid content in the extract. When the extract in acetone was washed with diethyl ether, (Figure 4.15) the diethyl ether fraction was found to be greenish showing richness in chlorophyll pigment.

At this stage the concentration of total chlorophyll in the petroleum ether fraction was found to be 1.596 mg/L [Table 4.14(b)] while the

concentration of total chlorophyll in the diethyl ether fraction was found to be 19.618 mg/L [Table 4.15(b)].

Table 5.1 Comparison of the concentrations of total chlorophyll obtained from the different methods of extraction.

Method	Chromatographic Column	Solvent system	Concentration of total chlorophyll
Method 1	Alumina method	Butanol, ethanol & water	2.013 mg/L
Method 2	Silica method	Petroleum ether	14.529 mg/L
Method 3	Improved Silica method	Petroleum ether	27.005 mg/L
Method 4	Winter/Silica method	Diethyl ether	25.751 mg/L

From the comparison shown in Table 5.1, it can be observed that the concentration of total chlorophyll increased with improvement in the method of extraction employed in the extraction and purification of chlorophyll.

The improved silica gel method of extraction could be seen as an efficient and convenient method to obtain chlorophyll-*a*. This method is also cost-effective and reliable especially where advanced analytical chemistry laboratory automations are lacking. Thus, this method of extraction is highly recommended for isolation of chlorophyll and pheophytin from plant material.

5.2 CHARACTERIZATION

5.2.1 ULTRAVIOLET-VISIBLE SPECTROSCOPY

The absorption spectrum of chlorophyll-*a* shows a strong absorption band in the red region of the spectrum and a more intense absorption band in the blue region of the spectrum.

In some of the spectra, Figure 4.16, a prominent shoulder appears on the high-energy side of the blue band. The ultraviolet and visible spectra of chlorophyll-*a* show four distinct absorption bands labelled B_y, B_x, Q_x and Q_y bands in order of decreasing transition energies. The absorption spectra of pheophytin-*a*, on the other hand show six absorption bands.

These bands are observed at 430 nm (B_y) and 451 nm (B_x) in petroleum ether Figure 4.10 and at 429 nm (B_y) and 530 nm (B_x) in diethyl ether (Figure 4.16). The Q_x and Q_y bands are observed at 616 nm (Q_x) and 663 nm (Q_y) in petroleum ether (Figure 4.10), whereas in diethyl ether, these bands are observed at 618 nm (Q_x) and 661 nm (Q_y) (Figure 4.16).
These absorption bands are in complete agreement with data obtained by other researchers. [19,140]

The spectra can be understood on the basis of the four orbital model for porphyrins and their derivatives.

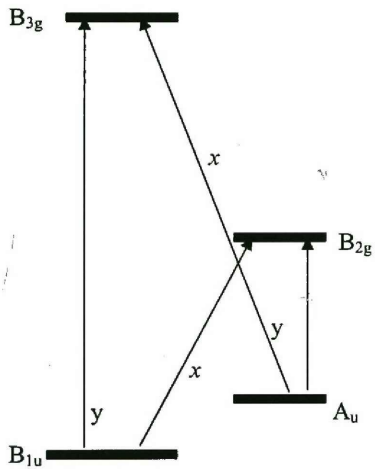


Figure 5.4 Frontier orbitals of chlorophyll

For D_{4h} metalloporphyrins, the two degenerate lowest unoccupied molecular orbitals (LUMO, e_g^*) and two nearly degenerate highest occupied molecular orbitals (HOMO, a_{1u} and a_{2u}) give rise to a strong soret band in the near-UV region and weak Q bands in the visible region. However, in the D_{2h} symmetry, the degenerate e_g^* (D_{4h}) LUMOs split into x and y components (b_{3g} and b_{2g}). The b_{3g} and a_u orbitals are more destabilized relative to b_{2g} and b_{1u} because of their orbital nodal pattern.[113] This is illustrated in Figure 5.4.

These possible electronic transitions in the above Figure, account for the peaks observed in the spectra of chlorophyll shown in Figure 4.16. The aromatic nitrogen heterocycles are known to possess low-lying n-π^* states attained by the promotion of a nonbonding electron localised on nitrogen into the lowest antibonding level of the π-system. The π^*

level is assumed to remain fixed since the main red band in the visible absorption spectra of chlorophyll-*a* and pheophytin-*a*, the first π-π^* transition differs by only 5 – 8 nm (λ_{max} 663 and 667 nm (Figure 4.10) and 661 and 666 nm (Figure 4.16).

5.2.2 INFRARED SPECTROSCOPY

The modern interpretation of chlorophyll infrared spectra is based mainly on the work of Katz and his coworkers.[57,110-112]

The region of greatest significance is the carbonyl region containing the stretching frequencies of the *C_7,**(C_{17}) propionic ester, the *C_{10} **(C_{13}^2) methylcarboxylate, the *C_9,**(C_{13}^1) carbonyl and the conjugated ring systems. The various chlorophyll-numbering systems are shown in Figure 5.5

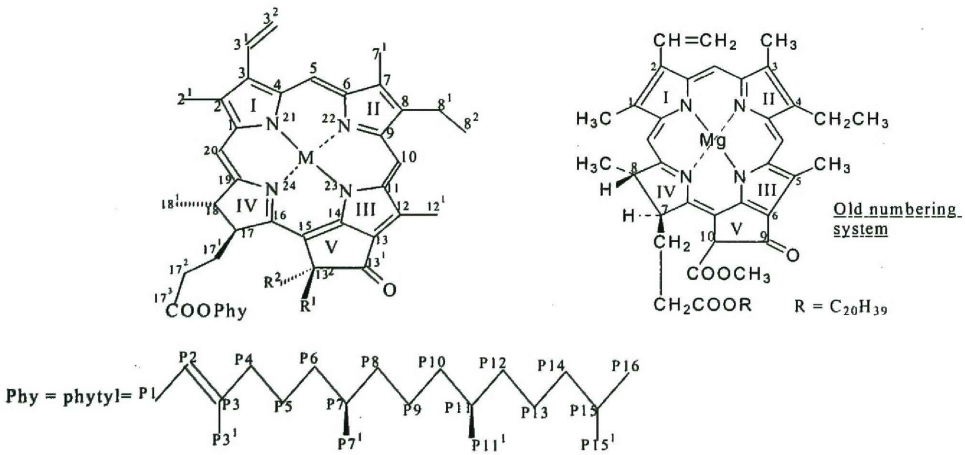


Figure 5.5 New(**) and old(*) numbering systems for Chlorophyll

The two ester groups absorb in the range 1735 – 1740 cm^{-1} in monomeric chlorophyll, the C_9 carbonyl absorbs near 1695 cm^{-1} and

in dimeric chlorophyll where the chlorophyll is bound to magnesium, it absorbs near 1650 cm^{-1}.

Infrared studies have shown that the coordination number of magnesium in chlorophyll is always larger than 4 and the coordination properties of magnesium determine the state of chlorophyll in solution. In electron donor solvents, the solvent molecules relieve the coordination unsaturation. [31,57,112,118,119]

In solvents such as pyridine, tetrahydrofuran, acetone and the like, chlorophyll is monomeric with solvent molecules in the axial positions. In non-polar solvents, the coordination unsaturation of the magnesium cannot be satisfied by the solvent, and coordination interaction of the ketone oxygen function of one chlorophyll molecule with the magnesium of another is the option that is exercised.

Thus in non-polar solvents, chlorophyll occurs as dimeric or as oligomers held together by *C=O---Mg* interactions. Figure 5.6 shows a model of C=O----Mg bond between two chlorophyll molecules. The coordination number of chlorophyll in this model is 4.

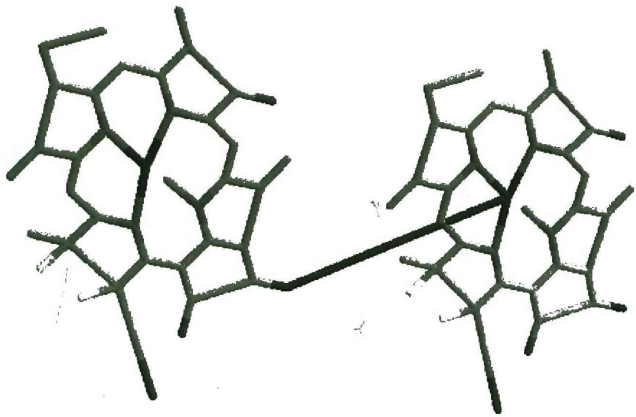


Figure 5.6 Dimeric chlorophyll held by *C=O---Mg* interaction showing magnesium with four bonds.

The presence of water in chlorophyll extraction has a special relationship.[112] The decrease of the free keto *C=O* absorption peak at 1698 cm^{-1} and the increase in the peak near 1650 cm^{-1} is due to the presence of water. Water acts as a nucleophile for chlorophyll-*a* in carbon tetrachloride (CCl_4) solution, equation [5.1].

$$Chl_2 + 2H_2O \rightleftharpoons 2Chl.H_2O \qquad [5.1]$$

Infrared analysis of chlorophyll-*a* extract in petroleum ether in the improved silica gel method, Figure 4.24 obtained from the liquid sample shows prominent absorption bands. C—H aliphatic stretching vibrations of the ligand macrocyclic ring are observed as strong bands at 2961, 2919 and 2851 cm^{-1}. The strong bands at 1455 and 1378 cm^{-1} could be regarded as alkyl C—H bending asymmetric vibrations and

bending symmetric vibrations originating from the phytal chain. And could also be due to C=C vibrations of the porphyrin ring system.
An important vibrational signal observed here is the weak signal at 3021 cm^{-1} due to N—H stretching vibration of chlorophyll converted to pheophytin. In this infrared spectra, the absorbance due to the two esters and $*C_9$ ketones (C=O), which should be observed at 1735 - 1740 cm^{-1} for monomeric chlorophyll and at 1695 – 1650 cm^{-1} are observed as weak vibrations. The fact that this very important vibration is found in this infrared spectra coupled with the presence of charge transfer transitions in the ultraviolet and visible spectra (Figure 4.11) at 615, 579 & 535nm shows that the solution obtained at this point in the analysis is chlorophyll-*a*.

The use of silica gel as the stationary phase in the purification of chlorophyll was employed. The chlorophyll-*a* obtained using this procedure were also analysed in the infrared region, Figure 4.24.
The absorption bands observed here are those of the alkyl C—H stretching vibrations at 2970, 2927 & 2876 cm^{-1}, which are in close agreement with published assignments.[31,57,112,119] There is the absence of the band at 3021cm^{-1}, which is an N—H stretching vibration arising from pheophytins.

The two ester and ketone absorption bands which appears as two peaks at 1700cm^{-1} is observed at 1719 cm^{-1} which could mean the presence of water in the chlorophyll extract.

After modification of the extraction procedure, Figure 3.3, the ultraviolet and visible spectral analysis of the chlorophyll-*a* and pheophytin-*a* obtained, show the presence of absorption bands that are consistent with literature values.[31,57,112]

The infrared spectra of this chlorophyll-*a* are shown in Figure 4.24 and 4.25. In the carbonyl stretching region, there are four notable absorption peaks at 1736, 1693, 1642 & 1557 cm^{-1}. The peak at 1736 cm^{-1} and the shoulder at 1720 cm^{-1} are ester carbonyl peaks consistent with chlorophyll absorption.[57,112]

The 1693cm^{-1} band is due to the free keto carbonyl and the peak at 1642 cm^{-1} is the peak due to aggregation of chlorophyll in solution. The broad band at 3404 cm^{-1} could be due to N—H stretching vibration and O—H stretching vibration probably originating from the acetic acid solvent.

5.2.3 MASS SPECTRAL ANALYSIS

Electrospray ionization mass spectra of chlorophyll-*a* produced several fragmentation peaks. These spectra are displayed in Figures 4.32 - 4.35.

Important fragmentation peaks for chlorophyll-*a*, observed and calculated mass to charge (m/z) ratios and their assignments are displayed in Table 5.2.

The most important peaks in this analysis are the peak with *(m/z)* 591.3_{obs} ($590.9_{calc.}$) and 613.2_{obs} ($613.9_{calc.}$) The peak at 613 has a relative abundance of 100%. This peak is due to the fragmentation of chlorophyll with the loss of the phytyl chain. The relative abundance of this peak shows the extract to be chlorophyll-*a*.

The peak *(m/z)* 591.3 results from the fragmentation of pheophytin-*a* formed in solution as a degradation product. The relative abundance of this peak at 591.3 (~10 %) shows that the percentage of chlorophyll that has converted into pheophytin is low.

In the mass spectrum of pheophytin-*a*, (Figures 4.32 and 4.33) the peak due to the loss of the phytyl chain during fragmentation is observed at a mass to charge (m/z) ratio of 593.2. This peak has a relative abundance of 100% also indicating the loss of the phytyl chain during fragmentation.

The molecular ion peak (M^{+1} or M^{+2}) of chlorophyll at *(m/z)* 894_{cal} or (895_{cal}) has a relative abundance of less than 5%.

Chlorophyll-*a* in water forms a dimer with a hydrogen bond, see [Figure 5.7(a and b)]. The peak at *m/z* $1823_{obs\ \&\ cal}$ indicates that the chlorophyll in acetic acid solution had dimerized.

Table 5.2. Fragmentation analysis for chlorophyll.

Observed *m/z*	**Assignment/Analysis**	**Calculated *m/z***
537.4		
555.3	Chla – phytyl - $COOCH_3$	893.5 – 278.6 – 59 = **555.9**
591.3	Chla – phytyl – Magnesium	893.5 – 278.6 – 24 = **590.9**
613.2/614.3	Chla – phytyl – proton	893.5 – 278.6 – 1 = **613.9**
635.2		
673.3	Chla – phytyl + $COOCH_3$	893.5 – 278.6 + 59 = **673.9**
695.1	Chla - $COOCH_3$ – $CH_2CH_2COOCH_3$ – $2H_2O$ – CH_3	893.5 - 59 – 87 – 36 – 15 = **696.5**
873.2	Chla – Magnesium + 2protons	893.5 – 24 + 2 = **871.5** (M+2)
1823	Chla. + water + chla + water (dimer)	893.5 + 18 + 893.5 +18 = **1823**
1799	Chla + chla	893.5 + 893.5 = **1797**
1039.9	1823 – 2[CH_2CH_2COO phytyl] + 2(water) – 2($COOCH_3$)	1823 – 700 + 36 – 118 = **1041**
1097.9	1823 – 2[CH_2CH_2COO phytyl] + 2(water) – $COOCH_3$	1823 – 700 + 36 – 59 = **1099**
1157.0	1823 – 2[CH_2CH_2COOphytyl] + 2(water)	1823 – 700 + 36 = **1159**
1203.2	[Chla + H_2O + chla +H_2O] – 2phytyl - $COOCH_3$	1823 – 557.2 – 59 = **1206.8**
1227.3	Chla + chla – 2phytyl	1787 – 557.2 = **1229.8**

The presence of these peaks and their fragmentation products at the above *m/z* values are indicative of the fact that the substance extracted is chlorophyll.

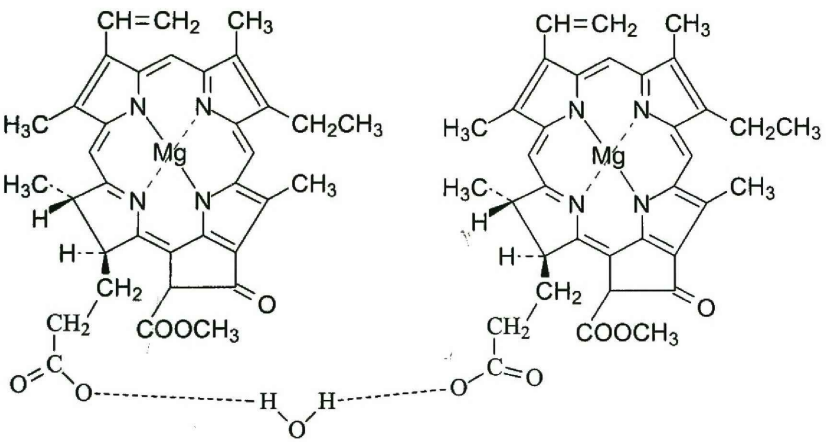


Figure 5.7(a) Chlorophyll-*a* and water dimer

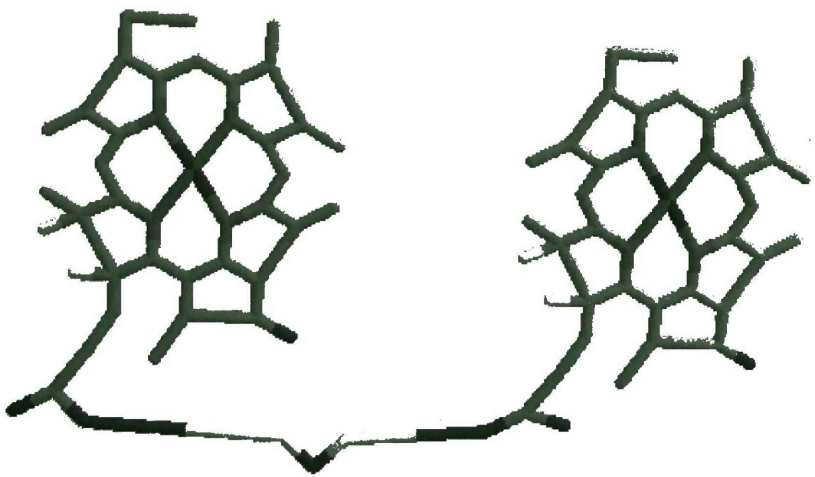


Figure 5.7(b) Chlorophyll-*a* –water dimer molecule model

The fragmentation of chlorophyll-*a* is as follows:

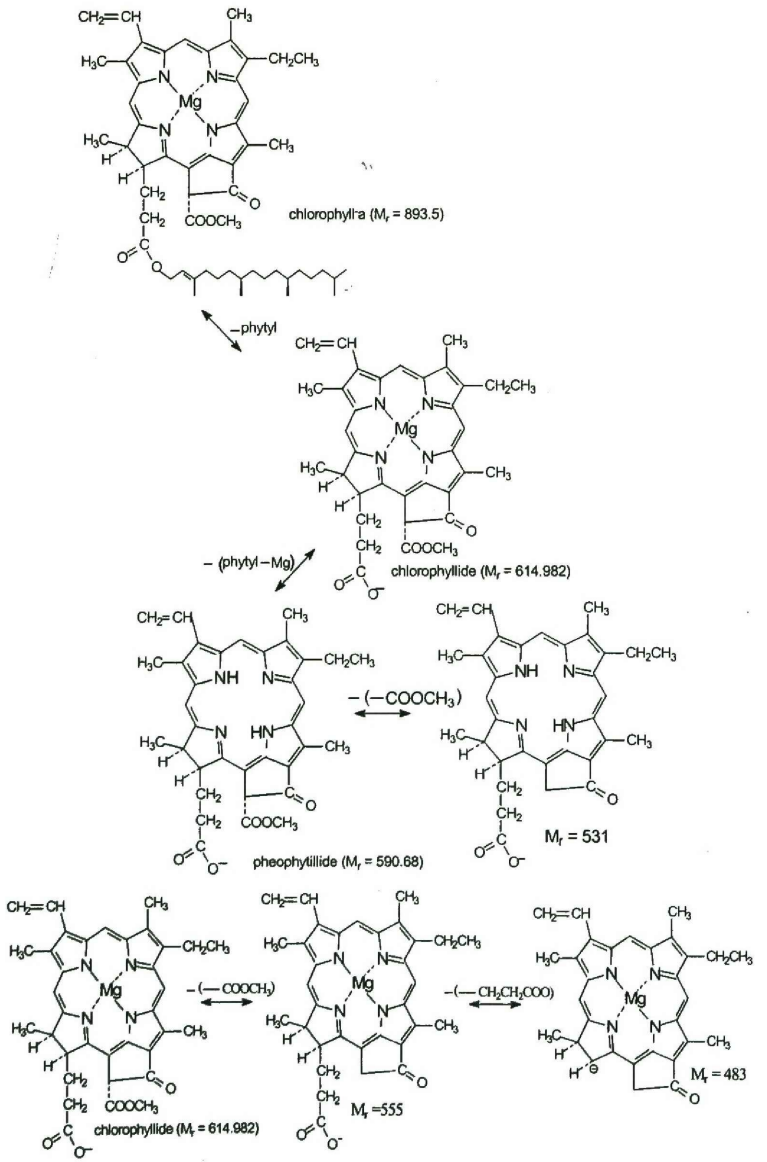


Figure 5.8 Fragmentation scheme for chlorophyll-*a*

The fragmentation pattern for the pheophytin could also be described similarly to that of chlorophyll-*a*.

The pheophytin molecular ion peak at *m/z* 871.5_{cal} is observed, but the pyrrolic ion without the phytyl moiety is a strong signal (nearly 100%) observed at *m/z* 593.2_{obs} (Figure 4.32). Other signals of interest (Figure 4.33) are those of dimeric pheophytin-*a* at *m/z* 1777.3_{obs} and the peaks due to the fragmentation of dimeric pheophytin-*a* at *m/z* 1064, 1185, 1321, & 1362. The fragmentation pattern of pheophytin-*a* is summarized in Table 5.3 and illustrated in Figure 5.9.

Table 5.3. Fragmentation analysis for pheophytin-*a*.

Observed *m/z*	**Assignments/Analysis**	**Calculated *m/z***
593.2	Pheo - phytyl	871.5 – 278.6 = **592.9**
533.3	Pheo – phytyl – $COOCH_3$	871.5 – 278.6 – 59 = **534**
1777.3	Pheo.H_2O.pheo.H_2O	871.5 + 18 + 871.5 + 18 = **1779**
1185.0	Pheo.H_2O.pheo.H_2O – 2phytyl – $2H_2O$	1779 – 557.2 – 36 = **1185.8**
1124.0	Pheo.H_2O.pheo.H_2O – 2phytyl – $2H_2O$ – $COOCH_3$	1185.8 – 59 = **1126.8**
1064.1	Pheo.H_2O.pheo.H_2O – 2phytyl – $2H_2O$ – $2COOCH_3$	1185.8 – 118 = **1167.8**
1601.9	Pheo.H_2O.pheo.H_2O – $2CH_2CH_2COOCH_3$	1779 – 2 x 87 = **1605**
1569.2	Pheo.H_2O.pheo.H_2O – $2CH_2CH_2COOCH_3$ – $2H_2O$	1779 – 174 – 36 = **1569**
1291.0	1569 - phytyl	1569 – 278.6 = **1290.4**
1321.1	1291 + methanol	1291.0 + 32 = **1323**
1362.0	Pheo.H_2O.pheo.H_2O – $2CH_2CH_2COOCH_3$ - $2H_2O$ – $COOCH_3$	1779 – 322 – 59 – 36 = **1362**

The fragmentation scheme for pheophytin-*a* is given below:

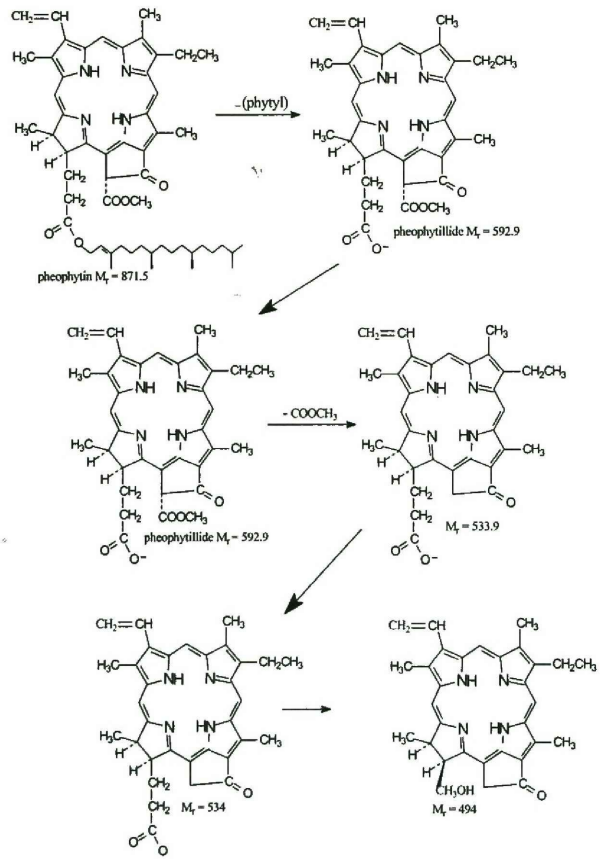


Figure 5.9 Fragmentation scheme for pheophytin-*a*.

5.3 METAL INSERTION

The metals cobalt, zinc, copper, nickel, and chromium were inserted in the centre of the chlorophyll-*a* tetrapyrrole ring.

5.3.1 ULTRAVIOLET-VISIBLE SPECTRA OF METALLO-CHLOROPHYLLS

Complexation of pheophytin-*a* to obtain the desired metal complex in this research was successful as shown by the absorption spectra of chlorophyll-*a* (Figure 4.16), pheophytin-*a* (Figure 4.17) and metal pheophytin complexes (Figure 4.18 – 4.23)

The absorption spectrum of chlorophyll-*a*, shows two prominent absorption bands characteristic of chlorophyll-*a*, one at 429 and the other at 662 nm (Figure 4.16), which are shifted upon demetallation. The absorption band at 429 nm shifts to 409 nm while the absorption band at 661 nm shifts to 666 nm in pheophytin-*a*. The absence of magnesium in the centre of the tetrapyrrole ring of chlorophyll also results in the appearance of a new band at 505 nm (Figure 4.17).

When pheophytin-*a* is complexed (Figure 4.18 – 4.23), the absorption bands at 409 nm and 666 nm are again shifted, for example, in cobalt(II) pheophytin-*a*, Figures 4.18-431 nm and 655 nm, respectively. The new absorption band at 505 nm, Figure 4.17, which is observed when chlorophyll-*a* is demetalled is not found in metalled pheophytins, Figures 4.18 – 4.23 confirming successful metal insertion.

The metallation reaction is expected to follow the following process in Figure 5.10. In this reaction process, chlorophyll-*a* is converted to pheophytin-*a* in acidic medium and pheophytin-*a* combines with the appropriate metal ion [M^{2+}/M^{3+}] to form a metallochlorophyll

$$\text{Chl-}a + 2H^{+} \longrightarrow \text{Phe-}a + Mg^{2+}$$

$$\text{Phe-}a + M^{2+} \longrightarrow \text{Mphe} + 2H^{+}$$

Figure 5.10 Metallation of chlorophyll equation

Acetic acid has been used in this metallation process because acetic acids acts to protonate the conjugated keto groups at position C-13[1] and or C-3[1] increasing the s-character and acidity of the N-atoms of ring I or III or both.

Reducing the acidity of the amino nitrogens is expected to lower the rate and yield of metal insertion.[10,59]

The absorption spectrum of the solution obtained with cobalt(II) acetate (Figure 4.18) shows two absorption bands at 431 and 655 nm. The change in this absorption spectrum, Figure 4.18, is confirmation of successful metallation of the pheophytin. The metal pheophytins obtained, are hereby referred to as metal pheophytin complexes.

Other metal acetates were also employed to obtain metal pheophytins of these metals. Metal pheophytins obtained are cobalt, zinc, copper, chromium, nickel and trisodium copper chlorophillin (Merck) (Figures 4.18 - 4.24). The general structural formula of the metal pheophytin complexes is shown in Figure 5.11.

Spectral variation influenced by the central metal atom results from the demetallation of chlorophyll-*a* to pheophytin-*a* and metallation of pheophytin-*a* to metal pheophytin-complex.

The absorption bands in chlorophyll-*a* and pheophytin-*a* labelled B_y, B_x, Q_x and Q_y show pair wise dependences. When the central metal atom is changed from magnesium in chlorophyll to other metals, the B_x and Q_y transitions are only slightly affected by changing the central metal in the tetrapyrrole ring. On the other hand, strong and distinct shifts are observed in the B_y and Q_x bands. Shifts in these absorption bands with respect to chlorophyll-*a* and pheophytin-*a* are displayed in Table 5.4.

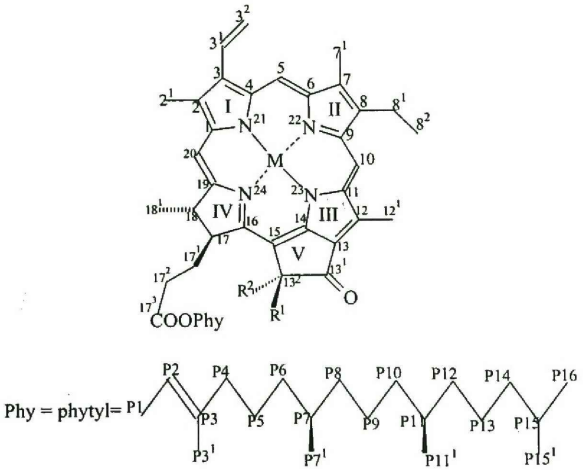


Figure 5.11 Metallated Chlorophylls

Complex	B_y	B_x	Q_x	Q_y	Figure
Mg^{2+}	429	530	617	661	4.16
$2H^{+}$	409	505	607	666	4.17
Co^{2+}	431	—	—	655	4.18
Cr^{3+}	422	—	—	594	4.20
Cu^{2+}	411	—	—	648	4.21
Zn^{2+}	428	—	—	659	4.23
Ni^{2+}	423	—	—	652	4.24

Table 5.4 Visible absorption spectral properties of prepared metallochlorophylls in acetic acid.

The large shifts of the Q_x and B_y bands can be rationalised qualitatively by the four orbital model. According to this model, the ultraviolet and visible spectra result from transitions among four orbitals. These are the two highest occupied molecular orbitals

(HOMO) and the two lowest unoccupied molecular orbitals (LUMO). These four orbitals are a_{2u} (HOMO-1), a_{1u} (HOMO), e_{gx} (LUMO) and e_{gy} (LUMO+1).

From this assignment, the B_y is a transition from a_{2u} to e_{gy}, the B_x is a transition from a_{1u} to e_{gy}, the Q_x is a transition from a_{2u} to e_{gx} and Q_y is a transition from a_{2u} to a_{1u}. The a_{2u}orbital have high electron densities around the four nitrogens nearest to the metal in the centre of the tetrapyrrole ring of the ligand, whereas the e_{gx} and e_{gy} orbitals have substantial electron densities on only two nitrogens and the a_{1u} orbital has almost no electron density at the nitrogens.

The metallation of a tetrapyrrole molecule in solution is believed to consist of the following steps: (a) deformation of the tetrapyrrole ring, (b) outer-sphere association of the solvated metal ion and tetrapyrrole, (c) exchange of a solvent molecule with the first pyrrolenine nitrogen atom, (d) chelate-ring closure with the expulsion of more solvent molecules, (e) first deprotonation of a pyrrole nitrogen and (f) second deprotonation of the other nitrogen, which will lead to the formation of the metallochlorophyll.[109]

The protons on two of the pyrrole nitrogen atoms prohibit the metal ion to reside in the centre of the porphyrin plane; rather, the metal ion will lie above the ring plane and form bonds to a number of solvent molecules. [45]

5.3.2 INFRARED SPECTRA OF METALLOCHLOROPHYLLS

Infrared spectra of chlorophyll-*a*, pheophytin-*a* and metallochlorophylls prepared are displayed in Figures 4.24 - 4.31. Prominent absorption bands of metallochlorophylls are displayed in Figure 5.12 to 5.17.

The frequencies of these prominent absorption bands of the metallochlorophylls are collected in Table 5.5. The infrared spectra obtained compare favourably with published data[31,112] for the structure of metallochlorophylls shown in Figure 5.11.

The infrared spectra of the metallochlorophylls have several prominent absorption bands among these bands is the ester carbonyl absorption band which is found at about 1735cm^{-1}.

The free keto carbonyl absorption band is around 1695cm^{-1} and the coordinated keto carbonyl absorption band C=O---Mg is observed at 1625 cm^{-1}. The skeletal C=C & C=N absorption is at ~1608 cm^{-1} and the aggregation peak at 1652 cm^{-1}. The skeletal C=C absorption band in metallochlorophylls show stretching vibrations that are metal sensitive, that shift upon metal insertion into the ligand. [57,112,118]

The bands at 1739-1710 cm^{-1} in these metallochlorophylls have been assigned as ester carbonyl absorptions. The bands at about 1642 – 1625 cm^{-1} are aggregation peaks. These peaks are absent in some metallochlorophylls. The most important metal sensitive absorption band is that described as IR4 by Masuo Fujiwara and Mitsuo

Tasumi[119] found at 1555-1549 cm^{-1} depending on the metal and which arises from C=C stretching vibrations. These absorption bands are also found at the wavenumbers 1576-1565 cm^{-1} depending on the metal.

The peaks at 1584 – 1506 cm^{-1} are also metal sensitive resulting from the macrocyclic ring of the tetrapyrrole. In chlorophyll and pheophytin, this band is observed at 1506 and 1523 cm^{-1} respectively. This absorption band is at a higher frequency for the metallochlorophylls (1584 – 1548 cm^{-1}), this may be interpreted to indicate a greater stability for the metallochlorophylls than for chlorophyll.

Most of the pheophytin absorption positions are independent of the metal ion, while the C—C and C—N stretching absorption of the pheophytin macrocycle are sensitive to the particular metal ion present in the tetrapyrrole ring. The bands at ~1029cm^{-1} and ~740cm^{-1} in chlorophyll and pheophytin are due to C—O ester and π(C—H) stretching vibrations which do not change upon metal insertion.

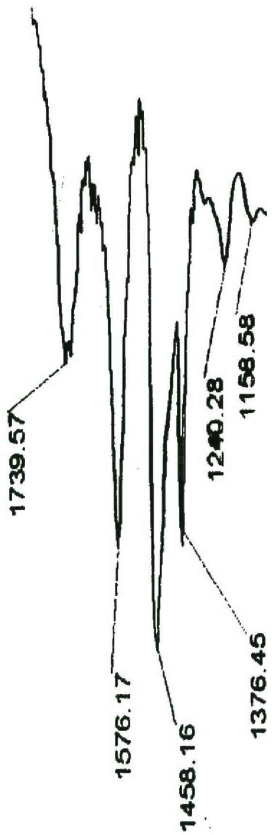


Figure 5.12 Cobalt(II) pheophytin-*a*

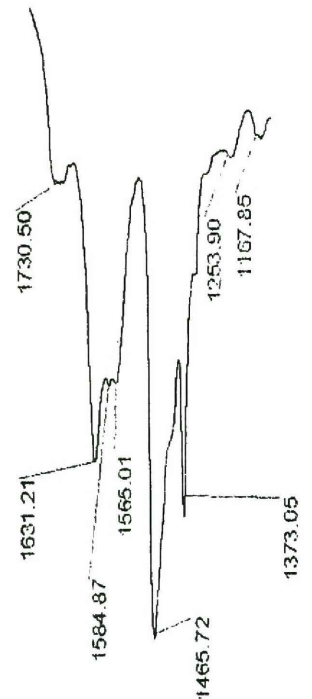


Figure 5.13 Copper(II) pheophytin-*a*

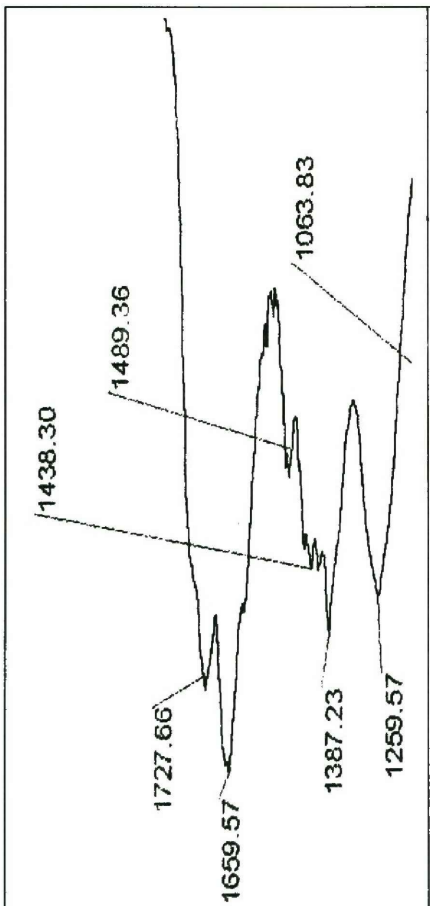


Figure 5.14 Chromium(III) pheophytin-*a*

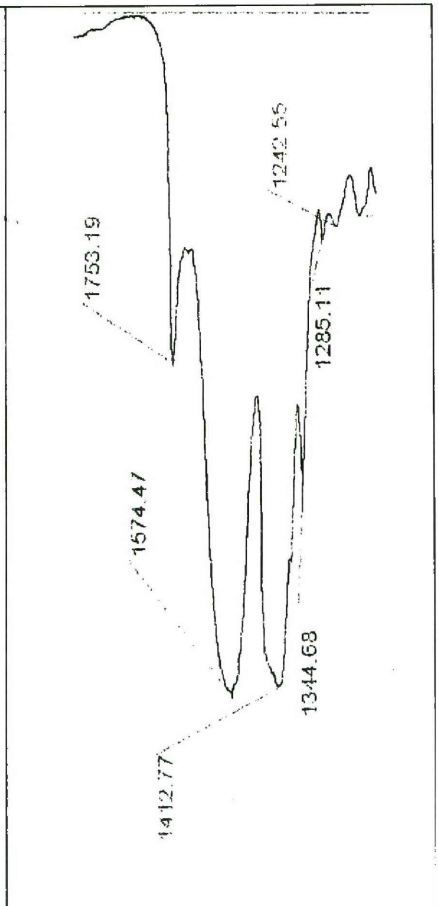


Figure 5.15 Nickel(II) pheophytin-*a*

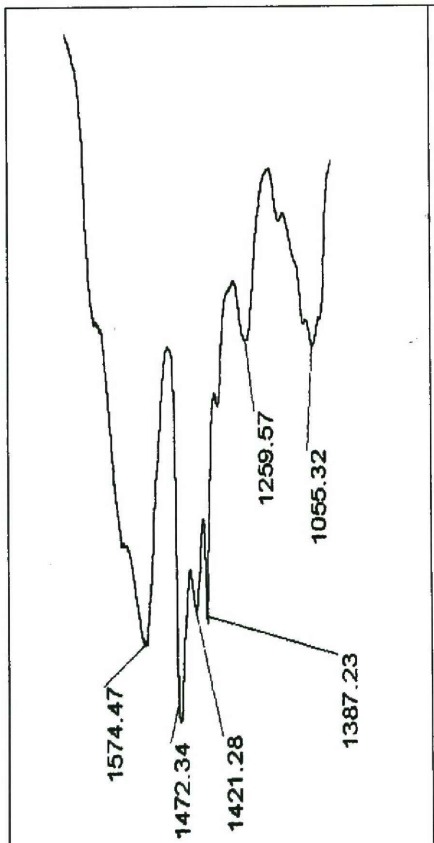


Figure 5.16 Zinc pheophytin-*a*

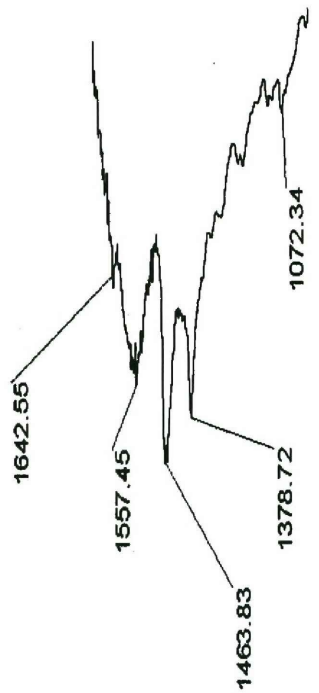


Figure 5.17 Trisodium copper pheophytin-*a*

Infrared absorption bands of synthesized metallochlorophylls and their assignments.

Complex	**Band**	**Signal strength**	**Assignment**
Cobalt(II) pheophytin-*a* (Cophe) (Figures 4.27 and 5.12)	1736 1719 1576 1458 1376 1240 1158 1058 1022 895 731	m sh sh sh m w w vw w w m	υ(C=O) υ(C=C) υ(C-O) ester (stretch) and υ(O-H) bending υ(C-H) υ(C=C) υ(C-C) υ(C-H)
Copper pheophytin-*a* (Cuphe) (Figures 4.28 and 5.13)	1730 1631 1584 1565 1465 1373 1253 1167 1055 1028 730 691	w m w w s sh w w w w m m	υ(C=O) υ(C=C) or (C=O---Metal) υ(C-O) ester υ(C-H) υ(C-C) υ(C-H)
Zinc pheophytin-*a* (Znphe) (Figures 4.31 and 5.16)	1574 1472 1421 1387 1259 1055 936 731	s s w sh w s vw vw	 υ(C=C) υ(C-O) ester (stretch) and υ(O-H) bending υ(C-H) υ(C-C) υ(C-H)

Nickel pheophytin-*a* (Niphe) (Figures 4.30 and 5.15)	1753	sh	υ(C=O)
	1574	s	
	1412	s	υ(C-O) ester (stretch) and υ(O-H) bending
	1344	w	
	1285	vw	
	1242	vw	υ(C-H)
	1165	w	υ(C=C)
	1114	vw	
	1063	vw	υ(C-C)
	740	vw	
	680	s	υ(C-H)
	621	vw	
Chromium pheophytin-*a* (Crphe) (Figures 4.29 and 5.14)	1727	s	υ(C=O)
	1659	s	υ(C=C) or (C=O---Metal)
	1489	w	υ(C-O) ester (stretch) and υ(O-H) bending
	1438	vw	
	1387	w	
	1259	s	υ(C-H)
	1106	sh	υ(C=C)
	1063	w	
	1012	w	υ(C-C)
	893	w	
	672	w	υ(C-H)

Table 5.5 Infrared absorption bands of cobalt(II) pheophytin-*a* (Cophe) in nujol

5.3.3 ELEMENTAL ANALYSIS

The insertion of cobalt and other metal ions in place of magnesium in the centre of the chlorophyll macrocycle was successful as shown by elemental analyses result obtained (Figures 4.38 – 4.42 and Table 4.25).

The percentage composition by mass of Carbon, hydrogen and nitrogen calculated and found are in close agreement with each other.

5.3.4 MASS SPECTRA OF COBALT(II) PHEOPHYTIN-*a*:

The insertion of cobalt(II) in the centre of the tetrapyrrole ring of chlorophyll in place of magnesium was successful. This is evident in the electrospray ionization mass spectrum (ESI-MS) of this complex (Figure 4.36).

The cobalt(II) pheophytin-*a* molecular ion peak at 928.13_{calc} is not a strong signal; this is because the chlorophylls provide only pyrrolitic fragments in mass spectral analysis.[126]

The most important signal is at *m/z* 648.66_{obs} due to the cobalt(II) pheophytin-*a* complex without the phytyl chain. The observed *m/z* of this signal at 648.66 and the calculated *m/z* of this signal at 648.53 is also an indication that cobalt was inserted.
This signal (*m/z* 648.66) is found in the spectrum of chlorophyll-*a* and pheophytin-*a* at *m/z* 613.2 and *m/z* 593.2 respectively. Whereas the relative abundance of this signal is about 100% in the spectrum of chlorophyll-*a* and pheophytin-*a*, in cobalt(II) pheophytin-*a*, the signal has an abundance of about 85%.

The other signals of interest in the cobalt(II) pheophytin-*a* mass spectrum are those observed at *m/z* 825.49 and 1002.32. These peaks result from the fragmentation and loss of the C(15)-CO_2Me group and rearrangement of these groups in the chlorophyll macrocycle.

The fragmentation analysis for cobalt(II) pheophytin-*a* is shown in Figure 5.18 and Table 5.6 respectively.

The fragmentation of cobalt(II) pheophytin-*a* is illustrated below:

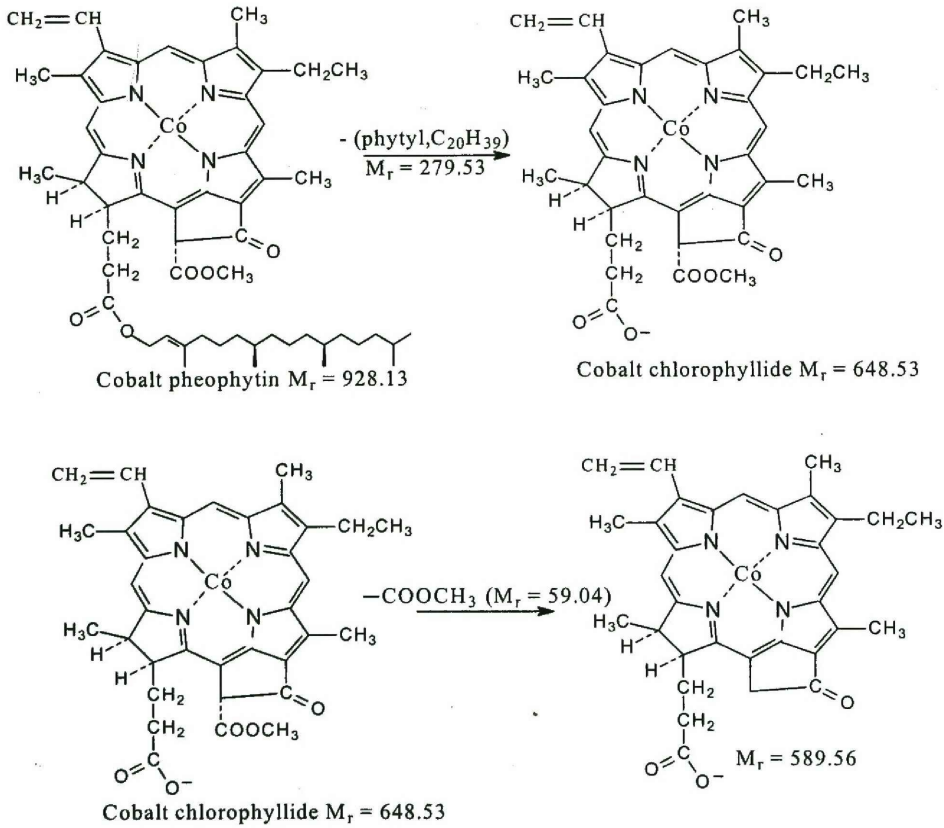


Figure 5.18 Fragmentation scheme for cobalt(II) pheophytin-*a*.

Table 5.6 Fragmentation analysis for cobalt(II) pheophytin-*a*.

Observed *m/z*	Assignments/Analysis	Calculated *m/z*
294.95	Phytyl + methyl	279.53 + 15.03 = **294.56**
312.63	Phytyl + methanol	279.53 + 32.04 = **311.57**
648.66	Cophe – phytyl	928.13 – 279.53 = **648.53**
825.49	Cophe – $CH_2CH_2COOCH_3$ – methyl	928.13 – 87.10 – 15.03 = **826.0**
1002.32	Cophe + $COOCH_3$ + methyl	928.13 + 59.04 + 15.03 = **1002.2**
1893	Cophe + water + Cophe + water	1893
1179.18	Cophe + methyl + 2(CH_3COOCo^+)	928.13 + 15.03 + 235.96 = **1179.12**
1356.2	Cophe + Cophe – 2phytyl + $COOCH_3$	1856.26 – 559.06 + 59.04 = **1356.24**

5.4 KINETICS OF OXIDATION OF COBALT(II) PHEOPHYTIN-*a* (Cophe) BY HEXAAQUACHROMIUM(III) CATION ($[Cr(H_2O)_6]^{3+}$)

The reaction of cobalt(II) pheophytin-*a* with hexaaquachromium(III) cation is a complementary reaction in which the cobalt(II) is oxidized to cobalt(III) and the chromium(III) is reduced to chromium(II), as shown in equation [5.2].

$$Co^{II}phe + [Cr(H_2O)_6]^{3+} \rightarrow Co^{III}phe + [Cr(H_2O)_6]^{2+} \qquad [5.2]$$

The oxidation reaction of cobalt(II) pheophytin-*a* by hexaaquachromium(III) cation followed a pseudo first order kinetics. The oxidation reaction was slow, an indication that the cobalt(II) ion is not easily oxidized to cobalt(III).

The kinetic stability of the cobalt ion in the centre of the chlorophyll macrocycle is comparable to results obtained by other workers [36,147-149] in this field, which show that transition metals coordinated to the chlorophyll macrocycle provide an increase in the stability[131] of the chlorophyll macrocycle. This stability is reflected in the activation energy of the electron transfer reaction.

In the study of the rate of pheophytinization of zinc bacteriochlorophyll-*a* and magnesium bacteriochlorophyll-*a* by Kobayashi and coworkers,[58] the rate of pheophytinization was found to be pseudo-first order. Zinc bacteriochlorophyll-*a* required a stronger acid for pheophytinization than magnesium bacteriochlorophyll-*a*.

The high resistance of zinc bacteriochlorophyll-*a* to acid pheophytinization was explained by invoking the inductive effects of the central metal by comparing the Mg—N bond with the Zn—N bond. Higher ionicity was expected for the Mg—N bond because the electronegativity (E_N) of magnesium (E_N = 1.2) is lower than that of zinc (E_N = 1.6).

The cobalt(II) pheophytin-*a* complex in this study is stable and less prone to degradation. The pseudo first order reaction observed could also be explained by invoking the inductive effect of the central metal by comparing the Mg—N bond and the Co—N bond. Higher ionicity is also expected for the Mg—N bond because the electronegativity

(E_N) of magnesium (E_N = 1.2) is also lower than that of cobalt (E_N = 1.7).

The higher electron density in the chlorophyll-*a* macrocycle and on the nitrogen atoms is expected to assist in electrophillic attack of proton on nitrogen resulting in lability of the magnesium when acidified. As a result, magnesium is easily exchanged by acidification to form the derivative or degradation product pheophytin in solution. This is also followed by a colour change from green to olive green.

The hexaaquachromium(III) cation[142-146] is acidic according to equation [5.3]

$$[Cr(H_2O)_6]^{3+} \rightleftharpoons H^+ + [Cr(H_2O)_5OH]^{2+} \qquad [5.3]$$

Since this could occur by the loss of a proton from coordinated water, the complementary oxidation reaction between cobalt and chromium may take place by electron transfer in this manner.

5.5 MECHANISM OF OXIDATION

The proposed mechanism of the oxidation of cobalt(II) pheophytin-*a* by hexaaquachromium(III) cation in solution is an outer-sphere reaction mechanism. [138]

This is because the pheophytin-*a* ligand to which the cobalt(II) is coordinated does not have a bridging group which is common to the coordination sphere of both cobalt(II) pheophytin-*a* and the hexaaquachromium(III) cation. Both reactants also have to rearrange

before electron transfer could be take place. The chlorophyll macrocycle being relatively large takes time for this rearrangement to occur.

This could explain the relatively slower rate of this reaction compared to the normal rates experienced in outer-sphere mechanisms.[138] As a result, the oxidation of cobalt(II) pheophytin-*a* by hexaaquachromium(III) cation in hydrochloric acid medium is a complementary outer-sphere electron transfer reaction in which, the cobalt is oxidized ($Co^{2+} \rightarrow Co^{3+}$) and the chromium is reduced ($Cr^{3+} \rightarrow Cr^{2+}$). This reaction could therefore be represented as shown in equation [5.2],

5.6 ROLE OF MAGNESIUM IN CHLOROPHYLL

The magnesium atom in chlorophyll plays an important electronic role in the excited states of chlorophyll. A look at the spectroscopic spectra of chlorophyll-*a*, pheophytin-*a* and cobalt(II) pheophytin-*a* complex shows the difference in the absorption spectra of chlorophyll-*a* and its magnesium free derivative pheophytin-*a* (Figures 4.16 and 4.17). When the spectra of chlorophyll-*a* and pheophytin-*a* are compared to the absorption spectra of the cobalt(II) pheophytin-*a* complex, it is evident that some electronic transitions in chlorophyll-*a* have been affected as a result of the removal of magnesium from the tetrapyrrole ring of chlorophyll. New absorption bands resulting from the demetallation observed at 505 – 507 nm in the pheophytin are not observed in the cobalt(II) pheophytin-*a* complex.

There is also a change in colour from green (in chlorophyll) to olive green (in pheophytin). The infrared spectra of chlorophyll-*a* and complexed pheophytin show shifts in absorption bands (Figures 5.12 to 5.17 and Table 5.5). This may have occurred due to expansion of the tetrapyrrole macrocycle once a different transition metal is inserted or co-ordinated in the tetrapyrrole macrocycle. Magnesium forms a five co-ordinate structure due to the lack of *d*-orbitals while transition metals could form six co-ordinates due to the presence of *d*-orbitals.

The most important use of chlorophyll in nature is in photosynthesis. Chlorophyll functions in the channelling of sunlight energy into chemical energy through the process of photosynthesis. The energy absorbed by chlorophyll transforms carbon dioxide and water into carbohydrates and oxygen as shown in equation [1.1]. [3,9,12,59]

In this photosynthetic reaction, electrons are transferred from water to carbon dioxide. The carbon dioxide is reduced by water in the process while the water is oxidized forming oxygen resulting in the transfer of four electrons in the process, equation [5.4].

$$4OH^- \rightarrow 2H_2O + O_2 + 4e^- \qquad [5.4]$$

Chlorophyll assists in this transfer when chlorophyll absorbs light energy, an electron in chlorophyll is excited from a lower energy state to a higher energy state. In this higher energy state, this electron is

readily transferred to another molecule. This starts a chain of electron transfer steps which ends with an electron being transferred to carbon dioxide.[1] Thus, chlorophyll is at the centre of the photosynthetic oxidation-reduction reaction between carbon dioxide and water.

The absence of magnesium in chlorophyll stops this vital photosynthesis reaction. How the magnesium supports this process is yet to be fully determined.

CHAPTER SIX

CONCLUSIONS

6.1 CONCLUSION

A simple, rapid and efficient method for extracting chlorophyll-*a* and pheophytin-*a* from spinach leaves has been developed

The purity of chlorophyll-*a* and pheophytin-*a* has been determined by ultraviolet-visible, infrared and mass spectroscopic methods and found to be in agreement with results obtained by previous workers[19,59,140] in this field.

The problem of extracting chlorophyll-*a* with aqueous acetone in winter[139] has also been solved. This has been achieved by modifying the extraction of chlorophyll using petroleum ether and diethyl ether instead of petroleum ether only.

As reported in the literature, acidification of chlorophyll-*a* has led to the removal of magnesium, enabling complexation of pheophytin by several metal ions. The metals cobalt(II), copper(II), chromium(III), nickel(II) and zinc(II) have been inserted into the chlorophyll macrocycle to give the corresponding metal pheophytin complexes. These have been fully characterised by spectrophotometric methods and by elemental analysis, thus opening up an area of study of natural metal pheophytin complexes that has been hampered by uncertainty in purity and difficulties in extraction.

In order to check on the mechanism of electron transfer in these systems, the oxidation of cobalt(II) pheophytin-*a* by hexaaquachromium(III) has been investigated. This is the first time that a study of this nature has been done, thus opening up a new area of reaction mechanism involving metal pheophytin complexes and macrocyclic ligands like porphyrin, porphrazines and phthalocyanines.

REFERENCES

1. R. Eder, Pigments in handbook of food analysis 1 (Physical characterization and nutrient analysis) edited by Leo M. L. Nollet: Marcel Dekker Inc. New York (1996) 952 – 1014
2. P. May, Chemistry symposium, School of chemistry University of Bristol, Bristol (2001)
3. J. B. Harborne, Phytochemical methods, 2nd ed. Chapman and Hall, London (1988) 214 – 219.
4. I. L. Finar. "Organic chemistry, Vol. 2: Stereochemistry of natural products". ELBS edition Longman. (1991), 899 – 909.
5. D. R. Ort and C. F. Yocum, (eds) Advances in photosynthesis: The light reactions. Kluwer academic publishers London (1996) 83 – 87.
6. C. A. Hampel & G. G. Hawley (editors); "The encyclopaedia of chemistry", 3rd edition. Van Nostrand Reinhold Company, New York, London (1973) 258-260.
7. H. W. Heldt; "Plant biochemistry and molecular biology" Oxford University Press, Oxford (1997) 43-47.
8. O. V. S. Heath, "The physiological aspects of photosynthesis"; Heinemann Educational Books Ltd. London, (1970), 10-23.
9. A. H. Jackson, "Structure, properties and distribution of chlorophylls" in Goodwin, T. W.; (editor), "Chemistry and biochemistry of plant Pigments, 2nd edition Vol. 1"

Academic press, London (1976) 2-21. (a) Fischer, H. and Wenderoth, H. *Ann. Chem.* 537 (1939) 170 – 177

10. K. M Smith, "Synthesis and preparation of porphyrin compounds" in Kevin M. Smith (editor), "Porphyrins and metalloporphyrins"; Elsevier Scientific Publishing Company, Amsterdam (1975) 16-777.
11. J. M. deMan: "Principles of food chemistry", Aspen Publishers, Inc. (1999) 239 – 245.
12. R. P. F. Gregory, "Biochemistry of photosynthesis"; 3rd edition, (John Wiley & Sons), New York (1989), 22-27.
13. R. E. Dickerson, H. B. Gray & G. P. Haight Jr.; "Chemical principles", 3rd edition, The Benjamin/Cummings publishing company, Inc. California (1979) 777-785.
14. G. R. Seely "Chlorophyll in model systems" in Barber, J.; (editor) "Primary process of photosynthesis, Topics in photosynthesis – 2." Elsevier Scientific Publishing Company Amsterdam (1977) 3-53.
15. J. J. da Silva, & R. J. P. Williams, "The biological chemistry of the elements" Oxford University Press, Oxford, New York, (1997) 262 – 263.
16. K. Nakanishi, T. Goto, S. Ho, S. Natori & S. Nozoe; (editors), "Natural products chemistry vol. 2" Academic press Inc, New York and London. (1975) 1145.
17. G. Wilkinson, R. D Gillard & J. A. McCleverty, "Comprehensive coordination chemistry, Vol. 2; Ligands". Pergamon press (1987) 813-983.

18. R. A. Morton, Biochemical spectroscopy, vol. 2, Adam Hilger Limited, London (1975) 515 – 520.

19. C. Long (ed), Biochemists' handbook, E & F. N. Spon Ltd London (1971) 1029 – 1033.

20. R. M. C. Dawson, D. C. Elliott; W. H. Elliott and K. M. Jones: Data for biochemical research 3rd edition, Oxford University Press, New York (1986) 232 – 237.

21. J. Buckingham, (editor): "Dictionary of natural products 1", Chapman & Hall, Chemical Database, London. (1994) 984 – 986.

22. J. Helaja: "Structural analysis of natural chlorin derivatives utilizing nmr spectroscopy and molecular modeling." Ph.D. dissertation, Department of Chemistry, University of Helsinki. (2000).

23. A. B. J. Parusel and S. Grimme. *J. Phys. Chem. B* (2000) 104, 5395 – 5398.

24. L. Sun, L. Hammarström, B. Åkermark and S. Styring. *Chem. Soc. Rev.* 30 (2001) 36 – 49.

25. F. Li, S. Gentemann, W. A. Kalsbeck, J. Seth, J. Lindsey, D. Holten and D. F. Bocian. *J. Mater. Chem.* 7 (1997) 1245 – 1262.

26. S. Yagai and H. Tamiaki, *J. Chem. Soc., Perkin Trans 1,* (2001) 3135 – 3144.

27. P. L. Dentuto, L. Catucci, P. Cosma, P. Fini, A. Agostiano. *Bioelectrochem.* 63 (2004) 117 – 120.

28. H. Furukawa, K. Kuroda, & T. Watanabe, *Chem. Letters* (2000) 1256 – 1257

29. J. Linnanto and J. Korppi-Tommola. *Phys. Chem. Chem. Phys.* 2 (2002) 4962 – 4970

30. S. G. Boxer, G. L. Closs and J. J. Katz. *J. Am. Chem. Soc.* 96 (1974) 7058 – 7066.

31. M. Fujiwara, & M. Tasumi, *J. Phys. Chem.* 90 (1986) 250 – 255.

32. P. Kuronen, K. Hyvärinen, I. Kilpeläinen and P. H. Hynninen. *J. Chromatogr. A.* 654 (1993) 93 – 104.

33. Y. Tan, J. H. Jiang, H. L. Wu, H. Cui and R. Q. Yu. *Anal. Chimi. Acta.* 412 (2000) 195 – 202.

34. T. Oba, M.Mimuro, Z. Wang, T.Nozawa, S. Yoshida & T. Watanabe, *J. Phys. Chem. B* 101 (1997) 3261 – 3268.

35. Kevin M. Smith Dane A. Goff & Daniel J. Simpson, *J. Am. Chem. Soc.* .107 (1985) 4946.

36. Kevin M. Smith, & Dane A. Goff, *J. Am. Chem. Soc.* 107 (1985) 4954 – 4964.

37. R. Livingston and E. Fujimori, *J. Am. Chem. Soc.* 80 (1958) 5610 – 5613.

38. A. R. Battersby. *Nat. Prod. Rep.* 17 (2000) 507 – 526.

39. V. Kleizaite, T. Cesniene and V. Rancelis. *Plant Science* 167 (2004) 1249 – 1256.

40. A. K. Chibisov, T. D. Slavnova & H. Görner. *J. Photochem. Photobiol. B: Biol.* 72 (2004) 11 – 16.

41. A. Dreuw, G. R. Fleming and M. Head-Gordon. *J. Phys. Chem. Chem. Phys.* 5 (2003) 3247 – 3256.

42. A. Prombona and J. Argyroudi-Akoyunoglou. *Plant Sci.* 167 (2004) 117 – 127.

43. Y. Amao, Y. Yamada, K. Aoki. *J. Photochem. Photobiol. A: Chem.* 164 (2004) 47 – 51.

44. K. Möbius. *Chem. Soc. Rev.* 29 (2000) 129 – 139.

45. Y. Shen and U. Ryde, *J. Inorg Biochem.* 98 (2004) 878 – 895.

46. R. R. Bucks, T. L. Netzel, I. Fujita & S. G. Boxer, *J. Phys. Chem.* 86 (1982) 1947 – 1955.

47. C. Yang, C. Peng, J. Duan, & Y. Chen, *Bot. Bull. Acad. Sin.* 43 (2002) 181 – 185.

48. C. C. Gradinaru, A. A. Pascal, F. van Mourik, B. Robert, P. Horton, R. van G. and H. van Amerongen. *Biochemistry* 37 (1998) 1143 – 1149.

49. C. Eijckelhoff & J. P. Dekker. *Photosynth. Res.* 52 (1997) 69 – 73.

50. V. Scheumann, S. Schoch and W. Rüdriger. *J. Biol. Chem.* 52 (1998) 35102 – 35108.

51. T. Bohn and T. Walczyk, *J. Chromatogr. A* 1024 (2004) 123 – 128.

52. K. Saitoh, I. Awaka and N. Suzuki. *J. Chromatogr. A,* 653 (1993) 247 – 251.

53. G. Zheng, M. Aoudia, D. Lee, M. A. Rodgers, K. M. Smith, T. J. Dougherty and Ravindra K. Pandey. *J. Chem. Soc., Perkin Trans. 1,* (2000) 3113 – 3121.

54. Y. Saiki and Y. Amao. *Inter. J. Hyd. Ene.* 29 (2004) 695 – 699.

55. P. Cosmas, F. Longobardi and A. Agostiano. *J. Electroanal. Chem.* 564 (2004) 35 – 43.

56. T. Watanabe, A. Hongu, & K. Honda, *Anal. Chem.* 56 (1984) 251 – 256.

57. L. J. Boucher, & J. J. Katz, *J. Am. Chem. Soc.* 89 (1967) 4703 – 4708.

58. M. Kobayashi, M. Yamamura, M. Akiyama, H. Kise, K. Inoue, M. Hara, N. Wakao, K. Yahara, & T. Watanabe. *Japanese J. Anal. Sci.* 14 (1998) 1149 – 1152.

59. M. Holden "Chlorophylls" in Goodwin, T. W.; (editor), "Chemistry and biochemistry of plant pigments", 2nd edition Vol. 2 Academic press, London (1976) 1-32.

60. McGraw-Hill. "Encyclopedia of Science and Technology", 8th edition Vol.3 (McGraw –Hill, Inc. New York (1997). 1256.

61(a) Pelletier and Caventou in I. L. Finar, "Organic chemistry, vol. 2: Stereochemistry of natural products". ELBS edition Longman. (1991), 899 – 909.

(b) Stokes in I. L. Finar, "Organic chemistry, Vol. 2: Stereochemistry of natural products". ELBS edition Longman. (1991), 899 – 909.

62. C. C. Leznoff, & A. B. P. Levers, (editors); "Phthalocyanines (Properties and applications)" VCH Publishers, Inc New York, (1996) 451 – 455.

63. M. Sekota and T. Nyokong. *J. Porphyrins and Phthalocyanines* 3 (1999) 477 – 487.

64. M. Thamae and T. Nyokong. *J. Electroanal. Chem.* 470 (1999) 126 – 135.

65. T. D. Smith, J. Livorness, H. Taylor, J. R. Pilbrow and G. R. Sinclair. *J. Chem. Soc., Dalton Trans.* (1983) 1391 – 1400.

66. R. Willstäter and A. Stoll, *Liebigs Ann. Chem.* 387(1911) 317.

67. H. Fischer & H. Helerlerger, *Ann. Chem.; (1930) 480, 235* in Nakanishi, Koji; Goto, Toshio; Ho, Sho; Natori, Shinsaku & Nozoe, Shigeo; (editors), "Natural products chemistry vol. 2" Academic press Inc, New York and London. (1975) 114.

68. H. Fischer & L. Medick, *Ann. Chem., (1935) 517, 245* in Nakanishi, Koji; Goto, Toshio; Ho, Sho; Natori, Shinsaku & Nozoe, Shigeo; (editors), "Natural products chemistry vol. 2" Academic press Inc, New York and London. (1975) 114.

69. I. Fleming, *J. Chem. Soc. C* (1968) 2765 – 2770.

70. H. H Strain and W. M. Manning, "Secondary process of photosynthesis, topics in photosynthesis – Vol.2." Elsevier Scientific Publishing Company, Amsterdam. **(1976)** 3 – 53.

71. H. Fischer and H. Wenderoth, *Ann. Chem.* 537 (1939) 170 – 177.

72. W. R. Kneen, M. J. W. Rogers & P. Simpson, "Chemistry, facts, patterns and principles" Addison-Wesley Publishers Limited, London (1972) 550 – 551.

73. R. O. C. Norman & D. J. Waddington, "Modern organic chemistry" Collin Educational Publishers, London (1993) 29 – 30.

74. M. Eagleson, "Concise encyclopaedia of chemistry" Walter de Gruyter Press, Berlin, (1993) 884.

75. A. F. H. Anderson and M. Calvin. *Nature* 194 (1962) 285 – 286.

76. P. H. Hynninen. *Acta. Chem. Scand. B.* 31 (1977) 829 – 835.

77. P. H. Hynninen and S. Lötjönen. *Synthesis.* (1980) 539 – 541.

78. P. H. Hynninen and S. Lötjönen. *Synthesis* (1983) 705 – 708.

79. P. H. Hynninen and K. Hyvärinen. *J. Org. Chem.* 67 (2002) 4055 – 4061.

80. Y. Lee. *J. Liquid Chromatography.* 18 (2001) 779 – 789.

81. M. D. Macías-Sánchez, C. Mantell, M. Rodriguez, E. M. dela Ossa, L. M. Lubian & O. Montero. *J. Food. Energy, in press* 2004.

82. R. B. Woodward, W. A. Ayer, J. M Beaton, F. Bickelhaupt, R. Bonnett, P. Buchschacher, G. L. Closs, H. Dutler, J. Hannah, F. P. Hauck, S. Ito, A. Langemann, E. Le Goff, W. Leimgruber, W. Lwoswski, J. Sauer, Z. Valenta & H. Volz. *J. Am. Chem. Soc.* 82 (1960) 3800 – 3802.

83. A. Nishigaki; S. Ohshima and K. Nakayama. *Plant Cell Physiol.* 41 (2000) 591 – 599.

84. P. Folly and N. Engel. *J. Biol. Chem.* 274 (1999) 21811 – 21816.

85. Leo P. Vernon, *J. Anal. Chem.* 32 (1960) 1144 – 1150.

86. A. Nakamura & T. Watanabe. *Japanese J. Anal. Sci.* 17 (2001) 503 – 508.

87. A. Nakamura and T. Watanabe. *FEBS Lett.* 426 (1998) 201 – 204.

88. T. Watanabe, A. Hongu, K. Honda, M. Nakazato, M. Konno, and S. Saitoh, *Anal. Chem.* 56 (1984) 251 – 256.

89. M. I. Minguez-Mosquera, B. G. Rojas, J. G. Fernandez. *J. Chromatogr. A.* 731 (1996) 261 – 271.

90. A. Cichelli and G. P. Pertesana. *J. Chromatogr. A.* 1046 (2004) 141 – 146.

91. J. S. Fritz and G. H. Schenk, Quantitative analytical chemistry, 5th edition, Prentice-Hall Inc. New Jersey 1987.

92. A. M. Gilmore, Shigeru S. Itoh and Govindjee. *Phil. Trans. R. Soc. Lond. B* 355 (2000) 1369 – 1382.

93. P. S. Woolley, A. J. Moir, R. E. Hester and B. J. Keely. *J. Chem. Soc., Perkin Trans. 2,* (1998) 1833 – 1839.

94. H. Küpper, M. Spiller and F. C. Küpper. *Anal. Biochem.* 286 (2000) 247 – 256.

95. T. R. Crompton. "Chemical analysis of organometallic compounds, vol.1." Academic press London & New York (1973) 86 – 87.

96. C. Weaver: The food chemistry laboratory, A manual for experimental foods, dietetics and food scientists. CRC Press Boca Raton (1996) 79 – 83.

97. N. A. Micheal Eskin: Biochemistry of foods, 2nd edition, Academic Press, Inc. San Diego (1990) 91 – 103.

98. P. H. Hynninen, M. R. Wasielewski and J. J. Katz. *Acta. Chem. Scand. B.* 33 (1979) 637 – 648.

99. S. Lötjönen and P. H. Hynninen. *Synthesis* (1983) 708 – 710.

100. S. Lötjönen and P. H. Hynninen. *Synthesis* (1980) 541 – 543.

101. K. Hyvärinen, J. Helaja, P. Kuronen, I. Kilpeläinen, and P. H. Hynninen. *Magn. Reson. Chem.* 33 (1995) 645 – 656.

102. K. Hyvärinen and P. H. Hynninen. *Res. Adv. In Organic & Bioorganic Chem. 1* (2001) 1 – 19.

103. J. J. Gooding, P. Eiokhin, D. Losic, W. Yang, V. Policarpio, J. Liu, F. M. Ho, M. Situmorang, D. B. Hibbert and J. G. Shapter. *Anal. Sci.* 17 (2001) 3 – 9.

104. Wilson, J. R.; Nutting, M. D. & Bailey, G. F. *J. Anal. Chem.;* 34 (1962) 1331 – 1332.

105. I. Bertini, H. B. Gray, S. J. Lippard, & J. S. Valentine, "Bioinorganic chemistry" University Science Books, Mill Valley, California (1994) 207 – 328.

106. W. Kaim & B. Schwederski, "Bioinorganic chemistry: Inorganic elements in the chemistry of life. An introduction and guide" John wiley and Sons, New York, Chichester, (1997) 57 – 59.

107. R. Croce, G. Cinque, A. R. Holzwarth & R. Bassi. *Photosynth. Res.* 64 (2000) 221 – 231.

108. J. Fiedor; L. Fiedor; J. Winkler; A. Scherz & H. Scheer: *J. Photochem. Photobiol.* 74 (2001) 64 – 70.

109. Stokes in Ş. Dere, T. Güneş and R. Sivaci. *Turk. J. Bot.* 22 (1998) 13 –17.

110. L. J. Boucher, H. H. Strain & J. J. Katz, *J. Am. Chem. Soc.*; 88 (1966) 1341 – 1346.

111. C. Houssier & K. Sauer, *J. Am. Chem. Soc.* 92 (1970) 779 – 791.

112. K. Ballschmiter, & J. J Katz, *J. Am. Chem. Soc.* 91 (1969) 2661 – 2677.

113. G. Hartwich, C. Geskes, H. Scheer, J. Heinze, & W. Mantele, *J. Am. Chem. Soc.* 117 (1995) 7784 – 7790.

114. A. Boussac; H. Kuhl; S. Un; M. Rogner and A. W. Rutherford. *Biochemistry* 37 (1998) 8995 – 9000.

115. L. J. Boucher & J. J. Katz, *J. Am. Chem. Soc.;* 89 (1967) 1340 – 1345.

116. C. Geskes, G. Hartwich, H. Scheer, W. Mantele & J. Heinze, *J. Am. Chem. Soc.* 117 (1995) 7776 – 7783.

117. J. R. Diers, Y. Zhu; R. E. Blankenship and D. F. Bocian. *J. Phys. Chem.* 100 (1996) 8573 – 8579.

118. R. L. Heald & T. M. Cotton, *J. Phys. Chem.* 94 (1990) 3968 – 3975.

119. M. Fujiwara & M. Tasumi, *J. Phys. Chem.* 90 (1986) 5646 – 5650.

120. G. Zweig & J. Sherman, (editors), "Handbook of chromatography, general data and principles"; Vol. 2 (CRC press) (1982), 2 – 3.

121. R. C. Dougherty, P. A. Dreifuss, J. Sphon, & J. J. Katz, *J. Am. Chem. Soc.* 102 (1980) 416 – 418.

122. J. E. Hunt, R. D. Macfarlane, J. J. Katz and R. C. Dougherty. *Proc. Natl. Acad. Sci. USA* 77 (1980) 1745 – 1748.

123. Q. Wang, Y. Lai, L. Yang & B. Huang, *Japanese J. Anal. Sci.* 17 (2001) 789 – 791.

124. J. E. Hunt, R. D. Macfarlane, J. J. Katz & R. C. Dougherty, *J. Am. Chem* 103 (1981) 6775 – 6778.

125. J. Grotonmeyer, U. Bosel, K. Walter & E. W. Schlag, *J. Am. Chem. Soc.* 108 (1986) 4233 – 4234.

126. B. Schoefs "Determination of tetrapyrrole pigments in foodstuffs" In: Proceedings of the 5th European symposium on food authenticity. Nantes, France: Eurofins Scientific, (2001) 34 – 39.

127. R. C. Dougherty, P. A. Dreifuss, J. Sphon & J. J. Katz. *J. Am. Chem. Soc.* 102 (1980) 416 – 418.

128. B. Gilbert "Investigation of molecular structure. spectroscopic and diffraction methods." Bell & Hyman Limited, Hong Kong, (1984) 9 – 122.

129. C. B. Faust, "Modern chemical techniques" Royal Society of Chemistry, London (1992) 1 – 184.

130. G. Hartwich, L. Fiedor, I. Simonin, E. Cmiel, W. Schafer, D. Noy, A. Scherz & H. Scheer. *J. Am. Chem. Soc.* 120 (1998) 3675 – 3683.

131. W. S. Caughey & A. H. Corwin, *J. Am. Chem. Soc;* 77 (1955) 1509 – 1513.

132. W. S. Kim, *Zeitschrift fur Naturforschung,* 22 (1967) No.10 1054 – 61.

133. A. Ghosh. *J. Phys. Chem. B* 101 (1997) 3291 – 3297.

134. M. J. Pilling and P. W. Seakins, Reaction kinetics, Oxford University Press, Oxford, 2001.

135. S. R. Logan. Fundamentals of chemical kinetics. Pearson Education Limited, (1996) 1 – 101.

136. F. Wilkinson. Chemical kinetics and reaction mechanism. Van Nostrand Reinhold Company, (1980) 171.

137. D. O. Cooke. Inorganic reaction mechanisms, The chemical society, (1979) 3 – 43.

138. M. L. Tobe. Inorganic reaction mechanism. Nelson London (1972)

139. F. C. Pennington, H. H. Strain, W. A. Svec and J. J. Katz. *J. Am. Chem. Soc.* 86 (1964) 1418 – 1426.

140. K. Kalyanasundaram, "Photochemistry of polypyridine and porphyrin complexes" Academic Press Limited (London), (1992) 430 – 435.

141. R. Kellner, J. M. Mermet, M. Otto, H. M. Widmer. Analytical chemistry. Wiley-Vch Weinheim, (1998) 710 – 760.

142. N. N. Greenwood and A. Earnshaw. Chemistry of the elements, Pergamon press, oxford (1989) pp1196 & 1310.

143. D. F. Shriver, P. W. Atkins and C. H. Langford. Inorganic chemistry (2nd edition). Oxford University press, Oxford (1994) pp814.

144. J. D. Lee. Concise inorganic chemistry. (5th edition) Chapman & Hall Ltd London (1996) pp 723.

145. F. A. Cotton and G. Wilkinson. Advanced inorganic chemistry 5th edition. John-Wiley & Sons New York (1988) pp 675.

146. J. Emsley. The elements. Oxford University press, Oxford (1991).

147. C. K. Poon and D. A. Isabirye. *J. Chem. Soc. Dalton* (1977) 2115 – 2120.

148. C. K. Poon and D. A. Isabirye. *J. Chem. Soc. Dalton* (1978) 740 – 743.

149. B. D. Bhosale and G. S. Gokavi. *Inter. J. Chem. Kinet.* 35 (2003) 9 – 14.

150. A. Tran. Ruthenium-manganese complexes as model systems for artificial photosynthesis. Ph.D. dissertation, department of chemistry, Royal Institute of Technology, Stockholm, Sweden (2001).

151. K. E. Berg, A. Tran, M. K. Raymond, M. Abrahamsson, J. Wolny, S. Redon, M. Andersson, L. Sun, S. Styring, L. Hammarström, H. Toftlund and B. Åkermark. *Eur. J. Chem.*, (2001) 1019 – 1020.

152. A. H. Squier, D. A. Hodgson and B. J. Keely. *J Chem. Soc. Chem. Commun.* (2003) 624 – 625.